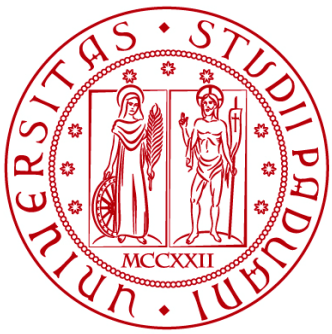

UNIVERSITÀ DEGLI STUDI DI PADOVA

DIPARTIMENTO DI SCIENZE MEDICO-DIAGNOSTICHE E TERAPIE SPECIALI

SCUOLA DI DOTTORATO DI RICERCA IN : Scienze Mediche, Cliniche e Sperimentali
INDIRIZZO: Metodologia Clinica e Scienze Endocrinologiche
CICLO XXIII

EVALUATION OF THE ROLE OF AIP, CDKN1B, MIR-107 AND AHRR IN THE PATHOGENESIS OF SPORADIC AND FAMILIAL PITUITARY ADENOMAS

Direttore della Scuola : Ch.mo Prof. Gaetano Thiene
Coordinatore d'indirizzo: Ch.mo Prof. Roberto Vettor
Supervisore : Ch.ma Prof.ssa Carla Scaroni

Dottorando : Giampaolo Trivellin

TABLE OF CONTENTS

List of publications

1. Ceccato F, Occhi G, Albiger NM, Rizzati S, Ferasin S, **Trivellin G**, Mantero F, and Scaroni C (2010) Adrenal lesions in acromegaly: there is a role of metabolic aspects and AIP (Aryl Hydrocarbon Receptor Interacting Protein) gene? Evaluation at baseline and after long term follow-up. *J Endocrinol Invest*.

2. Igreja S, Chahal HS, King P, Bolger GB, Srirangalingam U, Guasti L, Chapple JP, **Trivellin G**, Gueorguiev M, Guegan K, Stals K, Khoo B, Kumar AV, Ellard S, Grossman AB, and Korbonits M (2010) Characterization of aryl hydrocarbon receptor interacting protein (AIP) mutations in familial isolated pituitary adenoma families. *Hum Mutat,* **31,** 950-960.

3. Occhi G, Jaffrain-Rea ML, **Trivellin G**, Albiger N, Ceccato F, De ME, Angelini M, Ferasin S, Beckers A, Mantero F, and Scaroni C (2010a) The R304X mutation of the Aryl hydrocarbon receptor Interacting Protein gene in familial isolated pituitary adenomas: mutational Hot-Spot or founder effect? *J Endocrinol Invest*.

4. Occhi G, **Trivellin G**, Ceccato F, De LP, Giorgi G, Dematte S, Grimaldi F, Castello R, Davi MV, Arnaldi G, Salviati L, Opocher G, Mantero F, and Scaroni C (2010b) Prevalence of AIP mutations in a large series of sporadic Italian acromegalic patients and evaluation of CDKN1B status in acromegalic patients with multiple endocrine neoplasia. *Eur J Endocrinol,* **163,** 369-376.

Abbreviations

ACTH	adrenocorticotropic hormone
AHRE	AhR response element
AIP	aryl hydrocarbon receptor-interacting protein
AIPL1	aryl hydrocarbon receptor-interacting protein like 1
AhR	aryl hydrocarbon receptor
AHRR	aryl hydrocarbon receptor repressor
AR	androgen receptor
ARA9	Ah receptor-activated 9
ARNT	aryl hydrocarbon receptor nuclear translocator 1
BIR	baculovirus IAP repeat
bp	basepair
cAMP	cyclic nucleotide adenosine 3’,5’-monophosphate
CDK	cyclin dependent kinase
CDS	coding sequence
cDNA	complementary deoxyribonucleic acid
CHIP	carboxyl terminus of Hsc70-interacting protein
CNC	Carney complex
co-IP	co-immunoprecipitation
CREB	cAMP response element binding protein
Cyp40	cyclophilin 40
DQ	dosage quotient
EGFR	epidermal growth factor receptor
FIPA	familial isolated pituitary adenoma
FKBP	FK506-binding protein
FSH	follicle-stimulating hormone
GAPDH	glyceraldehyde-3-phosphate dehydrogenase
GH	growth hormone
GPCR	G protein-coupled receptor
GR	glucocorticoid receptor
GST	glutathione *S*-transferase
HBV	hepatitis B virus
Hop	Hsp70/Hsp90 organizing protein

Hsc70	heat shock cognate 70
Hsp90	heat shock protein 90
IAP	inhibitor of apoptosis
IGF-1	insulin-like growth factor 1
LH	luteinising hormone
LOH	loss of heterozygosity
LR-PCR	long-range PCR
MAS	McCune-Albright syndrome
MEN	multiple endocrine neoplasia
miRISC	miRNA-induced silencing complex
miRNA	microRNA
MLPA	multiplex ligation-dependent probe amplification
MRI	magnetic resonance imaging
mRNA	messenger RNA
MTC	medullary thyroid carcinoma
ORF	open reading frame
PAP	pituitary adenoma predisposition
PAS	Per-ARNT-Sim
PCR	polymerase chain reaction
PDE	phosphodiesterase
PKA	protein kinase A
PP5	protein phospatase 5
PPARα	peroxisome proliferator-activated receptor α
PPIase	peptidyl-prolyl *cis-trans* isomerases
PR	progesterone receptor
PRL	prolactin
PRKAR1A	protein kinase A regulatory subunit-1-alpha
PVN	paraventricular nucleus
RET	rearranged during transfection
RT	reverse transcription
RXRα	retinoid X receptor α
QMPSF	quantitative multiplex PCR of short fluorescent fragments
SA	somatostatin analogue
SD	standard deviation

SEM	standard error of the mean
siRNA	small inhibitory RNA
SNP	single nucleotide polymorphism
SRIF	somatostatin
T_3	triiodothyronine
TCDD	2,3,7,8-tetrachlorodibenzo-*p*-dioxin
TNNI3K	cardiac troponin I-interacting kinase
TOMM	translocase of the outer membrane of mitochondria
TPR	tetratricopeptide repeat
TR	thyroid hormone receptor
TSG	tumour suppressor gene
TSH	thyroid-stimulating hormone
UCR	upstream conserved region
UTR	untranslated region
wt	wild-type
XAP2	X-associated protein-2
Y2H	yeast two-hybrid

Abstract (English)

Pituitary adenomas are common benign intracranial neoplasms, with the vast majority of such tumours being sporadic. The pathogenesis of sporadic pituitary adenomas remains unclear; however, abnormal microRNAs (miRNAs) expression profiles have been recently associated with these adenomas, suggesting that miRNAs can contribute to tumour formation. In about 5% of cases, pituitary adenomas occur in a familial setting, often as part of multiple endocrine tumours syndromes, such as multiple endocrine neoplasia type 1 (MEN1) or Carney complex (CNC). Recently, germline mutations in the *aryl hydrocarbon receptor-interacting protein* (*AIP*) and in the *CDKN1B* (encoding the $p27^{Kip1}$ protein) genes have been identified as causing pituitary adenoma predisposition (PAP) or associated to the development of multiple endocrine tumours, respectively. Several studies revealed *AIP* mutations in about 15% of kindreds with familial isolated pituitary adenomas (FIPA), a clinical entity in which pituitary tumours are the sole phenotypic manifestation among family members, while sporadic cases are only rarely mutated. Regarding *CDKN1B*, so far point mutations have been reported only in few subjects with clinical features of MEN1, including pituitary adenomas, but without *MEN1* mutations, suggesting that they rarely cause a MEN-like phenotype in both sporadic and familial MEN1 patients.

The aim of the present investigation was to study some of the tumorigenic mechanisms involved in pituitary adenoma formation both in sporadic and familial settings.

Genomic DNA of a homogeneous cohort of Italian patients with either sporadic acromegaly or FIPA was analysed for point mutations and gross rearrangements in the *AIP* and *CDKN1B* genes. I detected three novel, presumably pathogenic, *AIP* variants in four apparently sporadic cases, and one known mutation (p.R304X) in a FIPA family. Interestingly, I found that another Italian FIPA family shares the same mutation and haplotype associated with the mutated gene, strongly supporting the presence of a founder effect. No known mutations were found in the *CDKN1B* gene.

The analysis of miR-107, a miRNA involved in the pathogenesis of different types of tumours and predicted to downregulate AIP expression, revealed that it is overexpressed in pituitary adenomas and may act as a tumour suppressor gene. I

also provided experimental evidences that *AIP*-3'UTR is a functional and direct target of miR-107.

The study of aryl hydrocarbon receptor repressor (AHRR), a molecule which participates in one of the AIP-related pathways potentially involved in pituitary tumorigenesis, demonstrated an increased expression in GH-secreting adenomas compared to normal pituitaries.

In conclusion, the main contribution of this PhD thesis was to provide new knowledge about the pathogenesis of pituitary adenomas. In particular, I found that:

- mutations in the *AIP* and *CDKN1B* genes seem relatively uncommon in the Italian sporadic acromegalic patients, confirming what already reported in the literature for other populations;
- a founder effect for the *AIP* p.R304X mutation exists in a region of central Italy;
- the miRNA miR-107 interacts with AIP and may play roles in pituitary adenoma pathogenesis;
- AHRR is overexpressed in somatotropinomas.

Abstract (Italian)

Gli adenomi ipofisari rappresentano delle comuni neoplasie intracraniche benigne, che nella maggior parte dei casi insorgono in maniera sporadica. La patogenesi degli adenomi ipofisari sporadici rimane tuttora poco chiara; recentemente, tuttavia, degli anormali livelli di espressione dei microRNA (miRNA) sono stati associati con questi adenomi, suggerendo che i miRNA possano contribuire al loro sviluppo. In circa il 5% dei casi, gli adenomi ipofisari insorgono invece in forma familiare, spesso come componenti di neoplasie endocrine multiple, quali la neoplasia endocrina multipla di tipo 1 (MEN1) o il complesso di Carney (CNC). Recentemente, mutazioni germinali nei geni *aryl hydrocarbon receptor-interacting protein* (*AIP*) e *CDKN1B* (codificante la proteina $p27^{Kip1}$) sono state identificate, rispettivamente, come predisponenti l'insorgenza di adenomi ipofisari o associate allo sviluppo di tumori endocrini multipli. Diversi studi hanno dimostrato come mutazioni in *AIP* siano presenti in circa il 15% delle famiglie con adenoma ipofisario isolato (FIPA), un'entità clinica nella quale i tumori ipofisari sono l'unica manifestazione fenotipica tra i soggetti affetti, mentre siano solo raramente ritrovate nei casi sporadici. Relativamente a *CDKN1B*, ad oggi mutazioni puntiformi sono state descritte solo in alcuni pazienti con caratteristiche cliniche associabili al fenotipo MEN1, tra cui la presenza di adenomi ipofisari, ma privi di mutazioni nel gene *MEN1*. Ciò fa quindi ritenere che tali mutazioni causino solo raramente un fenotipo associabile a MEN sia nei casi sporadici che familiari.

Lo scopo di questo lavoro è stato quello di studiare alcuni dei meccanismi tumorigenici coinvolti nello sviluppo degli adenomi ipofisari, sia nelle loro forme sporadiche che in quelle familiari.

Il DNA genomico di una coorte omogenea di pazienti acromegalici Italiani sia sporadici che familiari è stato analizzato per ricercare la presenza di mutazioni puntiformi e grossi riarrangiamenti nei geni *AIP* e *CDKN1B*. Ho individuato tre nuove varianti, presumibilmente patogeniche, nel gene *AIP* in quattro pazienti apparentemente sporadici, e una mutazione nota (p.R304X) sempre in *AIP* in una famiglia FIPA. E' interessante notare come un'altra famiglia FIPA Italiana condivida la stessa mutazione e lo stesso aplotipo associato con il gene mutato, dimostrando quindi la presenza di un effetto fondatore. Nessuna mutazione nota nel gene *CDKN1B* è stata invece riscontrata nella coorte analizzata.

L’analisi di miR-107, un miRNA coinvolto nella patogenesi di diversi tipi di tumore e predetto regolare negativamente l’espressione di AIP, ha rivelato come tale miRNA sia sovraespresso negli adenomi ipofisari e svolga verosimilmente un ruolo da gene oncosopressore. Ho inoltre dimostrato sperimentalemente che il 3’UTR di *AIP* è un reale e diretto bersaglio di miR-107.

Lo studio del repressore del recettore degli idrocarburi (AHRR), una molecola coinvolta in una delle vie correlate ad AIP e potenzialmemente coinvolta nella tumorigenesi ipofisaria, ha dimostrato una sua incrementata espressione nei tumori GH-secernenti rispetto alle ipofisi normali.

In conclusione, il contributo principale di questa tesi di dottorato è stato il fornire nuova conoscenza sui meccanismi patogenetici negli adenomi ipofisari. Più specificatamente, ho dimostrato che:

- mutazioni nei geni *AIP* e *CDKN1B* sono relativamente rare nei pazienti acromegalici sporadici Italiani, in accordo con quanto riportato in letteratura per altre popolazioni;
- esiste un effetto fondatore in una regione del centro Italia per la mutazione p.R304X del gene *AIP*;
- il miRNA miR-107 interagisce con AIP e potrebbe avere un ruolo nella patogenesi degli adenomi ipofisari;
- AHRR è sovraespresso nei somatotropinomi.

1 Introduction

1.1 The pituitary gland

1.1.1 Anatomy

The pituitary gland, also known as hypophysis, is a central endocrine organ that regulates basic physiological functions incuding growth, reproduction and metabolic homeostasis. It situates at the base of the brain, under the optic chiasm, inside a depression on the upper surface of the sphenoid bone, the sella turcica. The pituitary gland consists of two major parts, the adenohypophysis and the neurohypophysis. The neurohypophysis is of neuronal origin and can be divided into the posterior lobe, or pars nervosa, consisting mainly of terminal processes of hypothalamic neuronal cell bodies, and the infundibulum, which consists of an elongated infundibular stem and the median eminence. The adenohypophysis can be divided into the intermediate lobe, or pars intermedia, which exists in most animals and in the human fetus although less prominent in the mature human pituitary gland, the pars tuberalis (a collar of tissue that usually surrounds the pituitary stalk), and the anterior lobe, or pars distalis (Figure 1.1) (1).

The glandular adenohypophysis, particularly the anterior lobe, is composed of six distinct types of differentially distributed, hormone-secreting cells. These cells are named according to the hormones that each cell type produces and secretes: somatotrope cells produce growth hormone (GH), lactotrope cells produce prolactin (PRL), corticotrope cells produce adrenocorticotropic hormone (ACTH), thyrotrope cells produce thyroid-stimulating hormone (TSH), gonadotrope cells produce gonadotropins (follicle-stimulating hormone, FSH, and luteinising hormone, LH). A small population of mammosomatotrope cells producing both GH and PRL also exists. These secretory cells are arranged in clumps or in branching cords of cells separated by capillary and sinusoids. The hormonal peptides are released by exocytosis of the secretory storage granules and diffuse through the perivascular extracellular space to the blood vessels. There is also a non-hormonal structural cell type, called folliculostellate cells, located between the secretory cells, that exerts a supportive function.

The posterior lobe releases two hormones, oxytocin and antidiuretic hormone (ADH) or vasopressin, which are synthetised in different cells in the supraoptic and paraventricular nuclei of the hypothalamus (2;3).

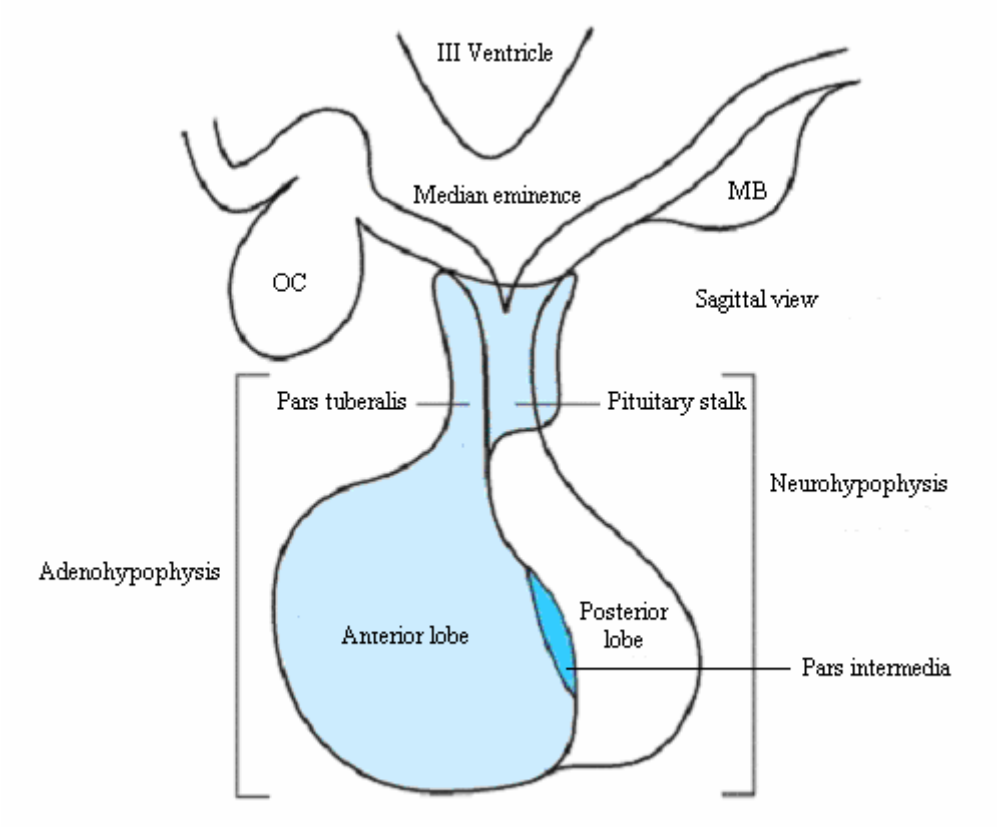

Figure 1.1 Schematic representation of the pituitary gland. OC, optic chiasm; MB, mammilary body. Adapted from (4).

1.1.2 Regulation of hormone secretion

Each of the hormone-secreting cell type of the anterior lobe expresses G protein-coupled receptors (GPCRs) specific for hypothalamic releasing and inhibiting hormones. These hormones reach the corresponding adenohypophyseal cells through the pituitary stalk via the hypophyseal portal system. The hypothalamic releasing hormones stimulate hormone's production by inducing gene transcription, usually through activation of the cyclic adenosine-monophosphate (cAMP) signalling pathway. The GH-releasing hormone (GHRH) induces GH secretion, the corticotropin-releasing hormone (CRH) stimulates ACTH secretion, the thyrotropin-releasing hormone (TRH) stimulates TSH secretion, and the gonadotropin-releasing hormone (GnRH) induces FSH and LH production. The

negative regulation of the pituitary hormones production is conferred by hypothalamic inhibiting hormones, such as somatostatin for GH and dopamine for PRL, and by a negative feedback mechanism exerted by the secreted products of the target glands (Figure 1.2) (2;3).

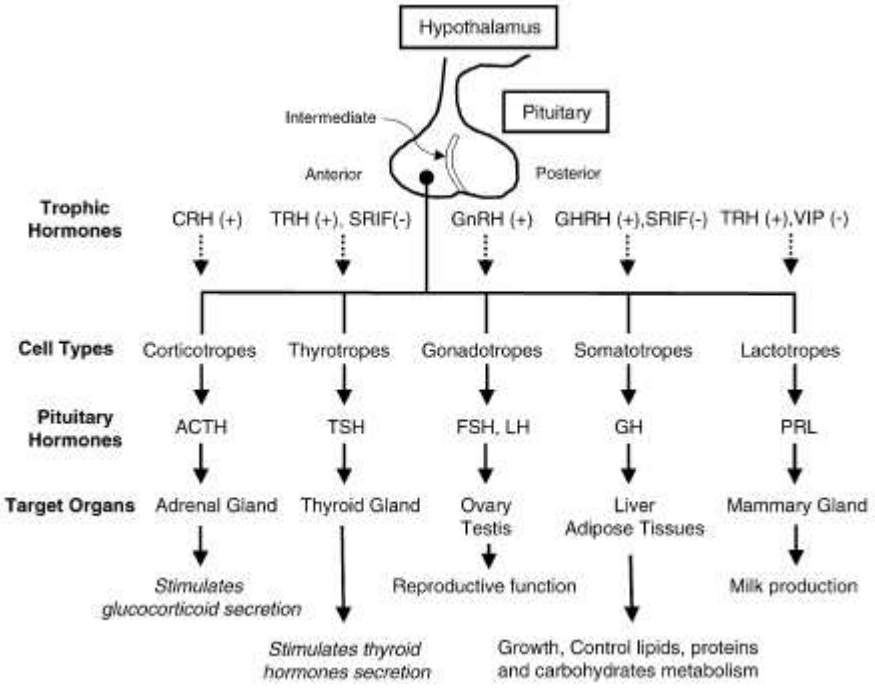

Figure 1.2 Trophic hormones, cell types of the anterior pituitary, hormones secreted and target organs. Hypothalamic trophic hormones act on specific cell types in the pituitary to induce the release of pituitary hormones, which in turn act on target organs to regulate various physiological processes. (+), stimulation; (−), inhibition; CRH, corticotropin-releasing hormone; TRH, thyrotropin-releasing hormone; SRIF, somatostatin; GnRH, gonadotropin-releasing hormone; VIP, vasoactive intestinal peptide; GHRH, GH-releasing hormone. Adapted from (3).

1.2 Pituitary tumours

Each cell type of the anterior lobe can give rise to pituitary tumours. They are the result of excessive proliferation and they can over-produce the specific hormones leading to endocrine syndromes, or they may be functionally silent. Pituitary tumours are usually well-differentiated, common (accounting for up to 25% of all intracranial tumours) benign neoplasms which often grow invasively but very rarely progress to true carcinomas. Although classified as benign, they may cause significant morbidity in affected patients due to aberrant hormone secretion, as well as compressive effects on nearby tissues, such as the optic chiasm, or the healthy pituitary (hypopituitarism) (5). The majority of pituitary adenomas are monoclonal in origin, arising from monoclonal expansion of a single neoplastic cell,

which has acquired genetic or epigenetic defects that confers growth advantage (6).

1.2.1 Classification of pituitary tumours

Pituitary tumours are classified according to the hormones secreted, the immunohistological hormone staining and the tumour size:

1) The clinical hormone-secreting types are:

- GH-secreting adenomas (or somatotropinomas)
- PRL-secreting adenomas (or prolactinomas)
- GH- and PRL-secreting adenomas (or mammosomatotroph adenomas)
- ACTH-secreting adenomas (or corticotropinomas)
- TSH-secreting adenomas (or thyrotropinomas)
- FSH- and LH-secreting adenomas (or gonadotropinomas)
- non-functioning adenomas (NFPAs).

The majority of NFPAs are derived from FSH- or LH-cells and are clinically silent. Mixed tumours co-secreting GH with PRL, TSH or ACTH can also occur (7). The most common pituitary adenoma types are prolactinomas (approximately 50%), NFPAs (30%), somatotropinomas (15-20%), corticotropinomas for (5-15%), thyrotropinomas and LH-FSH adenomas (less than 1%) (8;9).

2) The immunohistochemical staining often reflects the clinical phenotype, but provides additional informations that together with the cytological and histological appearances of tissue and cells have an impact on the perceptions of potential future aggressive behaviour.

3) The classification of pituitary tumours according to their size include:

- microadenomas, when the diameter is <10 mm
- macroadenomas, when the diameter is >10 mm. When the diameter is >40 mm they are defined as large or giant pituitary adenomas (10).

Most pituitary adenomas are microadenomas (7).

1.2.2 Clinical manifestations of pituitary tumours

1.2.2.1 Acromegaly/Gigantism

GH hypesecretion leads to acromegaly or gigantism, depending on the age of onset. The term acromegaly was first used by Pierre Marie in 1886 (11), but patients with acromegaly have been described much earlier. It was only at the beginning of the 20th century with post-mortem examinations of acromegalic patients that it became clear that the cause of the disease was associated with pituitary adenomas and that gigantism had a similar cause with onset during childhood or adolescence, before the growth plates have fused. Giant patients have increased structure and are slightly better proportioned than acromegalics (12). In 99% of the cases acromegaly is due to a somatotropinoma, whereas the rest are the result of increased secretion of GHRH by hypothalamic tumours or ectopic secretion of GH or GHRH by neuroendocrine tumours. The incidence of acromegaly is estimated to be 3 to 4 new cases per million per year, and the prevalence is about 60 cases per million people (13).

The majority of the symptoms seen in acromegalic patients occur as consequence of the deleterious impact of elevated serum concentrations of GH, which in turn increases the production of insulin-like growth factor 1 (IGF-1). The classic clinical features are coarse facial features, macrognathia, enlarged feet and hands, increased sweating, snoring, maxillary widening and skin thickening. Local mass effects of the tumour include headaches, visual disturbances, cranial nerve palsies and hypopituitarism/hyperprolactinemia. Pathologic effects include impaired glucose tolerance, hyperglycemia, visceromegaly, increased risk for cardiorespiratory complications and colonic polyps or tumours (14;15).

The onset of acromegaly is insidious and disease progression usually slow. Several treatment options are available for acromegaly. Transsphenoidal surgical resection of the adenoma, pharmacologic therapy with somatostatin analogues (SAs), dopamine agonists and a GH-receptor antagonist, and various modes of radiation therapy are used to treat GH-secreting adenomas (13).

1.2.2.2 Hyperprolactinemia

Hypersecretion of PRL compromises fertility in both sexes. In pre-menopausal women hyperprolactinemia causes oligomenorrhea or amenorrhea, in addition to galactorrhea due to decreased estrogen levels, whereas the main presenting symptoms in men are galactorrhea and sexual impotence, due to decreased testoterone levels. Other symptoms include headaches and visual field defects, as well as variable degrees of hypopituitarism (1).

1.2.2.3 Cushing's disease

ACTH hypersecretion from a corticotroph adenoma (known as pituitary-dependent Cushing's syndrome or Cushing's disease) induces bilateral adrenocortical hyperplasia and an excess production of cortisol, adrenal androgens and 11-deoxycorticosterone. The typical signs and symptoms of hypercotisolism are: central obesity, easy bruisability, hyperpigmentation, myopathy, striae, hypertension, hirsutism, menstrual irregularities, mood changes, osteoporosis, poor wound healing, hyperglycemia (16).

1.2.2.4 Hyperthyrodism

Thyrotropinomas cause mild hyperthyrodism by chronically stimulating an intrinsically normal thyroid gland. Goiter and clinical thyrotoxicosis are the most common presenting symptoms. Partial hypopituitarism is also common. Visual field defects are present in about two thirds of patients, loss of gonadal function in one third, and headache in one fifth (1).

1.2.2.5 Gonadotropinomas

Symptoms caused by excessive FSH/LH secretion include ovarian hyperstimulation in women and gonadal hyperplasia and elevated serum testosterone levels in men. Visual impairment and headache are also common (1).

1.2.2.6 NFPAs

NFPAs produce hormones that can be detected by immunostaining, but do not cause elevation of the blood hormone levels; thus no manifestations typical of a hormone oversecretion syndrome are seen. Their clinical presentation is only related to the mechanical effects of an expanding macroadenoma (hypopituitarism, headache, visual defects) (1).

1.3 Pituitary tumorigenesis

Tumorigenesis has been extensively studied in the pituitary and it has been suggested to occur as a result of activation of proto-oncogenes, inactivation of tumour suppressor genes (TSGs), and by epigenetic mechanisms in combination with these processes. A proto-oncogene is a gene involved in cell division and activation of one allele is sufficient to cause gain of function or upregulation and subsequent tumourigenesis. In contrast, a TSG inhibits cell cycle progression and only if both alleles are lost [Knudson's "two-hit" hypothesis (17)] it leads to uncontrolled cell division. In hereditary tumours, the first mutational event is inherited via the germ cells and the second occurs in somatic cells. The "second-hit" is usually the result of the loss of the remaining gene copy by a mechanism known as loss of heterozigosity (LOH). In the non-hereditary forms both mutations occur in somatic cells (18).

Alterations in common TSGs such as *p53* and *Rb* or oncogenes such as *Ras* and *c-Myc* are only rarely implicated in the development of pituitary tumours, whereas they seem to occur in more aggressive tumours (19). Several other alterations have been implicated in pituitary tumorigenesis including cell cycle dysregulation, abnormal miRNAs expression profiles, epigenetic mechanisms such as promoter hypermethylation, hormonal and/or growth factors overstimulation, increased expression of pituitary tumour transforming gene (*PTTG*), and other mechanisms such as pituitary senescence (Figure 1.3).

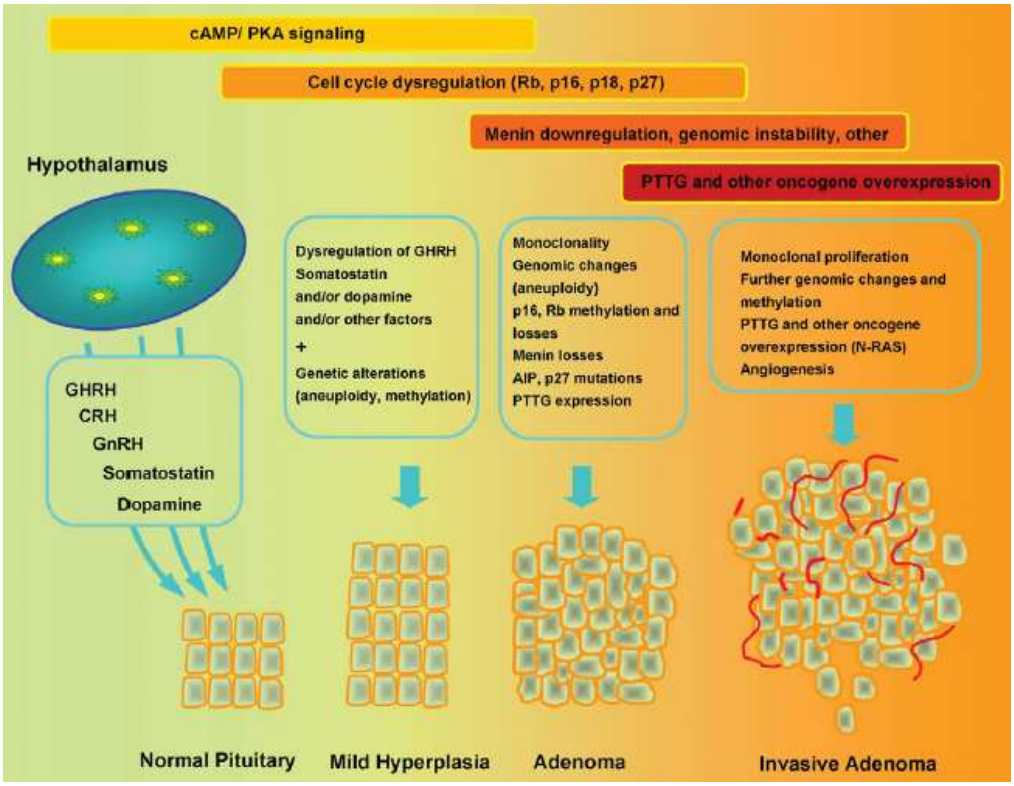

Figure 1.3 Model of pituitary tumorigenesis. Abnormalities linked to quantitative (i.e., excessive stimulation by hypothalamic factors) or qualitative (i.e., constitutively activating *GNAS* mutations) dysfunction of the cAMP signalling pathway lead to the first steps of neoplastic transformation (mild polyclonal hyperplasia, small adenoma). Growth of a monoclonal pituitary tumour is initiated and/or assisted by cell cycle dysregulation, aneuploidy and methylation of certain target genes. Aneuploidy and/or disruption of genomic integrity in a greater scale lead to a well-growing pituitary adenoma. PTTG overexpression, mutations in common oncogenes and increased angiogenesis lead to the formation of larger tumours and invasive adenomas. This model of tumorigenesis is not necessarily linear (not all steps have to occur for a given tumour to form). Adapted from (20).

1.3.1 Cell cycle dysregulation

Disruption of the cell cycle machinery frequently leads to pituitary adenomas. Cell division is divided into four phases: S phase (synthesis of DNA), M phase (mitosis), and two phases of growing and transition, called G (gap) phase (Figure 1.4). The progression of cells through the different phases of the cell cycle is controlled by several protein kinases. Among these kinases there are the cyclin dependent kinases (CDKs). CDK activity is modulated by fluctuations in the cellular concentration of their activators (cyclins) or inhibitors (CKIs), which are regulated by mitogenic and anti-mitogenic pathways and by proteolysis of the ubiquitin-proteasome system. A variety of cyclin-CDK complexes participate in the regulation of the cell cycle. D-type cyclins act as sensors of multiple mitogenic signals to activate CDK4 and CDK6 and to facilitate the progression during G1.

CDK2–cyclin E complexes participate in the transition from G1 to S phase. E-type cyclins are substituted by A-type cyclins to activate CDK2 and CDK1 at the end of S phase and during G2. Finally, the CDK1–cyclin B complex is involved in the progression through G2 and entry into M phase. The primary substrates of the CDKs in G1 progression are the members of the retinoblastoma protein family (pRB). pRB negatively regulates entry into the cell cycle and G1/S progression by binding to the transcription factor family E2F to target cell cycle-specific genes for repression (21).

CKIs as well are essential for cell cycle control, being mediators of antimitogenic signals or checkpoint responses in order to counteract CDK function. There are two families of CKIs, the INK4 and the Cip/Kip family. The INK4 family ($p16^{INK4a}$, $p15^{INK4b}$, $p18^{INK4c}$ and $p19^{INK4d}$) inhibits progression through G1/S by binding to CDK4 and CDK6, whereas members of the Cip/Kip family ($p21^{Cip1}$, $p27^{Kip1}$ and $p57^{Kip2}$) have different roles depending on which CDK–cyclin complex they bind to.

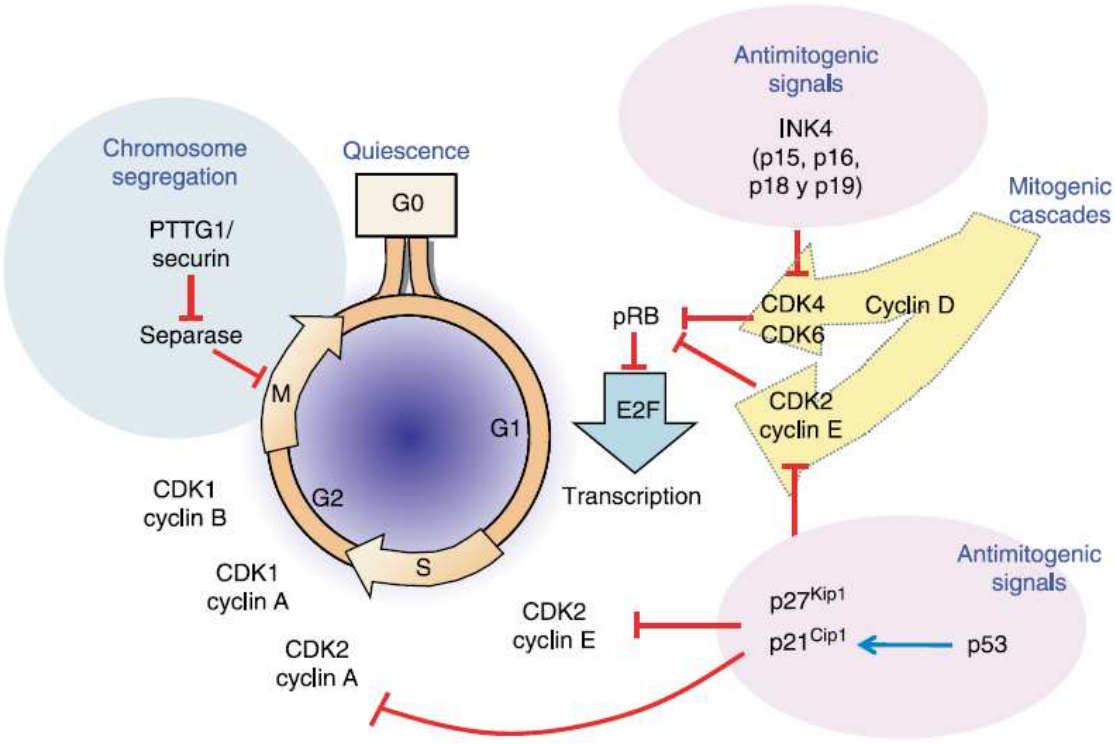

Figure 1.4 Control of the cell cycle by the principal regulators involved in pituitary biology. Adapted from (22).

In the last years several mouse models of cell cycle regulators, such as CKIs, have suggested that the pituitary gland is a critical target of cell cycle deregulation in cancer (22). For instance, a significant incidence of pituitary tumours was

described in p18-deficient mice (23), while $p27^{Kip1}$-null mice develop intermediate lobe pituitary adenomas as the sole tumour phenotype (24-26). In pituitary adenomas the site of most sensitivity appears to be the G1/S transition (22).

1.3.2 Abnormal miRNAs expression profiles

MicroRNAs (miRNAs) are a class of 20–25 basepair (bp)-long noncoding RNAs that are found in the genomes of animals, plants and protozoa (27). miRNA sequences are dispersed throughout the genome and are classified as intergenic (between genes) or intronic (embedded within a gene) (28). miRNAs are initially transcribed as long transcripts (pri-miRNA) which are sequentially processed by different endonucleases. Mature miRNAs are then incorporated into the miRNA-induced silencing complex (miRISC), which associate with target messenger RNAs (mRNAs) (29). Generally, miRNA:mRNA duplexes consist of a 5' end "seed" region, a central loop region, and a 3' end tail region. The major determinant of the interaction between an miRNA and its mRNA targets corresponds to the "seed" region of the miRNA (from 6 to 8 nucleotides at position 1-8 at its 5′ end), which pair with mRNA complementary sequences commonly located in the 3′ untranslated region (3'UTR). However, the central loop has also been shown to be another important factor in miRNA functioning (30), and supplementary base pairing involving the 3' portion of the miRNA can enhance binding specificity and affinity (31). Depending on the overall degree of sequence complementarity, miRNAs negatively regulate post-transcriptional expression of target genes predominantly by inhibiting protein translation or degrading the target mRNA (Figure 1.5) (27).

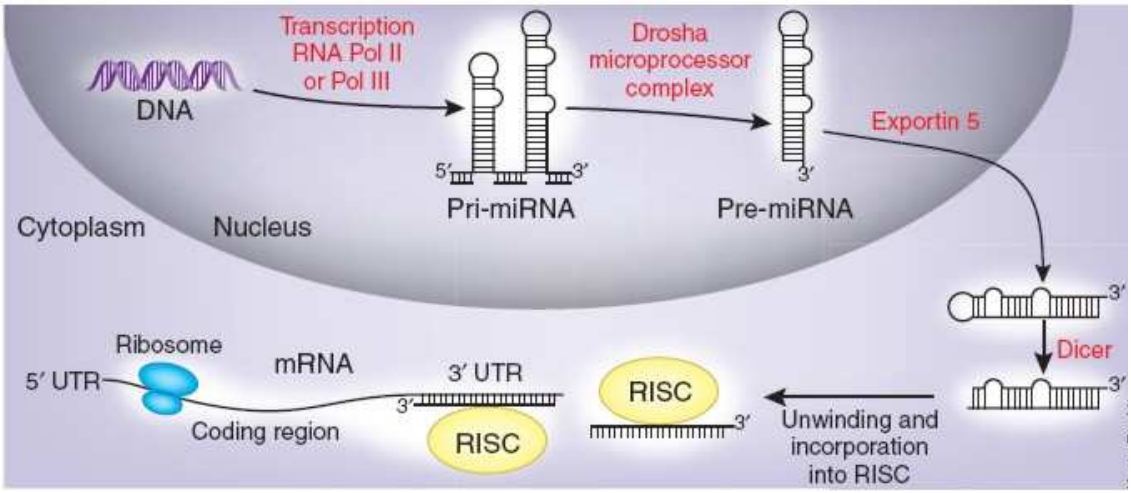

Figure 1.5 miRNA processing. In the nucleus, a miRNA gene is transcribed as a long pri-miRNA transcript (~0.5–7 kb), which is then cleaved by a microprocessor complex termed Drosha. The shorter transcript (~60–70 bp), now termed pre-miRNA, is transported in the cytoplasm, where is further processed by the enzyme Dicer. The hairpin loop is cropped off the double-stranded RNA, leaving a short miRNA duplex that is unwound by a helicase, cleaved into a mature miRNA and incorporated into the miRISC complex. The miRNA-miRISC complex negatively regulates post-transcriptional gene expression by hybridizing to complementary sequences located in the 3'UTR of a target mRNA. Adapted from (32).

Recent studies have shown the abnormal expression of certain miRNAs in various human cancers, demonstrating that some miRNAs may function as oncogenes or TSGs (33-35). Pituitary tumours have also recently been shown to be associated with abnormal miRNAs expression profiles, suggesting that miRNAs might contribute to pituitary adenoma development (36-42).

1.3.3 Epigenetic mechanisms

Many regions of the genome contain large clusters of CpG dinucleotides called CpG islands. They are present in approximately 70% of human promoters, usually in an unmethylated status (43). Promoter methylation is an epigenetic mechanism that has been shown to occur in pituitary tumorigenesis. For instance, in pituitary adenomas the genes *CDKN2A*, *MEG3A*, *ZAC1*, and *GADD45γ* are downregulated due to promoter hypermethylation (44).

1.3.4 Growth factors

Hypothalamic hormones and their receptors could have an effect in pituitary tumorigenesis. Excessive hormone stimulation can lead to an increased number of cells in the pituitary in various physiological or pathological states such as pregnancy (lactotrophs), untreated primary hypothyroidism (thyrotrophs and lactotrophs), primary hypoadrenalism (corticotrophs) and ectopic GHRH-secreting tumours (somatotrophs). Animal models also provide data that in the presence of excessive hypothalamic hormone stimulation, adenoma formation can occur. However, the monoclonal origin of the pituitary adenomas makes it unlikely that hypothalamic factors could initiate pituitary transformation, but they could still create an environment where there is a higher chance that a possible causative

tumourigenic mutation may occur in one or several of the overstimulated pituitary cells (45).

1.3.5 Pituitary senescence

Cellular senescence is an anti-proliferative response which leads to irreversible cell cycle arrest. It can be initiated by DNA damage, chromosomal instability and aneuploidy, loss of tumour suppressive signalling or oncogene activation, and its ultimate aim is to protect the cell from proliferative signals and to act as a buffer against malignant transformation (46). Cellular senescence is associated with the activation of inhibitors of cell cycle progression, such as p19, p21 and p16, and the subsequent modulation of the expression of additional gene pathways, such as those involved in tissue remodeling (i.e. angiogenesis) (47). Premature senescence may account for the predominance of benign versus malignant GH-secreting pituitary tumours. Pituitary adenoma cells may indeed undergo premature senescence in order to escape from the deleterious consequences that proliferative pressure of oncogenes, hormones and transformation factors could exert on their crucial physiological function on homeostasis control. More than 70% of GH-secreting tumours overexpress the *PTTG* gene, which leads to aneuploidy and induction of senescence markers, including p21 and senescence-associated β-galactosidase. In contrast, p21 is weakly expressed in normal pituitary tissue and undetectable in pituitary carcinomas (48;49).

1.4 Sporadic and familial pituitary tumours syndromes

1.4.1 Sporadic pituitary adenomas

The majority of pituitary adenomas occur sporadically (95%). However, their molecular pathology remains poorly understood. The only mutational changes unequivocally associated with sporadic pituitary adenomas are somatic mutations in the *GNAS* gene, which occur in around 40% of GH-secreting adenomas and in the McCune-Albright syndrome (MAS, MIM# 174800). These mutations are caused by a change in residue 201 or 207 (Figure 1.6) (50-52).

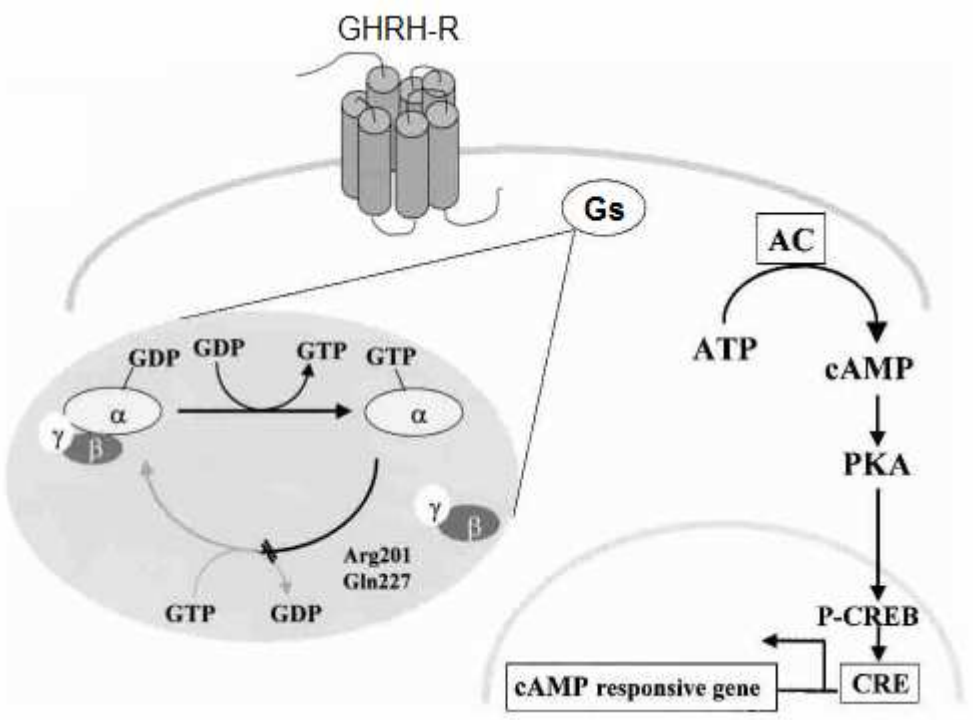

Figure 1.6 Schematic representation of the constitutive activation of the Gs protein in the presence of activating mutations of the *GNAS* gene. Ligand binding stabilises the association of GHRH receptor with Gs and induces the exchange of GDP with GTP on the α subunit, which in turn dissociates from the ß and γ subunits. *GNAS* mutations, by inhibiting the GTP hydrolysis, prevents the formation of the inactive heterotrimer αßγ. The downstream members of the pathway are thus in a state of constant activation. GHRH-R, GHRH receptor; Gs, stimulatory G protein; AC, adenylyl cyclase; PKA, protein kinase A; CREB, cAMP response element binding protein. Modified from (19).

GNAS is a ubiquitously expressed gene encoding for the stimulatory G protein $G\alpha_s$ (MIM# 139320). $G\alpha_s$ activates adenylyl cyclase, which in turn increases the cyclic nucleotide adenosine 3',5'-monophosphate (cAMP) cellular levels. cAMP functions as an intracellular second messenger in several signalling pathways, often acting as a promoter of both differentiation and apoptosis. However, in certain tissues such as in thyroid, adrenal cortex and pituitary somatotroph cells, cAMP stimulates cell proliferation (53). The cAMP overproduction constitutively activates the protein kinase A (PKA), which phosphorylates the cAMP response element binding protein (CREB) and leads to sustained GH hypersecretion and cell proliferation (54). An altered cAMP pathway could result in hypertrophy and hyperplasia of the pituitary, which could lead to the development of pituitary adenomas. MAS is a sporadic pituitary tumour syndrome caused by *GNAS* mutations occuring as an early a post-zygotic event. This disease is characterized by endocrinological

abnormalities, including precocious puberty, hyperthyroidism, Cushing's syndrome and gigantism/acromegaly (55).

1.4.2 Familial pituitary adenomas syndromes

Reports of familial pituitary adenomas date back to more than a century ago, though information is sparse. Several genetic syndromes are now known to be associated with the development of pituitary adenomas: multiple endocrine neoplasia type 1 (MEN1), multiple endocrine neoplasia type 4 (MEN4), Carney complex (CNC), and familial isolated pituitary adenomas (FIPA).

1.4.2.1 Multiple endocrine neoplasia type 1 (MEN1)

Multiple endocrine neoplasias (MEN) are autosomal dominant syndromes characterized by tumours involving two or more neuroendocrine tissues. Two such syndromes have been clinically and genetically well characterized: the MEN type 1 (MEN1, MIM# 131100) and type 2 (MEN2a, MIM# 171400 and MEN2b, MIM# 162300) .

MEN1 is an autosomal dominant condition with high age-related penetrance, characterized by the occurence of tumours of the parathyroids, pancreas and anterior pituitary. Familial MEN1 is defined as MEN1 plus one first-degree relative with a tumour in one of these three tissues. Hyperparathyroidism is the most common manifestation of MEN1, with a penetrance of nearly 100% by the age of 50 years. Enteropancreatic tumours occur in 30-75% of MEN1 patients and pituitary tumours in up to 65%. The most frequent type of pituitary adenoma is the prolactinoma and tumours are twice likely to be macroadenomas than in sporadic cases. Other endocrine tumours can also be detected (56). The disease is caused by mutations in the *MEN1* gene, a TSG located on chromosome 11q13, which consists of 10 exons encoding a 610 amino-acids protein, referred to as menin. Menin is a ubiquitous protein, located predominantly in the nucleus, which is involved in the regulation of gene transcription, cell division, cell proliferation, apoptosis and genomic stability (56). 25 menin partners have been identified so far; however, none has been shown conclusively to be important in the pathophysiology of MEN1 (57). Approximately 90-95% of MEN1 families carry

pathogenic *MEN1* mutations. More than 560 different germline or somatic mutations have been described to date, scattered throughout the whole gene sequence, with only a few potential hot-spots (58).

1.4.2.2 Multiple endocrine neoplasia type 4 (MEN4)

About 10-20% of the cases which exhibit MEN1 features test negative for mutations in the *MEN1* coding sequence (CDS) (59). These patients are described to have an "MEN1 phenocopy" (60;61). It is likely that some of these cases are explained by mutations outside the CDS (i.e. promoter, UTRs, intronic regions); however, theoretically MEN1 may exhibit genetic heterogeneity, with other predisposing genes harboring pathogenic mutations. In 2006, Pellegata *et al.* (62) identified *Cdkn1b* (Cyclin dependent protein kinase 1B, encoding for the CDK inhibitor $p27^{Kip1}$) as the gene predisposing to a MEN-like phenotype, termed MENX, in a rat model. The animals exhibited a phenotype resembling both the human MEN1 and MEN2 syndromes: bilateral pheocromocytomas, parathyroid adenomas, thyroid hyperplasia, paragangliomas, and endocrine pancreas hyperplasia. Based on this model, a heterozygous germline nonsense mutation in the human homologue gene *CDKN1B* (MIM# 600778) was then identified in a patient suspected for MEN1 (presenting with a somatotropinoma and a parathyroid tumour), but tested negative for *MEN1* mutations. The mutation segregated in the patient's family, with several members exhibiting endocrine neoplasia (62). Subsequently, germline point mutations have been reported in other five MEN-1 like subjects (only one was a sporadic case), tested negative for mutations in *MEN1* and *RET* (63-65). These affected patients developed parathyroid and pituitary tumours, as well as other malignancies, but considering the few cases identified, the full spectrum of affected organs associated to this *CKNN1B*-related syndrome remains to be established (66). Other studies, however, failed to detect *CDKN1B* mutations in MEN1-like patients, suggesting that such mutational events are only rarely associated with a MEN1-like phenotype (estimated prevalence around 1.5-2.8%) (67-71). In addition, different groups examined familial and sporadic cohorts of patients with pituitary adenomas, parathyroid tumours, pancreatic endocrine tumours or pheochromocytomas, but no *CDKN1B* mutations have been identified in any of these settings (Appendix, Table 1) (64;70-75).

A new nomenclature has recently been proposed for the human MEN1-like condition caused by *CDKN1B* mutations, namely multiple endocrine neoplasia type 4 (MEN4, MIM# 610755).

1.4.2.3 Carney complex (CNC)

Carney complex (CNC, MIM# 160980) is a rare (has been described in about 500 people so far) autosomal dominant disease, characterized by spotty-skin pigmentation, primary pigmented nodular adrenocortical disease (PPNAD), thyroid tumours and nodules, testicular tumours, cardiac and other myxomas, endocrine tumours (including pituitary adenomas) and schwannomas (76;77). Pituitary tumours are present in 10% of CNC patients and are mainly GH- or GH and PRL-secreting adenomas. CNC is familial in 70% of cases (78).

Two gene loci have been identified to be responsible for this syndrome: the gene encoding for protein kinase A regulatory subunit-1-alpha (*PRKAR1A*) located on chromosome 17q22-24 and an as yet uncharacterized locus on chromosome 2p16 (79). About 40 distinct germline inactivating mutations in *PRKAR1A* have been reported so far in up to 60% of CNC patients (78;80). The functional inactivation of PRKAR1A results in the constitutive activation of the catalytic subunit of PKA, which leads to increased cAMP levels in the affected tissues (81).

1.4.2.4 Familial isolated pituitary adenomas (FIPA)

Familial pituitary tumours have also been described in several families with no other associated endocrine diseases or tumours. These adenomas are inherited in an autosomal dominant manner with incomplete penetrance. This condition is commonly referred to as familial isolated pituitary adenomas (FIPA, MIM# 102200), which includes all types of familial pituitary tumours where no clinical or genetic evidence suggest MEN1 or CNC (82). FIPA comprises the subgroup of isolated familial somatotropinomas (IFS) (83;84) and the aryl hydrocarbon receptor-interacting protein (AIP) mutation-positive group termed pituitary adenoma predisposition (PAP) (85). Currently over 200 FIPA families have been described; however, this number will increase as this condition is being more recognized. The majority of FIPA cohorts consists of families with 2–5 members

having pituitary adenomas. FIPA is characterized by a predominance of prolactinomas (41%) and somatotropinomas (30%), with other tumour types being NFPAs (13%), mammosomatotroph adenomas (7%), corticotropinomas (4%), gonadotropinomas (4%), and thyrotropinomas (1%). There is a female prevalence (62%) probably due to the high incidence of prolactinomas in women within the cohort. FIPA kindreds are divided in those that present either the same pituitary tumour type (referred to as homogeneous families), or different tumour types (heterogeneous families) (86). Within the heterogeneous FIPA families somatotroph, lactotroph and mammosomatotroph adenomas are the most common (87), but other combinations involving NFPAs, corticotroph and gonadotroph adenomas have also been reported (86). Patients with FIPA have significantly larger pituitary adenomas than sporadic pituitary adenoma patients (86-88). Moreover, in the FIPA setting somatotroph adenomas often behave aggressively and respond poorly to somatostatin analog therapy (86). Patients from later generations tend to be significantly younger at diagnosis compared to earlier generations (89), probably because of increased awareness of symptoms due to the family history rather than genetic anticipation (86).

Linkage studies have found that the locus for one of the genes causing FIPA is located on chromosome 11q13.3, but it is independent of the *MEN1* gene (84;90-93). In 2006 Vierimaa *et al.* (85) reported heterozygous mutations in the *AIP* gene (MIM# 605555), located in the 11q13 area 2.7Mb downstream of *MEN1* (Figure 1.7).

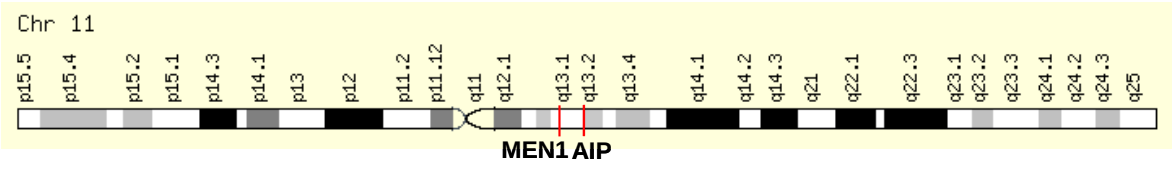

Figure 1.7 *MEN1* and *AIP* location on chromosome 11q13. The two genes are located respectively at 64.3 and 67.0 Mb.

Since then mutations have been found in more than 35 FIPA families (85;87;88;94-100). FIPA patients are on average four years younger at diagnosis than those with sporadic pituitary adenomas (87;94), but *AIP* mutation-positive families show an even younger age of onset, with most having members with childhood onset disease (96). The observed LOH at the *AIP* locus in affected individuals suggests the role of *AIP* as a TSG, with loss of the wild-type (wt) allele

causing PAP in concordance with the Knudson's two hit hypothesis (101). Penetrance is suggested to be incomplete at around 30%; however, this figure varies widely between families (86;87;97;102).

1.5 AIP

1.5.1 AIP structure and conservation

The *AIP* gene consists of 6 exons, encoding a 330 amino acid cytoplasmic protein of 37 kDa, also known as X-associated protein-2 (XAP2) (103), Ah receptor-activated 9 (ARA9) (104) or FK506-binding protein 37 (FKBP37) (105). Structurally it shares a significant degree of homology with immunophilins, such as FKBP52 (52 kDa FK506-binding protein) as it has a peptidyl-prolyl *cis-trans* isomerases (PPIase)-like domain. Immunophilins are a huge family of ubiquitous and conserved proteins which possess PPIase domains that bind immunosuppressant drugs of the FK506 or of the cyclosporin A groups (106). However, AIP does not function as an immunophilin. AIP lacks affinity for the immunosuppressant drugs FK506 and rapamycin (107;108) and the PPIase-like domain displays no enzymatic activity (107), so AIP could not be considered a true immunophilin. These data are consistent with a weak homology between the PPIase domains of AIP and FKBP12 [only five of the 14 amino acids of the FK506-binding domain of FKBP12 are conserved in AIP (108)] and explains the different biochemical properties of AIP.

AIP belongs to the family of tetratricopeptide repeat (TPR) domain containing proteins, such as the aryl hydrocarbon receptor-interacting protein like 1 (AIPL1), protein phosphatase (PP5), FKBP51, FKBP52, and Hop (109), and has three TPR motifs and a final α-7 helix at the C-terminus (Figure 1.8).

A

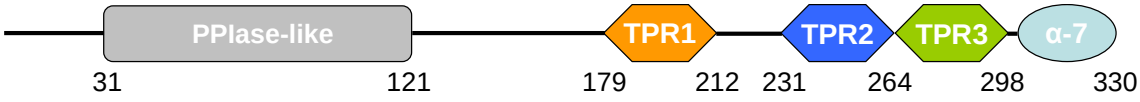

B

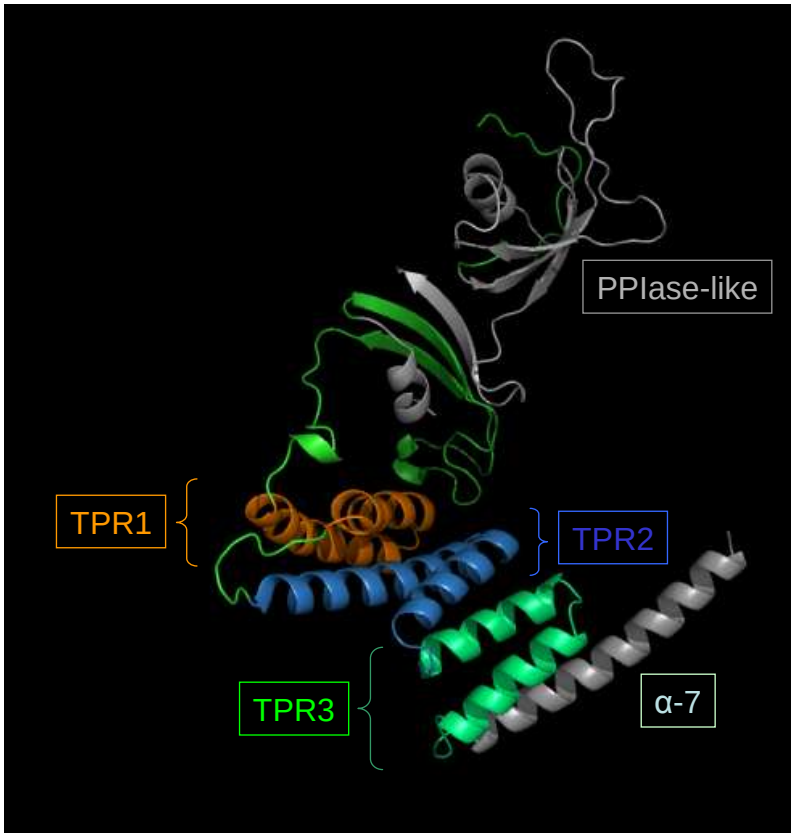

Figure 1.8 A) Schematic structure of the AIP protein. Structurally, AIP is similar to immunophilins. AIP contains a PPIase-like domain at the N-terminus, which show a weak identity to the low molecular weight FKBP12 (12 kDa FK506-binding protein) (104), but does not show immunophilin activity (107;108). The C-terminal part of the molecule contains three TPR domains which are conserved 34 amino structures consisting of two antiparalell alpha helices. There is a terminal α-7 helix which is crucial for protein-protein interaction. Numbers underneath the protein structure represent amino acids. Boxes with different shapes represent different domains. **B) Hypothetical structure of AIP based on the crystal structure of the related protein FKBP51** [adapted from (96)]**.** The PPIase-like domain, the three TPR motifs with three pair of antiparallel α-helices and the final extended α-helix, α-7, are highlighted. PPIase-like, peptidyl-prolyl cis-trans isomerase-like domain; TPR, tetratricopeptide repeat domain.

TPR domains are highly degenerate consensus sequences of 34 amino acids, often arranged in tandem repeats, formed by two α-helices forming an antiparalell amphipathic (having both hydrophilic and lipophilic properties) structure that mediate intra- and inter-molecular interactions in many proteins (110).

The AIP protein sequence is evolutionary conserved among species. For example, the protein sequence of human AIP is 100, 94 and 93% identical to chimpanzee, mouse and rat AIP, respectively. Furthermore, *AIP* is located on a conserved synthenic block in human, mouse and rat (Figure 1.9).

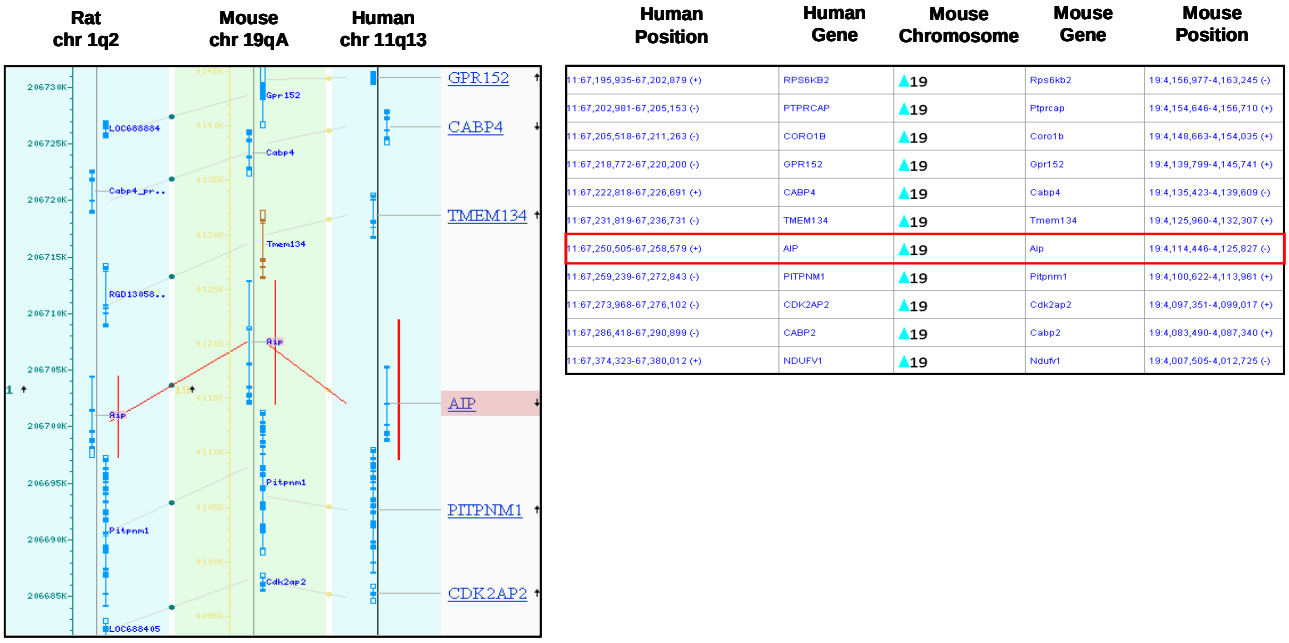

Human Position	Human Gene	Mouse Chromosome	Mouse Gene	Mouse Position
11:67,195,935-67,202,879 (+)	RPS6KB2	19	Rps6kb2	19:4,156,977-4,163,245 (-)
11:67,202,981-67,205,153 (-)	PTPRCAP	19	Ptprcap	19:4,154,646-4,156,710 (+)
11:67,205,518-67,211,263 (-)	CORO1B	19	Coro1b	19:4,148,663-4,154,035 (+)
11:67,218,772-67,220,200 (-)	GPR152	19	Gpr152	19:4,139,799-4,145,741 (+)
11:67,222,818-67,226,691 (+)	CABP4	19	Cabp4	19:4,135,423-4,139,609 (-)
11:67,231,819-67,236,731 (-)	TMEM134	19	Tmem134	19:4,125,960-4,132,307 (+)
11:67,250,505-67,258,579 (+)	AIP	19	Aip	19:4,114,446-4,125,827 (-)
11:67,259,239-67,272,843 (-)	PITPNM1	19	Pitpnm1	19:4,100,622-4,113,961 (+)
11:67,273,968-67,276,102 (-)	CDK2AP2	19	Cdk2ap2	19:4,097,351-4,099,017 (+)
11:67,286,418-67,290,899 (-)	CABP2	19	Cabp2	19:4,083,490-4,087,340 (+)
11:67,374,323-67,380,012 (+)	NDUFV1	19	Ndufv1	19:4,007,505-4,012,725 (-)

Figure 1.9 Human-mouse-rat synteny map around the AIP locus (highlighted in red) (http://www.ncbi.nlm.nih.gov/projects/homology/maps/human/chr11/).

The fact that AIP is a highly conserved protein could be expected for two reasons: first because *AIP* is associated with a human disease (85), and several studies have found that genes causing human disease are more conserved than non-disease genes (111), and second because *AIP* has been demonstrated to be essential in cardiac development in mice (112) and previous studies in mammals and other eukaryotes showed that essential genes are usually located in highly conserved genomic regions (111).

1.5.2 AIP interacting partners

As expected from the presence of TPR motifs in the AIP protein, several proteins have been identified to interact with AIP. 19 interactions have been described so far. 14 proteins directly interact with AIP: two viral proteins (HBV X and EBNA-3), two chaperone proteins (hsp90 and hsc70), two PDEs (PDE4A5 and PDE2A3), three nuclear (AhR, PPARα and TRβ1) and a transmembrane (RET) receptors, two G proteins ($G\alpha_{13}$ and $G\alpha_q$), an inhibitor of apoptosis (survivin), and a mitochondrial import receptor (TOMM20). Three non confimed interactions with a cytoskeletal protein (actin), a growth factor receptor (EGFR) and a cardiac-specific kinase (TNNI3K), have also been described. The association of AIP with the GR

and the co-chaperone protein p23 was proved to be mediated by hsp90 (Figure 1.10 and Appendix 1, Table 2).

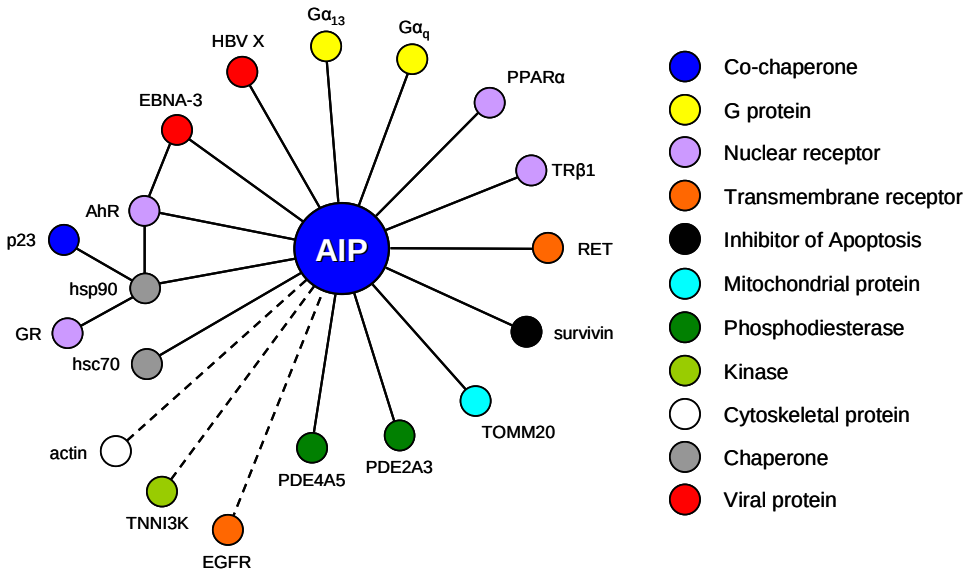

Figure 1.10 AIP interactome. The protein-protein interaction network was rendered with NAViGaTOR 2.1.13 (http://ophid.utoronto.ca/navigator) (113). Nodes correspond to proteins and edges to physical protein-protein interactions. Solid edges signify confirmed interactions, whereas dashed edges represent uncertain associations. Node colors discriminate between different classes of proteins.

1.5.2.1 Viral proteins

- *HBV X protein*

AIP was originally described as a protein associated with the X protein of the hepatitis B virus (HBV) (103), a small human DNA virus that causes acute and chronic hepatitis. Among the few genes contained in the genome of HBV, there is an open reading frame (ORF) that encodes a 154 amino acid regulatory protein, termed X protein. This protein, which does not have a human homologue, activates the transcription of a wide variety of different genes through interaction with cellular factors (114). In order to identify new proteins that may interact with X, the authors used the yeast two-hybrid (Y2H) method. Among the several potential complementary DNAs (cDNAs) coding the protein X binding protein, six were found to be overlapping clones of a full-length cDNA encoding the same gene. The gene was named XAP2 since it was the second protein found to interact with the HBV X protein by this technique. The full-length AIP cDNA was subsequently isolated and *in vitro* translated in a rabbit reticulocyte lysate. The translated product was perfectly corresponding to the native AIP from HeLa cells, and had an

apparent molecular mass of 36 kDa. AIP RNA expression was evaluated and detected in several different tissues and cell lines, but very low levels were found in the liver (103). The ubiquitous expression of AIP was subsequently confirmed in human and murine tissues at the mRNA and protein level (115-118).

The X protein-AIP interaction was also demonstrated to occur *in vitro* by testing the ability of a glutathione *S*-transferase (GST)-X fusion protein to bind to a ^{35}S-labeled AIP. By using different X mutants the interaction with AIP was then shown to be mediated by X protein residues 13–26, a region highly conserved among all mammalian hepadnaviruses. A third evidence regarding this interaction shows similar cytoplasmic distributions of X protein and AIP with immunocytochemistry in X protein-transfected mammalian cells.

Overexpressing AIP resulted in inhibited X protein transcriptional activity suggesting that AIP is an important negative regulator of the X protein, and that their interaction may play a role in HBV pathology (103).

- *EBNA-3*

EBV-immortalized lymphoblastoid cell lines express, among others, six nuclear antigens (EBNA 1-6) and three latent membrane proteins (LMP 1, 2a, 2b), whose concerted action is essential for the immortalization and transformation of B-cells (119). Since the identification of cellular proteins that can interact with the transformation associated EBNAs was not yet complete, Kashuba *et al.* (120) searched for proteins that can bind to the transcriptional regulator EBNA-3, which again does not have a human homologue, in a Y2H system. Among the several clones identified, one corresponded to the AIP protein. Subsequently, this interaction was also confirmed *in vitro* using a GST pull-down assay.

Concordant to what was shown for the aryl hydrocarbon receptor (AhR, (MIM# 600253)) (see section 1.5.2.2), AIP was also found to translocate to the nucleus upon expression of EBNA-3. The authors hypothesized that since AIP can bind to the transforming proteins of two evolutionarily distant viruses and also to the AhR, that is a phylogenetically ancient protein conserved in vertebrates and invertebrates (121), the AhR signal transduction pathway could be involved in virus induced cell transformation. This hypothesis was further supported by a following demonstration from the same group that besides AIP, EBNA-3 can also directly interact with the AhR, with AIP enhancing the stability of the complex. As a

result of this association, an enhanced transcription of AhR responsive genes has been observed (122).

1.5.2.2 AIP-AhR-Hsp90 Complex

More or less paralell to the discovery of the binding with HBV X protein (103), AIP was independently identified by three laboratories to interact also with other two proteins: the AhR (104;115;117) and the heat shock protein 90 (hsp90) (107;108;118;123-126).

- *AIP-AhR*

The AhR, a basic helix-loop-helix protein of the PAS (Per-ARNT-Sim) family of transcriptional regulators, is a cytoplasmic transcription factor that can be activated by a wide variety of structurally diverse exogenous ligands, the prototype of which is the dioxin (TCDD), as well as by some endogenous compounds, such as cAMP (127-129). Ligand-free AhR in the cytoplasm binds to two molecules of hsp90 (130) and to the co-chaperone proteins p23 (131) and AIP (104;115;117). The interaction with hsp90 shapes the AhR's ligand binding domain into a state competent for ligand binding, and it also negatively regulates AhR until ligand binding occurs (132). p23 is part of the AhR complex through interaction with hsp90 (131) and its presence is thought to stabilise the complex (133) and to favour its nuclear import (134). The presence of p23 in the AhR complex seems, however, not to be essential for the AhR physiology (135;136).

Using the Y2H method with AhR as the bait, a human cDNA (termed at the time ARA9) (104) and a murine cDNA (termed AIP) were described (115), both shown to be identical to XAP2. At the same time, since an uncharacterized protein of about 43 kDa was found to be part of the AhR-hsp90 complex (137), a third group decided to identify this protein. After purification from simian COS-1 cells the molecular mass was reassigned from 43 kDa to 38 kDa and the protein sequence was found to be 98% identical to human AIP (117).

There is considerable controversy regarding the effect of AIP on AhR function. Some studies reported that AIP can enhance the activity and expression of the AhR (104;115-117;138;139), while others described an inhibitory function (140-142). This variability is due to several factors, including species- and tissue-

specific differences. Apart from these conflicting results, AIP was repeatedly shown to protect the AhR from ubiquitin-dependent degradation through the proteasome (143;144). Consistent with that low levels or loss of AIP correlate with low expression of AhR (145).

After ligand binding AhR undergo a conformational change that exposes a nuclear localisation sequence, resulting in traslocation of the complex into the nucleus. In mouse ligand binding leads to the dissociation of AIP from the complex as it enters the nucleus (115), whereas in human the association is maintained in the nucleus (104;146). Once into the nucleus, the AhR forms a heterodimer with the aryl hydrocarbon receptor nuclear translocator 1 (ARNT, MIM# 126110), which lead to the activation of AhR sensitive genes. One of these genes, namely the *aryl hydrocarbon receptor repressor* (*AHRR*), plays a role in AHR regulation by forming a negative regulatory loop (147): expression of AhRR is regulated by the AhR, and AHRR, in turn, acts as a transcriptional repressor of AhR function (147-149). AHRR represses the transcription activity of AhR by competing for heterodimer formation with ARNT (150) and subsequently binding to the AhR response element (AHRE) sequence (149). However, additional repressing mechanisms that do not involve competition for ARNT and are independent of AHRE binding by AHRR have been described (151).

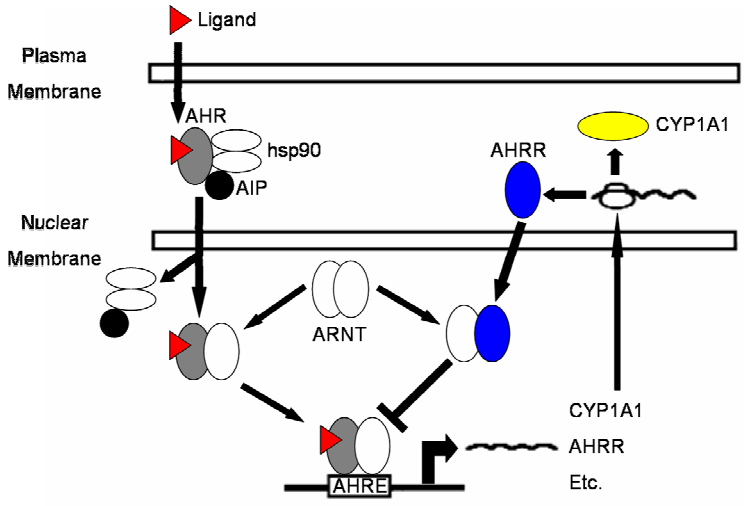

Schematic representation of the AHR-AHRR feedback loop. CYP1A1: cytochrome P450, family 1, subfamily A.

The effect of AHRR varies widely across different tissues because AHRR is not equally expressed nor equally inducible in various cells and tissues (152;153). In

the pituitary, high basal mRNA and protein levels of AHRR have been described, suggesting a tight control of the AhR pathway. Moreover, AHRR expression was shown to be rapidly and considerably induced by xenobiotic compounds in this tissue, supporting the notion that AHRR exerts a tissue-specific regulatory role (152;154). This upregulation of AHRR expression induced by dioxin was demonstrated to require AIP expression (139).

- *AIP-Hsp90*

Hsp90 is a highly abundant molecular chaperone which associates as a dimer with a set of highly different client proteins. Hsp90 is required to maintain signalling proteins in an active conformation that can be rapidly triggered by ligands. Hsp90 functions as the core component of a dynamic set of multiprotein complexes, involving a set of co-chaperones. Structurally, hsp90 can be divided into five domains: a highly conserved N-terminal domain involved in nucleotide and drug binding, a charged domain, a middle domain with ATPase activity involved in client protein binding, a second charged domain, and a C-terminal domain involved in dimerisation and binding of TPR-containing proteins (mediated by a conserved EEVD motif) (155).

The direct but moderate association of AIP with hsp90 has been demonstrated in different studies (107;108;118;123-126). Hyperacetylation of hsp90 was found to lead to the loss of complex formation with AhR, p23 and AIP (156). Discordant findings arose about the role exerted by hsp90 in assisting the AIP-AhR interaction. One study demonstrated that AhR, in order to bind AIP, needs to fold into the mature ligand-binding conformation with the help of hsp90 (123). This requirement of hsp90 was instead proved to be not essential in another report (125).

- *AIP-Hsc70*

In the absence of AhR, AIP was shown to interact - with higher affinity - with another heat shock protein, the heat shock cognate 70 (hsc70, MIM# 600816), rather than to hsp90 (118). Hsc70 is a constitutively expressed co-chaperone protein which is involved, as hsp90, in protein folding and in mitochondrial protein import (discussed later in section 1.5.2.8) (157), but it also functions as an ATPase in the disassembly of clathrin-coated vesicles during transport of membrane

components through the cell (158). Hsc70 is a member of the hsp70 family. Although human hsc70 shares 85% sequence identity with human hsp70, they play different cellular functions (159;160). Consistent with this, AIP was found to be not able to bind hsp70 (126).

- *AIP interactions with other proteins of the AhR signalling pathway*

Apart from AhR and hsp90 it was also investigated whether AIP binds to two other proteins involved in the AhR pathway, ARNT and p23.

ARNT was thought to be a good candidate since it belongs to the same family of transcription factors of AhR and they both share a similar modular structure. However, the results from three different studies demonstrated that AIP is excluded from the AhR-ARNT heterocomplex *in vitro* and *in vivo* (104;115;125). These findings agree with the AhR mapping data since AIP and ARNT have been shown to contact, at least in part, the same or an adjacent binding site on the AhR (117). Even if AIP does not interact with ARNT, two recent studies showed that the expression of ARNT protein is significantly reduced in AIP-mutated pituitary tumours, suggesting that loss of AIP leads to an imbalance in the AhR-ARNT complex formation (161;162).

p23 was then demonstrated to contact AIP in co-immunoprecipitation (co-IP) experiments (140), but only indirectly via hsp90, as previously demonstrated for AhR (131). AIP was also shown to be able to displace p23 from the AhR complex, an effect specific only for the AhR complex and not for hsp90 alone (140).

- *AIP self-association*

An interesting finding was the evidence that AIP can exist in multimeric complexes of at least two molecules even without requiring AhR or hsp90 (140). The self-association of AIP is very likely mediated by the TPR domain, as demonstrated for other TPR-containing proteins (163-165). This suggest that AIP can homodimerise without the association of other auxiliary proteins or at least others than AhR or hsp90, and also that more than one molecule of AIP could be present in the AhR complex. However, two previous studies, using different stoichiometric approaches to examine the AhR complex subunits composition, showed a AhR:hsp90:AIP ratio of 1:2:1 (137;166). If these ratios are correct, the authors suggested that the multimeric complexes of AIP act as a reservoir able to regulate the amount of

available monomeric AIP that can be included into the AhR complex (140), or maybe in the other complexes with which AIP has been shown to interact. Furthermore, the TPR-mediated self-association of AIP might be a mechanism to specifically regulate its biological functions, as reported for the TPR-containing proteins PP5 (protein phosphatase 5) and Sgt1 (164;167). For example, the phosphatase activity of PP5 is suppressed by an autoinhibited conformation maintained by the TPR domain-catalytic domain interaction (167).

- *Domains mediating AIP-AhR-Hsp90 interaction*

Different studies contributed to define the domains involved in AIP-AhR-Hsp90 interaction (Figure 1.11) and also, more specifically, the AIP residues essential for AhR and hsp90 binding.

Mapping experiments using AIP deletion mutants showed that the C-terminal half of AIP (residues 154–330), which contains the three TPR motifs, was necessary for binding both the AhR and hsp90 (108;125;143). An indispensable role in mediating AhR binding was shown for the α-helical C-terminus (α-7) of murine AIP: deletion of the last five amino acids abolishes almost completely AhR binding, without affecting AIP-hsp90 interaction (123). However, another study presented evidences suggesting that the human final α-7 helix binds more likely hsp90 rather than AhR (124). These contrasting results might be explained by species-specific differences. There are controversial results regarding the role played by the N-terminus of AIP. Some reports demonstrated that this region did not interact with either AhR or hsp90 (108;125;143), whereas Kazlauskas *et al.* (124) showed that the N-terminus contains an additional site of interaction with the AhR complex. Moreover, the N-terminal part of AIP was shown to confer stability to the complex and to be essential in the regulation of the subcellular localisation of AhR (124). Taken together, these results suggest that despite the C-terminal region of AIP is capable of interacting alone with the AhR complex, this interaction is not functional. This hypothesis is further supported by the finding that an AIP mutant lacking the first 17 amino acids, even if it did not loose the ability to bind hsp90, was expressed at lower levels compared to the wt protein, maybe as a result of a higher turnover in cells (125).

In the reciprocal mapping analyses, the boundaries of the AhR protein segment interacting with AIP were defined to be approximately between amino acids 380

and 419, which encompass the C-terminal portion of the PAS domain (PAS-B) (108;125;143). This interaction seems to be mediated by nonpolar or hydrophobic amino acids (140). It was also established that AIP, like other immunophilins found in hsp90 complexes, binds to the C-terminal segment of hsp90 (residues 629-732), whereas the AhR binds to the middle region (residues 272-617) (123;125). Hsp90 was found to interact with two spatially distinct motifs of the AhR, the PAS-B and the bHLH domains (168). The domains involved in the AIP-hsc70 interaction were not experimentally determined (118).

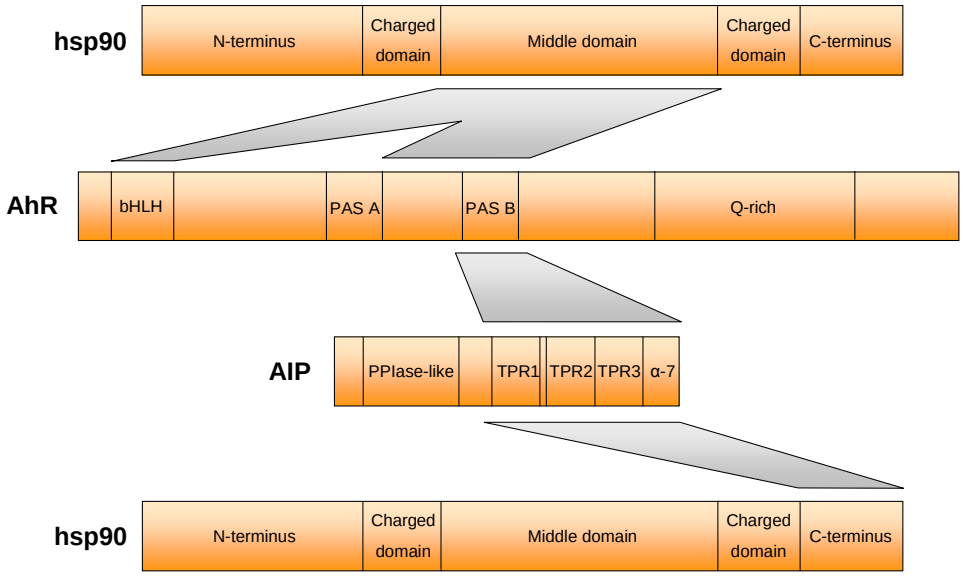

Figure 1.11 Location of key interacting domains of the AIP-AhR-Hsp90 complex. The size of domains is drawn to linear scale proportional to amino acid number. bHLH, basic helix-loop-helix; PAS, Per-ARNT-Sim homology domain; Q, glutamin-rich domain.

1.5.2.3 Cytoskeletal proteins

After ligand-dependent activation in the cytoplasm, signalling proteins that affect gene transcription, like the AhR or the glucocorticoid receptor (GR), move to their sites of action within the nucleus. Lots of evidences point out the essential role of the hsp90-binding immunophilins in mediating various phases of nuclear receptor movements. For instance, FKBP52, which is associated with several steroid receptor heterocomplexes, has been shown to interact with tubulin cytoskeletal networks. This interaction takes place through the PPIase domain of FKBP52 and the cytoplasmic dynein, the motor protein which processes along the microtubules in a retrograde direction toward the nucleus (169). It is thus conceivable to

suppose that AIP could also associate with actin or tubulin filaments in order to regulate the cytoplasmic localisation of the AhR.

Three studies addressed this matter. In one, by a co-immunoadsorption assay, it was shown that the PPIase-like domain of AIP does not bind, or binds only very weakly, the cytoplasmic dynein (170). In another study it was demonstrated that the well-documented AIP-mediated cytoplasmic retention of the AhR (122;124;138;143;166) involves the anchoring of the complex to actin filaments (171). By co-IP experiments this interaction was proven to involve a direct binding of AIP to actin and also to take place only in the non-activated AhR complex, since TCDD treatment induces the release of the complex from actin (171). However, it should be noted that the AIP-actin interaction was subsequently rejected by another group (172). The only difference between the two studies was the cell line used for the experiments. In absence of a conclusive demonstration, this interaction cannot be considered certain at the moment.

1.5.2.4 PDEs

caMP is generated in the cytoplasm by activation of adenylyl cyclase, while is inactivated by phosphodiesterases (PDEs). PDEs are a huge family of enzymes which catalyze the hydrolysis of cAMP and cGMP, generating the corresponding nucleotides 5'AMP and 5'GMP. The PDE superfamily can be subdivided into 11 subfamilies which differ by structure, enzymatic properties, sensitivity to different inhibitors, and specific expression profiles. Each subfamily comprises from one to four distinct genes and each gene, in turn, generates several transcripts (173). This multiplicity of PDE isoforms (currently more than 50 different PDE proteins with tissue-specific subtypes have been identified) ensures the compartmentalisation, fine-tuning and cross-talk of the cAMP and cGMP pathways (174). All the PDEs consist of a modular architecture, with variable regulatory domains located at the N-terminus and a highly conserved catalytic region at the C-terminus (175).

- *PDE4A5*

The cAMP-specific PDE4 group forms the largest PDE subfamily, which is the main enzyme responsible for cAMP degradation (176). PDE4s can be

distinguished from other PDE subfamilies by sequence identity in the catalytic region and by the presence of specific regions, located at the N-terminal portion of the proteins, called upstream conserved regions 1 and 2 (UCR1 and UCR2) (177;178). Four genes (*PDE4A*-*D*) encode at least 35 splice variants (176). Of these, the highly conserved PDE4A4/5 isoform (PDE4A5 is the rat homologue of the human PDE4A4) is characterized by an extended N-terminal region involved in subcellular targeting (177). PDE4A4/5 is expressed in a wide variety of tissues, including the pituitary (179;180), and both membrane and cytosolic localisation has been detected (181). PDE4A5 was demonstrated to interact with the SH3 domains of SRC family tyrosyl kinases (182;183), with AKAP3 (184) and with AIP (177). AIP was initially identified as a direct binding partner of PDE4A5 by a Y2H screening of a rat brain cDNA library. The interaction was subsequently confirmed by a GST pull-down assay and demonstrated also in mammalian cells. In addition, the ability of AIP to bind PDE4A5 was found to be unaffected by the concomitant binding of LYN, a member of the tyrosyl kinase family.

The interaction was proved to be highly specific, since other immunophilins or TPR-containing proteins such as the AIP homologue AIPL1, FKBP51 and FKBP52 were unable to bind PDE4A5, and do not involve other PDE4 isoforms. The domains mediating the interaction were mapped in the TPR region of AIP and in both the unique N-terminal region (amino acids 11–42) and the UCR2 domain (only the PDE4 conserved EELD motif) of PDE4A5. The binding of AIP to PDE4A5 was demonstrated to lead to three distinct functional consequences. One is a reversible, dose-dependent, inhibition of PDE4A5 catalytic activity by approximately 60%, which is directly mediated by the TPR domain of AIP. A second outcome, also leading to a decreased enzymatic activity, is the attenuation of PDE4A5 phosphorylation by PKA. The third consequence is an increased sensitivity of PDE4A5 to rolipram, the PDE4 specific inhibitor.

- *PDE2A3*

Three isoforms of PDE2A (PDE2A1, PDE2A2 and PDE2A3), generated from a single gene by alternative splicing, have been cloned from several different species. These three isoforms are identical except for the N-terminal regions, which are responsible for their different subcellular localisation. The human variant (PDE2A3), encodes a membrane-associated protein of 941 amino acids. PDE2A

functions as a homodimer and each monomer is formed by an N-terminal domain, two tandem GAF domains (GAF-A and GAF-B) and a catalytic C-terminal domain. PDE2A is able to hydrolize both cAMP and cGMP, but in the presence of cGMP, which binds to the allosteric GAF-B domain, the enzyme is activated and increases its affinity for cAMP, resulting in a greater hydrolyzing capacity for cAMP than for cGMP (173). This enzyme contributes thus to the cross-talk between these two second messengers pathways (174). PDE2A is strongly expressed in the brain with a moderate presence in peripheral tissues such as the adrenal gland, heart and skeletal muscle (185-188). In addition, PDE2A expression has been observed in rat (185;189) and human pituitary (180).

In 2007, de Oliveira *et al.* (190) identified an interaction between the human PDE2A and AIP by a Y2H screening of a human brain cDNA library. The interaction was subsequently confirmed by GST pull-down and co-IP experiments both in cell lines and brain tissue lysates. The two proteins were found to colocalise in the cytosol, with the occasionally involvement of the plasma membrane. The regions which mediate the interaction were mapped in the GAF-B domain of PDE2A and the C-terminal half (amino acids 170-330) of AIP. In addition, preliminary results suggested that AIP was able to interact with PDE2A and hsp90 at the same time.

Differently from what was previously showed for PDE4A5, the enzymatic activity of PDE2A was unaffected by AIP binding. Probably because of the intact ability of PDE2A to lower the local cAMP concentration in the compartment where the AhR complex is located, the TCDD and especially the forskolin-induced nuclear translocation of AhR was 40% (with TCDD) or 55% (with forskolin) lower in PDE2A transfected cells compared to PDE2A transfected cells. Furthermore, this inhibition was demonstrated to correlate with a reduction of the AhR function, as reported by a reporter gene assay.

At present it is unknown if both PDE4A5 and PDE2A can simultaneously associate via AIP to the AhR complex (178).

1.5.2.5 Nuclear receptors

Several studies demonstrated the involvement of AIP in various nuclear receptor signalling pathways.

- *GR*

The GR is a member of the nuclear receptor superfamily. Like the AhR, it has been demonstrated to exist in a multiprotein heterocomplex containing two molecules of hsp90 and other co-chaperone proteins, such as p23, PP5 and FKBP52 (191). Moreover, the GR signalling pathway shares some mechanistic similarities with the AhR pathway. Both the receptors reside in the cytoplasm in the absence of the respective ligands and, upon their binding, they undergo conformational changes which lead to nuclear translocation. Inside the nucleus, the GR homodimerises and the dimer binds to the recognized enhancer elements, activating the transcription of the target genes (192). The similar mechanism of action with the AhR and especially the presence of TPR-containing proteins as GR regulators, prompted different groups to test whether AIP is part of the GR complex.

The first studies by Carver *et al.*, conducted by a Y2H screening (104) and by co-IP experiments in yeast (108), demonstrated that AIP does not interact with the GR complex. However, subsequently co-IP assays in a mammalian cell line showed that this interaction occurs via hsp90 (107). The effect of AIP on the GR signalling is inhibitory due to a delayed nuclear accumulation of GR after ligand binding, with subsequent decrease of GR's transcriptional activity (107;126). A similar situation has occurred with FKBP51, which was found not to be associated with GR in yeast but was associated in mammalian cells. A possible explanation could be the lack of other TPR domain protein partners of the receptor resulting in suboptimal activity in yeast (107).

Apart from the GR, some evidences suggest the potential of AIP to interact with other steroid hormone receptors. In particular, AIP has recently been shown to strongly inhibit the transcriptional activity of the receptors for progesterone (PR) and androgen (AR) (126).

- *PPARα*

The peroxisome proliferator-activated receptor α (PPARα, MIM# 170998) is a soluble transcription factor belonging, as the GR, to the nuclear receptor superfamily. PPARα can be activated by different lipophilic compounds, and in turn it associates with the retinoid X receptor α (RXRα). This heterodimer activates the

transcription of several genes encoding enzymes involved in the lipid and lipoprotein metabolism (193).

By co-IP experiments using an antibody highly specific for the PPARα isoform, therefore not binding to the other PPARs subtypes PPARβ and PPARγ, the mouse PPARα was found to form a complex with AIP and hsp90 in the liver cytosol. However, since PPARα is predominantly nuclear, the authors hypothesized that this complex could exist as well in the nucleus (194). Similarly to the inhibition exerted on the transcriptional activity of the HBV X protein and GR (103;107), AIP was found to repress PPARα activity when overexpressed (194). However, the normally low expression levels of AIP in the liver in contrast to the high PPARα expression, suggest that the inhibitory effect of AIP is very weak or not explicated at all in physiological conditions.

- *TRβ1*

Thyroid hormone receptors (TRs) mediate the genomic actions of the thyroid hormone triiodothyronine (T_3). TRs are nuclear receptors derived from two genes, *THRA* and *THRB*. The *THRB* (MIM# 190160) gene encodes three isoforms, β1, β2, and β3 (195). TRβ1 is involved in the negative feedback of T_3 on TRH production in the paraventricular nucleus (PVN) and mediates the T_3-independent activation of TRH transcription. Since the mechanism by which TRβ1 exerts this activating role was unknown, Froidevaux *et al.* (196) decided to look for TRβ1 interacting proteins. By using a Y2H assay to screen a mouse PVN cDNA, AIP was identified as a new TRβ1 partner. More specifically, AIP and TRβ1 co-localised in the same neurons in the PVN, giving thus to this interaction a functional significance in the regulation of TRH activation. The AIP-TRβ1 interaction was demonstrated to be very specific both in yeast and in a mammalian cell line, since no other TR isoforms interacted with AIP. However, while in yeast the strength of the complex was T_3 dependent, in mammals the interaction was still happening in the absence of T_3, although the interaction was weaker. As it could be expected, AIP binds to TRβ1 via the TPR domain, since its deletion causes the loss of the interaction. AIP, however, does not change the subcellular localisation of TRβ1, regardless of the presence of the ligand T3. Finally, an *in vitro* small inhibitory RNA (siRNA) experiment demonstrated that the stability of the TRβ1 receptor was compromised by AIP knockdown. This finding was also

integrated by *in vivo* siRNA studies showing that AIP is indispensable for the T_3-independent TRβ1 activation of TRH transcription but not for the T_3-dependent repression.

1.5.2.6 Transmembrane receptors

- *RET*

The rearranged during transfection (*RET*, MIM# 164761) proto-oncogene encodes a transmembrane tyrosine kinase receptor involved in the development, maturation and survival-controlling functions of epithelial, neuronal and several neuroendocrine cells (197). RET has been shown to be expressed in two major splicing isoforms that differ at the C-terminal end: a long isoform of 1114 amino acids, termed RET51, and a short isoform, 1072 amino acid long, named RET9 (198). Structurally, RET can be divided into three domains: a large extracellular domain that includes a cadherin-like and a cysteine-rich region, a transmembrane domain, and an intracellular tyrosine kinase domain (197). In the presence of the ligand RET activates and in turn triggers various signal transduction pathways which ultimately promote survival, growth and extension/migration of cells, whereas in its absence it releases an intracellular fragment which induce apoptosis (199). RET activating mutations have been associated with the disorders MEN2A and MEN2B, familial medullary thyroid carcinoma (MTC, MIM# 155240), and RET inactivation mutations with Hirschsprung disease (MIM# 142623). None of these diseases are associated with pituitary adenomas and no RET mutations have been identified in FIPA families (197;200;201).

In order to identify novel signalling pathways induced by RET51, Vargiolu *et al.* (201) used the new split-ubiquitin Y2H assay (202) to screen a human fetal cDNA library. Among the 10 clones identified one corresponded to AIP. The AIP-RET interaction was subsequently validated by a co-IP assay and was also shown to occur with both RET isoforms. Moreover, the AIP-RET complex was demonstrated to be present in cells expressing endogenously both proteins and also *in vivo* in the rat pituitary gland tissue. The region of RET involved in the interaction was mapped between residues 707-999, a region common to both isoforms located within the intracellular proapoptotic fragment.

RET was also demonstrated to interfere with AIP-survivin interaction (201).

- *EGFR*

The epidermal growth factor receptor (EGFR, MIM# 131550) is a transmembrane glycoprotein which is is required for normal cellular proliferation, survival, adhesion, migration, and differentiation (203). EGFR interacts with a wide range of proteins, among which AIP was reported (204). AIP was identified in a large-scale MYTH screen, a split-ubiquitin based membrane Y2H assay which allows the systematic analysis of full-lenght membrane protein interactions in a cellular environment (205). However, this interaction was not subjected to further confirmations employing different techniques and thus, given the high rate of false positives in Y2H analysis (206), it cannot be considered certain.

1.5.2.7 G proteins

G proteins are heterotrimeric GTP-binding proteins formed by α, β and γ subunits (Gα, Gβ and Gγ), which mediates receptor-stimulated signalling pathways. Gα subunits are typically divided into four families: $G\alpha_s$, $G\alpha_i$/$G\alpha_o$, $G\alpha_q$/$G\alpha_{11}$ and $G\alpha_{12}$/$G\alpha_{13}$. $G\alpha_{13}$, similarly to AIP, is ubiquitously expressed and is an essential gene, since its deletion is embryonic lethal in mice (207).

Nakata *et al.* (208), looking for new $G\alpha_{13}$ interacting proteins, found by a Y2H screening of a mouse fetal brain cDNA that AIP is a binding partner of $G\alpha_{13}$. This interaction was confirmed *in vitro* by a GST pull-down assay and was shown to involve the whole AIP protein sequence. It was also determined that the interaction is independent of the GTP/GDP binding status of the α subunit and that it does not involve the β and γ subunits. The other three types of α subunits were also tested for their ability to interact with AIP, and it was found that the $G\alpha_q$ subunit also binds AIP, although weaker than $G\alpha_{13}$, while $G\alpha_s$ and $G\alpha_i$ do not bind AIP. It is interesting to note that another TPR protein, PP5, also binds $G\alpha_{12}$/$G\alpha_{13}$ (209).

$G\alpha_{13}$ activation was then demonstrated to disturb the AIP-AhR interaction through the destabilisation of the AhR protein via the ubiquitin-proteasome pathway, and was also shown to inhibit the ligand-mediated transcriptional activation of the AhR independently from RhoA binding (RhoA is a small GTP-binding protein that is activated after the interaction with $G\alpha_{13}$). $G\alpha_q$, despite its less tightly interaction with AIP, was also found to exert a strong inhibitory effect on the AhR (208). The

downstream signalling pathways regulated by $G\alpha_{13}$, apart from the activation of RhoA, are not well characterized (207). Since the $G\alpha_{13}$-mediated inhibition of AhR explicates in a RhoA-independent manner, what happens to $G\alpha_{13}$ signalling is at present unknown. However, it is interesting to note that there are some evidences reporting the involvement of the $G\alpha_{13}$ pathway in the regulation of cAMP responses (210;211). Specifically, the synergistic regulation of cAMP synthesis by the $G\alpha_s$ and $G\alpha_{13}$ pathways was shown to be mediated by a specific isoform of adenylyl cyclase, termed AC7 (211).

The AhR dissociation from AIP induced by $G\alpha_{13}$ was shown to cause the translocation of the AhR into the nucleus in a ligand-independent manner. However, the AhR that moves into the nucleus in this way does not form an active complex with ARNT, as also seen for the cAMP-mediated nuclear translocation of the AhR (129). This divergence suggests that the AhR adopts a unique structure in the cytoplasm, and that AhR does not undergo the same conformational change when moving to the nucleus with every nuclear transport-inducer (such as TCDD or $G\alpha_{13}$ or cAMP).

1.5.2.8 TOMM20 and mitochondrial preproteins

TOMM20 is an import receptor which, along with TOMM70 and other proteins, is part of the translocase of the outer membrane of mitochondria (TOMM) protein complex. This complex is involved in the recognition and translocation of the cytosolically synthesized mitochondrial preproteins into the organelle. To be able to cross the mithocondrial membranes the preproteins are maintained in the cytosol in an unfolded translocation-competent conformation by different molecular chaperones (212). Among them, hsp90 and hsc70 have been shown to mediate the import of TOMM70-dependent preproteins (157), whereas AIP was demonstrated to interact with TOMM20 (118). In humans, TOMM20 can be structurally subdivided into five regions: a transmembrane segment at the N-terminus, a linker segment, a TPR motif, a Q-rich region, and a conserved COOH-terminal acidic segment (213). This latter region is not required for preprotein binding but is specifically involved in an electrostatic interaction with the TPR motifs of AIP (118). In particular, an essential role has been found to be played by the very last five amino acids of TOMM20 (EDDVE), a segment similar to those

present in PDE4A5 (EELD, involved in AIP binding) (177) and hsp90 and hsc70 (EEVD, involved in the interaction with various TPRs) (214).
In the same study (118), AIP was also shown to interact with several mithocondrial preproteins. Differently from the AIP-TOMM20 interaction, both the PPIase-like and the TPR regions of AIP are required to bind the presequences or the internal import signals of the preproteins.
AIP was then demonstrated to maintain the loosely folded state of preproteins and to promote their transfer into mitocondria. This finding was confirmed by the demonstration that AIP forms a ternary complex with TOMM20 and the preprotein and by the fact that AIP interacts with preproteins less strongly than with TOMM20. Altogether, these results suggest the following scenario: mitochondrial preproteins may form a large complex in the cytosol with hsc70 and AIP, with both proteins contributing to maintain their unfolded conformation; once the complex has reached the outer membrane of the mitocondrion, AIP binds to TOMM20 and promotes the transfer of the preprotein to the import receptor.

1.5.2.9 Survivin

Survivin is a member of the inhibitor of apoptosis (IAP) gene family, which include evolutionary conserved members that suppress apoptosis by preventing the maturation and/or the proteolytic activity of its effector enzymes, the caspases (215). Survivin, apart from inhibiting apoptosis, is also implicated in other essential cellular functions like the control of cell division and the stress response (216-218). For instance, during harmful environmental stimuli a significant release of survivin takes place from the mitochondria to the cytosol (216) and survivin form complexes with hsp90 (217). Structurally, survivin is a 142 amino acid-long protein which exist as a functional homodimer. The dimerisation is mediated by the N-terminal baculovirus IAP repeat (BIR) domain, which is also involved in the interaction with other proteins, i.e. the caspases and hsp90 (217;219;220). The survivin-AIP interaction, discovered in a proteomics screening by Kang & Altieri (221), is instead mediated by the C-terminal α-helical coiled-coil region, with a key role played by the last residue of the protein. The reciprocal AIP region involved in the binding was mapped between residues 170-330, thus comprising the three TPR motifs. The interaction was demonstrated to be direct and to happen in pull-

down and co-IP experiments. The association of AIP with survivin was shown to stabilise survivin protein levels independently from hsp90 binding (217). Loss of both proteins leads to proteasomal degradation of survivin, resulting in enhanced apoptosis and, only for hsp90, also to cell cycle arrest. The reported association of AIP with TOMM20 (118), leaves room to speculate that AIP could stabilise survivin in the cytoplasm and facilitate its displacement into the mitochondria pool, increasing the reserves of survivin in this compartment readily for subsequent events that involves apoptosis (221). However, since several evidences suggest that *AIP* acts a TSG (87), it is not clear why it stabilises survivin, thereby elevating the cellular anti-apoptotic threshold. To further increasing the level of complexity of the system, the RET protein abolishes the binding of AIP to survivin (201) thus probably promoting apoptosis, a role already documented for RET (199;222). It is thus conceivable that when AIP and RET are co-expressed in the same tissue, RET acts to counteract the AIP-mediated stabilisation of survivin, in order to lower the anti-apoptotic threshold.

1.5.2.10 TNNI3K

In 2003, Zhao *et al.* (223) cloned a new cardiac-specific kinase gene named TNNI3K [cardiac troponin I (cTnI)-interacting kinase], belonging to the MAPKK family. In that study, by a Y2H screening, TNNI3K was found to interact with several proteins including AIP. The interaction with AIP was not further investigated with other techniques.

1.5.3 AIP mutations in FIPA and sporadic pituitary tumours

The first mutations on *AIP* published were from the study of Vierimaa *et al.* (85) in 2006. In that study, a germline inactivating mutation (p.Q14X) was identified in two large FIPA kindreds originating from Northern Finland and in 13% of sporadic acromegalic patients from a population-based cohort from the same geographical area, as a possible consequence of a founder effect. At the same time the p.R304X mutation was reported in an Italian sibling pair with acromegaly (85). Subsequently, nine different novel germline mutations (p.R16H, p.G47_R54del, p.Q142X, p.E174fsX47, p.Q217X, p.Q239X, p.K241E, p.R271W, p.Q285fsX16)

were detected in 11 families in a study consisting of 73 FIPA families from nine countries (88). Of the 167 FIPA families analysed so far for *AIP* mutations, 38 (22%) harbour *AIP* mutations, including 30 IFS families (224). Several studies searched also for *AIP* mutations in sporadic pituitary adenoma patients (68;85;87;94;99;225-230). To date, over 1100 patients have been studied, with 31 individuals having germline *AIP* mutations, giving an estimated prevalence of 2% for all the pituitary patients and 2.7% for patients with acromegaly. Most of the patients with *AIP* mutations in the sporadic cohort have acromegaly: 28 out of the 31 patients have GH-secreting tumours, whereas the other three mutations arised in two Cushing's disease patients and a prolactinoma patient (224). Interestingly, no somatic *AIP* mutations have been found in pituitary adenomas to date (99;225;229;231).

So far, 51 different *AIP* germline variants have been reported in the literature, including nonsense, missense, frameshift, splice site, large deletions, in-frame deletions, an in-frame insertion, and promoter mutations (Figure 1.12 and Appendix 1, Table 3).

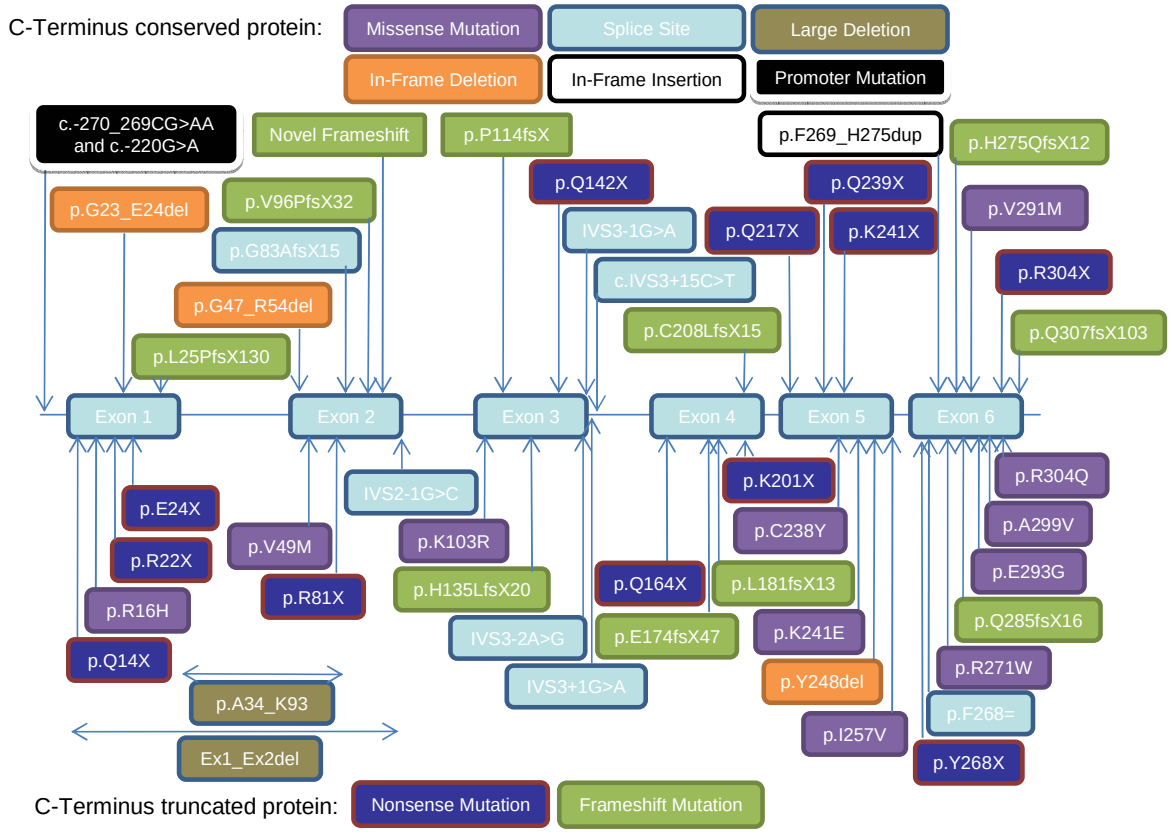

Figure 1.12 Localisation of germline *AIP* variants identified to date.

36 out of 51 variants result in deletion of the C-terminal end of the AIP protein and are scattered throughout the gene, whereas the 11 known missense variants and the in-frame insertion mostly affect the TPR domains or the C-terminal α-helix (87;88). The most common AIP mutation seems to occur at residue 304 (85;87;88;94;97;100;228). Other potential hot-spots involve codons 81 (87;232), 241 (71), and 271 (88;233).

1.5.4 AIP mutations in other tumours

In a subset of *AIP* mutation-positive FIPA families concomitant non-pituitary endocrine tumours, including thyroid, adrenal and MEN1-related tumours, have been reported (94;228;232). As mentioned earlier, a common feature of pituitary, thyroid and also adrenal tumours is the disruption of the cAMP signalling pathway. Since AIP is potentially implicated in this pathway through interactions with PDE2A3, PDE4A5 and the AhR, it is conceivable to hypothesize that mutations in this gene might also predispose to other endocrine tumours. Furthermore, the ubiquitous expression of AIP argue in favour of this hypothesis. Interestingly, previous genetic studies in adrenocortical tumorigenesis have also strongly suggested the existence of an as yet unidentified TSG at 11q13 (234-236).

So far, two studies performed a screening for somatic *AIP* mutations in endocrine tumours other than pituitary adenomas. The first study analysed 79 sporadic tumours of the endocrine system, including thyroid, adrenal and parathyroid lesions, carcinoids and adenocarcinoids, paragangliomas, and pancreatic endocrine tumours, but no somatic *AIP* mutations were found (229). In the second study, the index case of a homogeneous *AIP* mutation-positive FIPA family presenting also with an adrenocortical carcinoma and a grade II B-cell non-Hodgkin's lymphoma, was analysed for somatic *AIP* mutations in the extra-pituitary tumours. The analysis of the tumoral DNA revealed that the *AIP* wt allele was lost in the adrenocortical carcinoma, whereas no evidence of LOH was observed in the B-cell lymphoma. The finding of *AIP* inactivation in the adrenocortical tumour suggests a potential role of this gene in those tumours in which the cAMP and the 11q13 locus are implicated (232). Very recently, this was indeed demonstrated in hibernomas, benign neoplasms which consistently display cytogenetic rearrangements involving chromosome band 11q13. These

aberrations were demonstrated to be associated with concomitant deletions of *AIP* and *MEN1* (237).

Many genes involved in hereditary cancer syndromes are also somatically mutated in tumours that are not significantly related to the respective syndromes (238-241). Hence, to characterize the possible contribution of somatic *AIP* mutations to the development of common tumours, Georgitsi *et al.* (231) performed a mutation analysis in a series of colorectal, breast and prostate cancer samples. The authors found only a heterozygous variant (p.R16H) in 2 colorectal tumours. However, the same change was later found by the same group in a healthy control, suggesting it is a rare polymorphism (94). These results suggest that *AIP* does not seem to be involved in the initiation or progression of colorectal, breast and prostate cancer (231).

1.5.5 AIP expression in sporadic pituitary tumours

As reported in section 1.5.3, *AIP* mutations do not seem to play a role in the pathogenesis of sporadic tumours. However, in sporadic somatotroph adenomas, which arise from a cell type normally expressing AIP, lower AIP expression was seen in aggressive tumours (145;242). On the contrary, expression of AIP was shown to be consistently higher in NFPAs, a tumour type arising from gonadotroph cells which normally do not express AIP (87;145;242). In addition, while in both normal and adenomatous somatotroph cells AIP is located in the secretory vesicles, the aberrantly expressed AIP in NFPAs (of gonadotroph cell origin) and corticotroph adenomas has a different localisation in the cytoplasm (87). This suggests that the regulation of AIP is different in somatotroph and other cell types. The consequences of the aberrant localisation of AIP in non-GH-secreting adenomas as well as of its abnormal expression, independent of germline mutations, is at present unknown.

1.6 CDKN1B

1.6.1 *CDKN1B* functions and regulation

The CDKN1B gene is located on chromosome 12q13 and consists of 3 exons encoding a 198 amino acid protein known as $p27^{Kip1}$. In quiescent cells, $p27^{Kip1}$ accumulates in the nucleus where it controls the progression from the G1 to S phase of the cell cycle by binding to and inhibiting the activity of cyclinE/ and cyclinA/Cdk2 complexes (Figure 1.4) (243). In addition, $p27^{Kip1}$ is involved in cell migration, cell proliferation, neuronal differentiation and apoptosis (244-246). Moreover, it has been demonstrated that $p27^{Kip1}$ has a pro-oncogenic effect when it cannot bind to cyclin/Cdk complexes (247). The activity of $p27^{Kip1}$ is tightly regulated at transcriptional (248;249), translational (250;251) and post-translational levels. The latter mechanism is the best characterized and involves proteolysis via the ubiquitin-proteasome pathway (252) and interaction with two miRNAs (253). Interestingly, it has been shown that $p27^{Kip1}$ is a transcriptional direct target of menin (254) and the AhR (255), and a possible downstream target of RET in endocrine cells (256).

1.6.2 Roles of *CDKN1B* in pituitary tumorigenesis

A drastic reduction of $p27^{Kip1}$ expression has been observed in almost 50% of all human cancers (257;258). Consistent with that finding, lack of functional $p27^{Kip1}$ promotes tumour formation in several animal models (24;259;260), supporting a TSG role for $p27^{Kip1}$ (257;261). However, $p27^{Kip1}$ was only rarely found mutated or lost in human tumours (262-265), suggesting that its downregulation is mainly due to post-translational mechanisms rather than genetic alterations.

As detected in other tumour types, a significant reduction of $p27^{Kip1}$ protein expression levels, but not mRNA levels, is commonly observed in all subtypes of pituitary tumours compared to normal pituitary tissue, while $p27^{Kip1}$ is completely absent in corticotropinomas and pituitary carcinomas (266-270). However, similarly to that reported for several non-endocrine tumours, no somatic mutations in $p27^{Kip1}$ were found (271-274). Thus, these findings suggest a contribution of $p27^{Kip1}$ in the development of human sporadic pituitary adenoma by post-translational mechanisms (66).

Following the discovery that *CDKN1B* is a tumour susceptibility gene for multiple endocrine tumours, six germline mutations have been identified in MEN1-like patients (Appendix 1, Table 1). The *in vitro* functional studies performed on five of these changes demonstrated that they affect either the localisation, the stability or the binding abilities of $p27^{Kip1}$ (62;63;65).

2 Aims of the study

The overall aim of the present investigation was to study some of the tumorigenic mechanisms involved in pituitary adenoma formation.

The more specific objectives were:

1) To assess the prevalence of germline point mutations and gross rearrangements in the *AIP* and *CDKN1B* genes in a large serie of sporadic Italian acromegaly patients and in some Italian FIPA families (Study I).

2) After the identification of the *AIP* p.R304X mutation in a FIPA family, to evaluate if it shares a common ancestor with other two independent Italian FIPA families harbouring the same mutation (Study II).

3) To investigate the biological functions and the involvement in the pathogenesis of sporadic pituitary adenomas of a specific miRNA, referred to as miR-107. In addition, to investigate if miR-107 is able to interact with AIP (Study III).

4) To investigate the expression of AHRR, a molecule which participates in one of the AIP-related pathways potentially involved in pituitary tumorigenesis, in a cohort of GH-secreting adenomas (Study IV).

3 Materials and Methods

3.1 Subjects

3.1.1 Pituitary adenoma patients

Diagnosis and management of pituitary disease were established for each patient by physicians at each referring center following international criteria (13;275). The diagnosis of acromegaly was established with GH levels failing to drop below 1 mg/l after a standard glucose tolerance test or mean of seven samples above 2.5 mg/l, high insulin-like growth factor 1 (IGF-1) levels for age- and sex-related reference range, and radiological evidence of pituitary adenoma. Local ethical committees from each referring center approved the study, and all subjects gave written informed consent.

3.1.1.1 Sporadic patients (Studies I, III, IV)

- Study I

The survey sample of this study consisted of blood-extracted DNA samples from 131 Italian acromegalic patients negative for pituitary tumours within their family and therefore considered as apparently sporadic. Patients were recruited at the Endocrinology Division of Padova Hospital/University, at the Verona Hospital, at the Hospital/University of Udine, at S. Chiara Hospital in Trento, and at the Division of Endocrinology and Metabolism Diseases of the Ancona Hospital. 43% of patients were men, the mean age at diagnosis was 44±13 years (range 16–76 years), and in 89% of cases they presented a macroadenoma; 75% of patients underwent transsphenoidal surgery and 22% received pituitary radiotherapy.

- Study III, IV

Overall, 62 human pituitary tissue samples were analysed. This cohort consisted of: a) 34 (11+23) GH-secreting tumours; b) four GH+PRL-secreting adenomas; c) 24 NFPAs. Patients were recruited at St. Bartholomew's Hospital of London (Study III) and at the Endocrinology Division of Padova Hospital/University and the Pituitary Unit, Department of Neurosurgery San Raffaele Hospital in Milan (Study

IV). The tumour specimens were collected fresh during transsphenoidal surgery and were immediately frozen in liquid nitrogen and then stored at -80 ^{o}C until use.

3.1.1.2 FIPA families (Studies I, II)

- Study I

The survey sample consisted of six Italian FIPA families recruited at at the Endocrinology Division of Padova Hospital/University. Four FIPA families were homogeneous for PRL-secreting pituitary tumours and two were heterogeneous with PRL/NFPA tumours (pedigrees in Appendix 2, Figure 1). Mutations in the *MEN1* and *PRKAR1A* genes have been excluded in all patients.

- Study II

An heterogeneous two generations FIPA family (hereafter referred to as Family 1) presenting with a GH- and a PRL-secreting pituitary adenoma was recruited at the Endocrinology Unit in Padova, and a familial screening was proposed (pedigree in Results, Figure 4.5). After an *AIP* p.R304X mutation was recognized in both patients, three additional mutations carriers were identified. The two previously reported *AIP* p.R304X Italian FIPA families (85;88) were referred by the Neuromed Institute of Pozzilli (Family 2, pedigree in Results, Figure 4.7) and the Hospital of Treviso [Family 3, pedigree in (276)], respectively. Most individual characteristics of these patients were previously reported in details (88;276;277).

3.1.2 Healthy controls (Studies I, III, IV)

All subjects gave written informed consent.

- Study I

Blood-extracted DNA samples from 250 healthy, anonymous, unrelated individuals were available.

- Studies III, IV

A total of 20 normal pituitary (NP) tissues from autopsy were analysed.

3.2 Nucleic acids extraction and quantification

3.2.1 DNA extraction (Studies I, II)

- Study I

Whole blood from patients and control individuals was collected in tubes containing K_2EDTA. Genomic DNA was extracted using the QIAcube extractor (Qiagen, Milan, Italy) following the manufacturer's instructions. Briefly, the procedure consists of five steps: lysis of erythrocytes and isolation of lymphocytes, lysis of proteins with proteinase K, adsorption to a silica membrane, removal of residual contaminants and elution of pure DNA. DNA concentration was measured as described in section 2.2.3 and stored at 4^{o}C.

- Study II

Tumour DNA was extracted using the Trizol reagent (Invitrogen, Milan, Italy) following a modified protocol (http://www.mrcgene.com/tri.htm). Trizol is a ready-to-use reagent for the isolation of RNA, DNA and proteins from cells and tissues. During sample lysis, the reagent, a mono-phasic solution of phenol and guanidine isothiocyanate, maintains the integrity of the RNA, while disrupting cells and dissolving cell components. Addition of chloroform followed by centrifugation separates the solution into an aqueous phase containing RNA and an organic phase containing DNA and proteins. After removal of the aqueous phase, the DNA and proteins in the samples can be recovered by sequential precipitation. Precipitation with ethanol yields DNA from the interphase.

3.2.2 RNA extraction (Studies III,IV)

Total RNA was extracted from cells and tissues using the Rneasy Mini Kit (Qiagen) following the manufacturer's instructions. Briefly, biological samples were first lysed and homogenized in the presence of a highly denaturing guanidine-thiocyanate–containing buffer, which immediately inactivates RNases. An additional on-comun Dnase treatment was also performed to ensure high purification of intact RNA. Subsequently, ethanol was added to provide appropriate binding conditions, and the samples were then applied to a spin column, where the total RNA binds to the membrane and contaminants are efficiently washed away.

RNA concentration was measured as described in section 2.2.3 and stored at -20^{o}C.

3.2.3 Determination of nucleic acids concentration and purity

The concentration and purity of the isolated DNA and RNA were determined spectrophotometrically in a Nanodrop Spectrophotometer ND 1000 (Thermo Scientific, USA). This technique enables higly accurate UV analyses microvolume samples with remarkable reproducibility. The concentration of DNA in a given sample is automatically calculated by the NanoDrop software using the formula: A_{260} × 50 µg/ml x dilution factor, whereas the concentration of RNA is calculated by using the formula: A_{260} x 44 µg/ml x dilution factor. The purity of the nucleic acids is determined by the A_{260}/A_{280} ratio. A ratio of 1.8-2.0 indicated little or no protein contamination.

3.2.4 Determination of RNA integrity

RNA integrity was measured by Agilent Bioanalyzer 2100 System (Agilent Techonologies). This is an essential procedure in order to yield accurate quantification of RNA expression by qRT-PCR. The RNA was analysed with the RNA 6000 Nano Assay chip associated with the instrument, which allows a quick caracterization of total RNA using microvolume samples. The total RNA concentration and the amount of ribosomal impurities (18S/28S ratio) were automatically calculated by the Agilent Bioanalyzer software (Figure 3.1). Only samples with a 18S/28S ratio>1 were considered for qRT-PCR analyses.

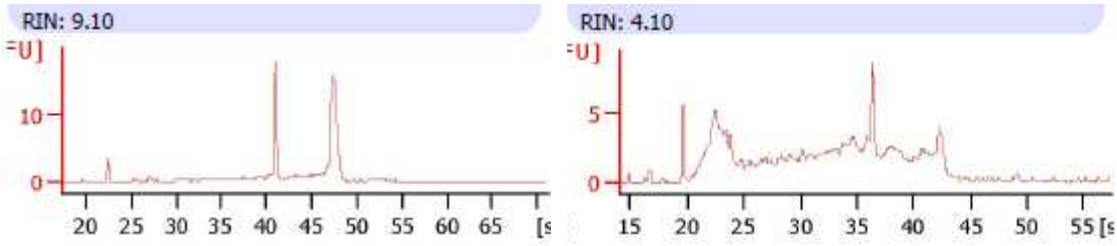

Figure 3.1 Example of chromatograms of micro-capillary electrophoresis from RNA samples showing different degrees of degradation. A) A typical electropherogram of high-quality RNA include a clearly visible 18S/28S rRNA peak ratio and a small 5S RNA. B) A partially degraded sample was indicated by a shift in the electropherogram to shorter fragment sizes and produce a decrease in fluorescence signal as dye intercalation sites are destroyed.

3.3 Polymerase chain reaction (PCR) and DNA sequencing (Studies I, II, III)

PCR reactions were usually performed according to the following conditions:

Master Mix (for a single sample)	Final concentration
DNA	25-50 ng
dNTPs	0,8 mM
10X Buffer	1X
$MgCl_2$	1,5 mM
Primers	0,4 µM
Taq Gold	0,4 U
ddH_2O	to final volume
Final Volume: 12,5 µl	

Enzyme activation	94℃	10’	
Denaturation	94℃	30”	X 35 cycles
Annealing	60℃	30”	
Extension	72℃	30”	
Final extension	72℃	5’	
Hold	4℃	∞	

This basic protocol was modified depending on the DNA sample (blood- or tissue-extracted DNA), the primers annealing temperatures, and the amplification outcome of the template. In some cases the use of different Taq polymerases and/or the addition of dimethyl sulfoxide (DMSO, ≤8%v/v) to favour the stretching of DNA filaments was necessary. For primer design, genomic sequences were retrieved from the University of California Santa Cruz (UCSC) Genome Browser (http://genome.ucsc.edu/cgi-bin/hgGateway, version February 2009) and primers were designed by the use of the publicly available software Primer3 (http://frodo.wi.mit.edu/primer3/input.htm) and Primer Express v3.0 (Applied Biosystems, Monza, Italy). All primer sequences used in this study are provided in Appendix 2. To assess the successful outcome of each reaction and the absence of contaminations, PCR products were run on 1-2% agarose gels stained with ethidium bromide.

3.3.1 Enzimatic purification of PCR products and DNA sequencing

PCR products were purified by ExoSAP-IT (USB Corporation, Cleveland, OH), according to the manufacturer’s instructions. This solution is a mixture of two

hydrolytic enzymes: Exonuclease I, which removes residual primer oligonucleotides, and Shrimp Alkaline Phosphatase, which removes unincorporated dNTPs.

DNA sequencing was performed using the BigDye 3.1 Termination Chemistry (Applied Biosystems) on an ABI 3730XL DNA sequencer (Applied Biosystems). This methodology uses fluorescent dyes attached to terminating dideoxynucleoside triphosphates (ddNTPs) and the DNA fragments are electrophoretically resolved. Each PCR product was sequenced in separate reactions with the forward and reverse primers. Sequencing chromatograms were visualized using the Chromas software (Technelysium Pty Ltd) and aligned to the wt reference sequence(s) using the Seqman Pro software (DNAStar, Madison, WI). All mutations and variants have been annotated according to the nomenclature for human genomic sequence variations of the Human Genome Variation Society (www.hgvs.org/mutnomen).

3.4 Detection of *AIP* and *CDKN1B* germline variants (Study I, II)

3.4.1 Point mutations

The whole coding region, intron–exon boundaries, and 5'- and 3'-UTRs of the *AIP* and *CDKN1B* genes were PCR-amplified and directly sequenced as described in the previous section. Previously unreported nucleotide changes in both genes and the already described *AIP* c.911G>A and *CDKN1B* c.426G>A variants were screened in healthy, anonymous, unrelated individuals by Tetra-primer ARMS-PCR (278) or, in the case of *AIP* IVS3+1G>A, by enzymatic digestion using MboII. The Tetra-primer ARMS-PCR system employs two primer pairs (termed outer and inner) to amplify, respectively, the two different alleles of a variant in a single PCR reaction (Figure 3.2).

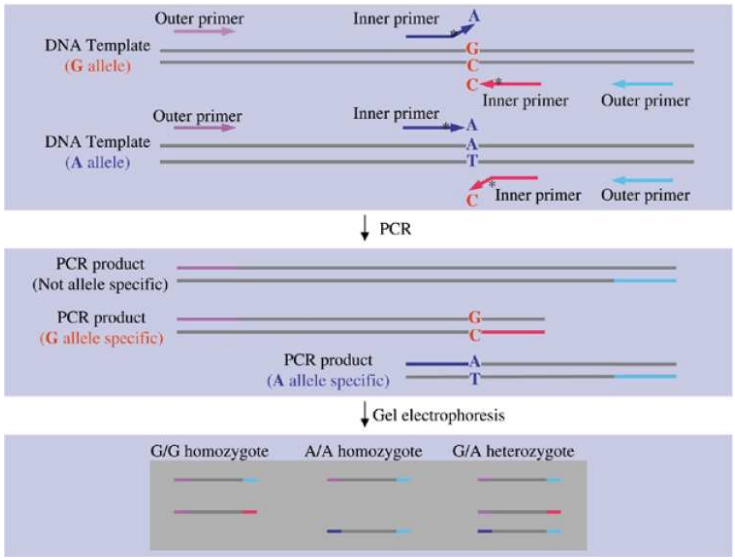

Figure 3.2 Schematic representation of the Tetra-primer ARMS-PCR method. The single nucleotide polymorphism used here as an example is a G→A substitution, but the method can be used to type other types of single base substitutions. Two allele-specific amplicons are generated using two pairs of primers, one pair (indicated by pink and red arrows, respectively) producing an amplicon representing the G allele and the other pair (indicated by indigo and blue arrows, respectively) producing an amplicon representing the A allele. By positioning the two outer primers at different distances from the target nucleotide, the two allele-specific amplicons differ in length, allowing them to be discriminated by gel electrophoresis. Adapted from (278).

3.4.2 Deletion analysis

3.4.2.1 AIP

Large rearrangements at *AIP* locus were evaluated using the SALSA multiplex ligation-dependent probe amplification (MLPA) assay (MRC-Holland, Amsterdam, The Netherlands), following the manufacturer's protocol. PCR products were run on an ABI 3730XL DNA sequencer (Applied Biosystems). Initially, electropherograms were visualized with GeneMarker v1.4 software (Softgenetics LLC, State College, PA), then data were exported as an Excel-compatible format using Peak Scanner v1.0 software (Applied Biosystems) (Figure 3.3).

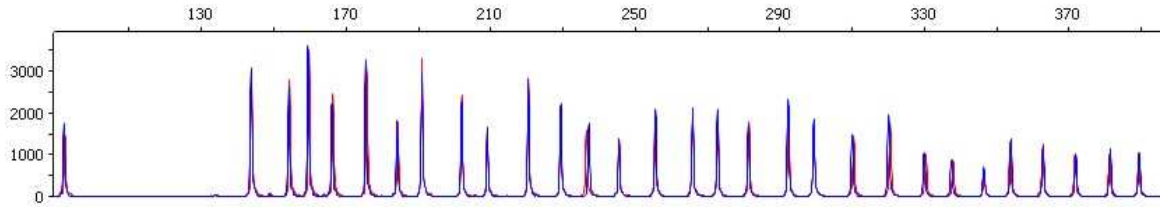

Figure 3.3 Electropherograms profiles generated by the Peak Scanner software. Each peak represents a different probe. Electropherograms from a control (in red) and a patient (in blue) were superimposed. For every peak, an area reduction to 0.5 compared with a control indicates a heterozygous deletion of the corresponding exon(s), whereas exonic duplications result in a 1.5-fold increase in this value.

Final gene dosage analysis was assessed for each patient by calculating a dosage quotient (DQ) with Coffalyser v6.0 software (MRC-Holland). Probes with a DQ less than 0.65–0.7 (for deletions) or higher than 1.3–1.35 (for amplifications) were examined for consistency by repeated testing.

3.4.2.2 CDKN1B

CDKN1B gene dosage alteration was assessed by the quantitative multiplex PCR of short fluorescent fragments (QMPSFs) and by long-range PCR (LR-PCR). For QMPSF, six short genomic fragments (115-276 bp) were simultaneously amplified in a single multiplex PCR with one primer from each pair 5'-labeled with 6-FAM fluorochrome using the Multiplex PCR Master Mix 2X and the Q-solution (Qiagen). Primers shared common melting temperatures of between 58 and 60 ℃ and no primer covered polymorphic regions (Appendix 2, Table 3). Samples underwent 24 amplification cycles, which ensured that the reaction ended during the exponential phase. An amplicon from a genomic region (19q13.3), whose deletion was not expected, was included as negative control. The amplified DNA fragments were then separated on an ABI 3730XL DNA sequencer (Applied Biosystems) and analysed using Peak Scanner software v1.0 (Applied Biosystems). Two different methods of comparison were used to calculate allele dosage: visual sample-to-control and numerical sample-to-control (279). For every peak, an area reduction to 0.4–0.6 compared with a control indicates a heterozygous deletion of the corresponding exon(s), whereas exonic duplications result in a 1.5-fold increase in this value.

LR-PCR on genomic DNA was used as an additional technique to detect rearrangements not detectable by QMPSF. Briefly, exons 1 and 3 were amplified using, for each exon, the most external primers employed in sequencing analysis (Figure 3.4).

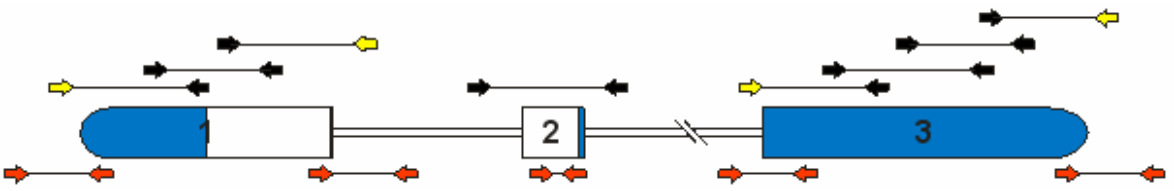

Figure 3.4 Location of primers used for *CDKN1B* analysis. In red, primers employed in QMPSF; in yellow, primers used in LR-PCR; in black, primers used in the sequencing analysis. Boxes represent exons.

3.5 LOH analysis (Study II)

A tumour sample obtained from the proband of family 1 was available. After DNA extraction, LOH was studied by *AIP* sequencing at the corresponding mutation position as described in section 2.4.1, and by analysis of informative microsatellite markers flanking the *AIP* gene as described in section 3.6. LOH on tumour-derived DNA was assessed by visual observation of the sequence chromatograms by comparing the peak heights/areas between the wt and mutant allele. Allelic loss was concluded when the wt allele was either completely invisible or significantly reduced when compared to the mutant allele. LOH was confirmed when the marker alleles segregating with the affected haplotype were retained, whereas the corresponding wt alleles were significantly reduced or lost.

3.6 Haplotype analysis (Study II)

Available members of families 1 and 2, and family 3's proband, were genotyped using 12 microsatellite markers surrounding both *AIP* and *MEN1* genes, and one single nucleotide polymorphism (SNP, rs4084113) located in intron 3 of *AIP*. Primer sequences for genetic markers were obtained from the UCSC Genome Browser website (http://genome.ucsc.edu/) and a previous publication (85) or were designed with Primer3. An additional tandem repeat was identified by Tandem Repeat Finder (http://tandem.bu.edu/trf/trf.html) (Appendix 2, Table 4). Markers were PCR-amplified from genomic DNA, separated on an ABI 3730XL DNA sequencer, and analysed with Peak Scanner v1.0 software (Applied Biosystems). For eight markers, the CEPH 1347-2 control was included to standardize allele sizes. For SNP genotyping, direct sequencing of *AIP* intron 3 was performed.

3.7 Reverse Transcription and Real-Time PCR (qRT-PCR) (Studies III, IV)

Total RNA was reverse transcribed (RT) into cDNA using the SuperScript® III Reverse Transcriptase Kit (Invitrogen) according to the manufacturer's protocol. First-strand cDNA was synthesized using 1 µg of RNA for each sample and employing random examers as primers. A RT-PCR reaction mix without the

reverse transcriptase enzyme was included in each experiment as a control for gDNA contamination. The exclusion of gDNA contamination from each sample were usually verified by PCR for the glyceraldehydes-3-phosphate dehydrogenase (GAPDH) gene. The cDNA samples were stored at -20℃ .

qRT-PCR is a combination of two steps: (1) the amplification of the cDNA using the PCR and (2) the detection and quantification of amplification products in real time by using fluorescent reporter dyes. The assay relies on measuring the increase in fluorescent signal, which is proportional to the amount of DNA produced during each PCR cycle. Furthermore, the use of probes labeled with different reporter dyes allows the detection and quantification of multiple target genes in a single (multiplex) reaction. Individual reactions are characterized by the PCR cycle at which fluorescence first rises above a threshold background fluorescence, a parameter known as the threshold cycle (Ct). The more target there is in the starting material, the lower the Ct (Figure 3.5). This correlation between fluorescence and amount of amplified product allows accurate quantification of target molecules over a wide dynamic range, while retaining the sensitivity and specificity of conventional end-point PCR assays.

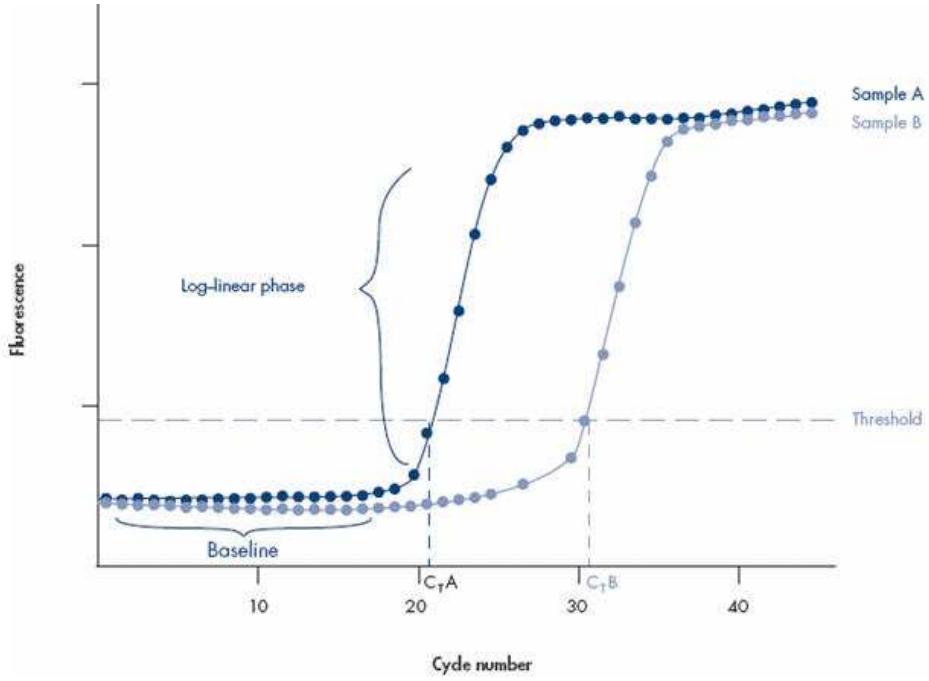

Figure 3.5 Amplification plot. The baseline region is automatically set up by the software and allows the exclusion of the intrinsic fluorescence of the reporter. An amplification threshold is set within the early exponential phase. The cycle number at which the amplification curves cross this threshold is the Ct of the samples. Adapted from the Qiagen website.

In this study gene expression assays were performed using the TaqMan® qRT-PCR system (Applied Biosystems). The assays consist in the quantification of a gene of interest using a mix of unlabeled PCR primers and a TaqMan probe (Figure 3.6).

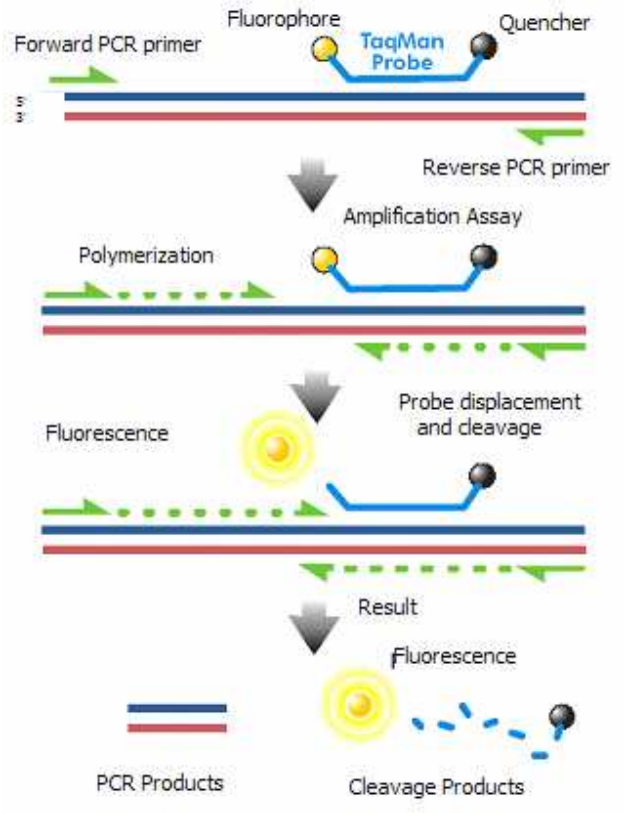

Figure 3.6 TaqMan probe chemistry mechanism. The TaqMan probes contain a FAM or VIC dye label and minor groove binder moiety on the 5' end, and a non-fluorescent quencher dye on the 3' end. The probe anneals to the template between the two primers. During the reaction, cleavage of the probe by the AmpliTaqGold DNA polymerase separates the reporter and the quencher dyes, resulting in increased fluorescence of the reporter. The accumulation of PCR products is detected by the increased fluorescence of the reporter dye. Adapted from http://en.wikipedia.org/wiki/TaqMan.

TaqMan reactions were performed as duplex reactions including the gene of interest and an endogenous control (reference gene). In each reaction, each sample was assayed in duplicate or triplicate. A standard curve for the quantification of the samples was also run in parallel with each assay. For the standard curve serial dilutions of 1:5 were made (Figure 3.7).

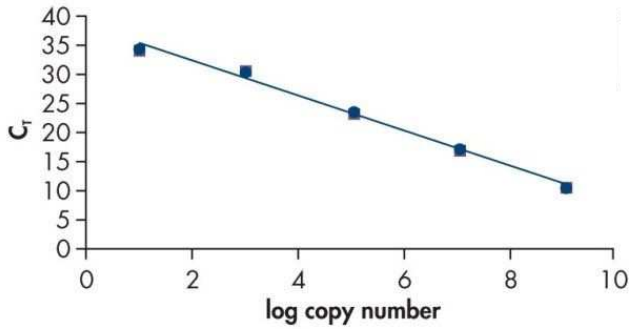

Figure 3.7 Standard curve. A standard curve can be generated using the Ct values from a dilution series of a sample with a known DNA or RNA quantity. The slope of a standard curve is used to estimate the PCR amplification efficiency of each reaction. A standard curve slope of –3.32 indicates a PCR reaction with 100% efficiency. Slopes more negative than –3.32 indicate reactions that are less than 100% efficient, whereas slopes more positive than –3.32 indicate sample quality or pipetting problems. Adapted from the Qiagen website.

Reactions were prepared according to the following conditions:

	Volume for a single sample (µl)
cDNA	5 (2 ng/µl)
2X TaqMan Universal PCR Master Mix	12.5
20X Assay Mix gene of interest (AIP or AHRR) (FAM)	1.25
20X Assay Mix reference gene (GAPDH or 18S) (VIC)	1.25
ddH_2O	5
Total Volume	25

Enzyme activation	95℃	10 min	
Denaturation	95℃	15 sec	} X 40 cycles
Annealing/Extension	60℃	1 min	

The cDNA was amplified in 96- or 384-well plates on a 7900HT Real-Time PCR System (Applied Biosystems). Data were analysed using the SDS v2.3 software (Applied Biosystems). All data were normalised to the expression levels of 18S or GAPDH. The normalisation to an endogenous control was done to correct for sample to sample variations in qRT-PCR efficiency and errors in sample quantification.

3.8 miRNA expression in pituitary tissues (Study III)

3.8.1 TaqMan™ Low Density Array (TLDA)

miR expression profile was analysed using TLDA Human MicroRNA Panel v.2 (Applied Biosystems), following the supplier's protocol. Briefly, 300 ng of total RNA per sample were reverse transcribed using Megaplex RT primer Pool A and B [part number (PN) 4399966, 4399968, Applied Biosystems] up to 380 stem-looped primers per pool and TaqMan MicroRNA Reverse Transcription Kit (PN 4366596). Preamplification was carried out by Megaplex Preamp Primers and TaqMan PreAmp Master Mix. qRT-PCR amplifications were run in TaqMan Human MicroRNA Array A and B (PN 4398965, 4398966) using Megaplex Primer Pools, Human Pools Set v3.0 (PN 4444750) on a 7900HT Real Time PCR System (Applied Biosystems). RNU6B (PN 4373381) was chosen as endogenous control based on supplier Application Note [Endogenous Controls for Real-Time Quantification of miRNA using TaqMan MicroRNA Assays (Applied Biosystems)]. Data were analysed using the $\Delta\Delta C_t$ method.

3.8.2 qRT-PCR

Expression levels of miR-107 (PN 4427975) were further validated by qRT-PCR using the specific TaqMan MicroRNA Assay (Applied Biosystems) according to the manufacturer's instructions. Quantification using the TaqMan MicroRNA Assays was done using a two-step qRT-PCR (Figura 3.8):

1. In the RT step, cDNA was reverse transcribed from total RNA samples using specific miRNA primers from the TaqMan MicroRNA Assay.
2. In the qRT-PCR step, PCR products were amplified from cDNA samples using the TaqMan MicroRNA Assay together with the TaqMan Universal PCR Master Mix.

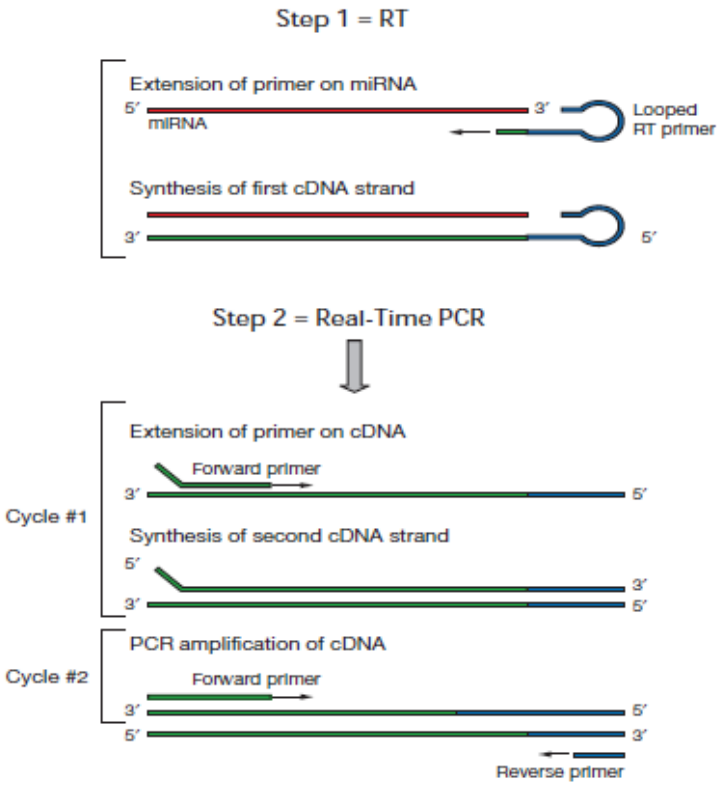

Figura 3.8 Schematic representation of the two-step qRT-PCR. Adapted from the Applied Biosystems website.

Reactions were performed in triplicate in 384-well plates on a 7900HT Real-Time PCR System (Applied Biosystems) using RNU6B as endogenous control. Data were analysed using the standard curve method.

3.9 Cloning (Studies I, III)

The cloning of DNA fragments into a cloning vector was utilised to study the functional implications of an *AIP* sequence variant identified in a sporadic acromegalic patient (Study I) and the interaction between miR-107 and the 3'UTR of *AIP* (Study III).

3.9.1 Minigene construction and *in vitro* splicing analysis (Study I)

To investigate the effect on *AIP* splicing of the novel synonymous variant c.153C>T, a minigene-based strategy was adopted, as suitable mRNA from the proband was not available. The procedure and the plasmid vectors have been

detailed in (280). Genomic DNA of the proband was amplified using primers containing a PstI sequence (Appendix 2, Table 5). The PCR fragment, comprising the 3' half of intron 1, exon 2 and the 5' half of intron 2, was cloned into the PstI restriction site of the pEGFP-N1-COQ2-ASL5-6-7 Vector. The ligation reaction was carried out with T4 DNA ligase (Promega, UK) according to the manufacturer's instructions. 0.4 µg of each wt or mutant minigene constructs were then transfected into $3x10^5$ HeLa cells. After an incubations of 48h, RNA was extracted and reverse transcribed as described in sections 2.2.2 and 2.7. cDNA was amplified with specific primers adjacent to the mutation to be tested.

3.9.2 Construction of 3'UTR reporter plasmid (Study III)

A 931 bp segment of human *AIP*-3'UTR containing the putative miR-107 target sites was PCR-amplified from genomic DNA and cloned into the pGEM®-T Easy Vector (Promega) (Figure 3.9A) using primers containing a XbaI binding site (Appendix 2, Table 5). The XbaI fragment was then subcloned into the pGL3-Control Vector (Promega) (Figure 3.9B), using the XbaI site immediately downstream from the stop codon of the luciferase reporter gene. For the subcloning procedure, the DNA fragment excised from the pGEM®-T Easy Vector was run on an agarose gel and then purificated prior to be ligated in the pGL3-Control Vector. The DNA purification was carried out with the Wizard® SV Gel and PCR Clean-Up System (Promega) according to the manufacturer's instructions.

A

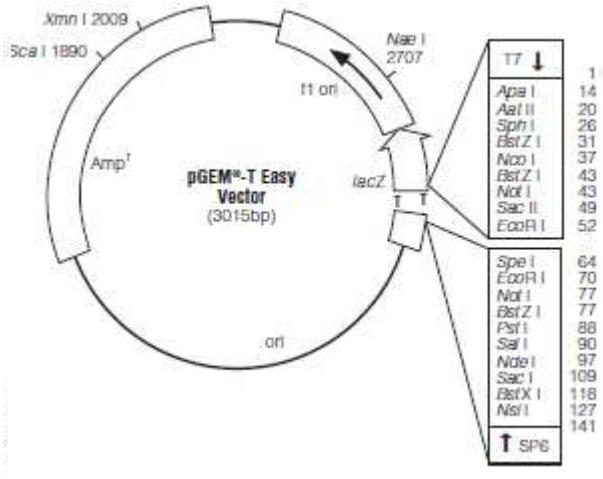

B

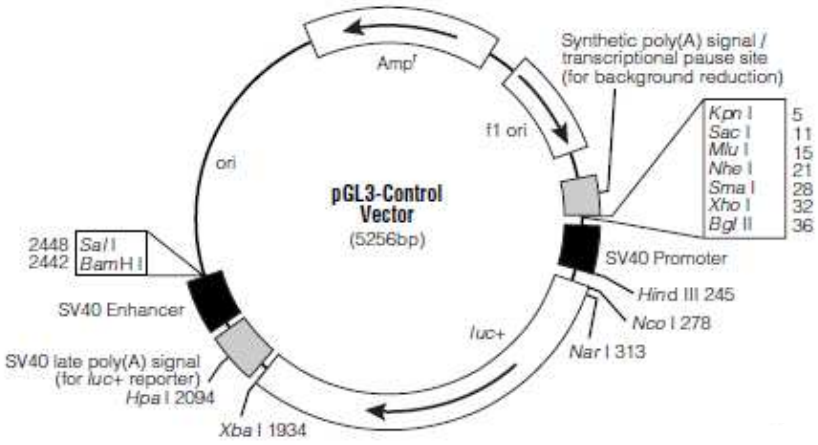

Figure 3.9 A) Schematic structure of the pGEM®-T Easy Vector. The pGEM®-T Easy Vector is a convenient system for the cloning of PCR products. The vector has a 3' terminal T in both ends (T overhangs). These single 3' T overhangs at the insertion site improve the efficiency of ligation of a PCR product into the plasmids by preventing recircularization of the vector and providing a compatible overhang for PCR products with 5′ A overhangs. **B) Schematic structure of the pGL3-Control Vector.** The pGL3-Control Vector is a luciferase reporter vector which allows the quantitative analysis of factors that regulate mammalian expression. Its backbone contains a modified coding region for firefly (*Photinus pyralis*) luciferase that is used for monitoring transcriptional activity in transfected eukaryotic cells.

To examine whether the observed repression of a reporter gene by miR-107 was specifically due to the presence of predicted binding sites in the *AIP*-3'UTR fragment, I also disrupted these sites by site-directed mutagenesis, a technique which allows the introduction of site-specific mutations in double stranded plasmids. For interrupting a perfect "seed" pairing, four nucleotides were deleted from each site of perfect complementarity using the QuikChange XL-site-directed mutagenesis kit (Agilent Technologies). Because there are two predicted binding sites for miR-107 in the *AIP*-3'UTR, three variants were generated, with one of each mutated and both mutated. Wt and mutant inserts were confirmed by sequencing. Mutagenic primers were designed using the Stratagene's QuickChange primer design program. Both oligonucleotides contained the desired mutation and annealed to the same sequence on opposite strands of the plasmid (Appendix 2, Table 6). The QuickChange XL site-directed mutagenesis kit was performed in three steps according to the manufacturer's instructions: synthesis of the mutant strand, digestion of the parental methylated strand that did not contain the mutation with DpnI, transformation of competent cells with plasmid DNA (see next session).

3.9.3 Transformation of competent bacterial cells with plasmid DNA

The high-efficiency JM109 competent cells were transformed with plasmid DNA. Briefly, 50 µl of cells were mixed with 2 µl of each ligation reaction and then heat-shocked for 50 sec at 42℃. 900 µl of SOC medium (Invitrogen) were then added to the ligation reaction transformations and shaked for 1h at 37^{o}C. After incubation, 100 µl of each transformation culture were plated onto LB/agar/ampicillin plates. Plates were incubated overnight at 37^{o}C. Transfromation was successful if the next day colonies were formed because of vector conferring resistance to ampicillin.

3.9.3.1 Small-scale plasmid DNA purification (miniprep)

A single colony from a plate was inoculated in 5 ml of LB medium containing 5 µl of 100 mg/ml ampicilin and shaked overnight at 37^{o}C. The next day plasmid DNA was purified using the QIAprep Spin MiniPrep Kit (Qiagen) following the manufacturer's instructions. The protocol consisted of four steps: preparation and cleaning of the bacterial lysate by alkaline lysis, adsorption of DNA onto a silica membrane in high-salt solution, washing with specific buffers to remove endonucleases and salts, elution of plasmid DNA. The concentration of each sample was determined as described in section 2.2.3. To confirm the integrity of the isolated plasmids a digestion with appropriate restriction enzymes was performed. The plasmids were confirmed to contain the desired mutations by sequencing.

3.9.3.2 Large-scale plasmid DNA purification (midiprep)

After confirming the constructs were correct, higher concentrations of plasmid DNA were obtained using the HighSpeed plasmid Midi Kit (Qiagen) following the manufacturer's instructions. Previous to purification, 100 µl of each plasmid were added to 150 ml of LB medium and 150 µl of ampicilin. Bacterial cultures were shaked overnight at 37^{o}C. The midiprep protocol is based on an alkaline lysis procedure and binding of plasmid DNA to an anion-exchange resin. RNA, proteins and impurities were removed by a salt-wash. The plasmid DNA was eluted in a

high-salt buffer, it was then concentrated and the salt was removed by precipitation in isopropanolol.

3.10 Luciferase gene reporter assay (Study III)

In order to determine whether the *AIP*-3'UTR could confer transcriptional or post-transcriptional control of gene expression and to study the interaction between miR-107 and the wt and mutant *AIP*-3'UTR constructs, the Dual-Luciferase Reporter Assay System (Promega) was utilised. This assay combines two luciferase reporter systems: the firefly (*Photinus pyralis*) and the *Renilla* (*Renilla reniformis*). The protocol was followed according to the manufacturer's instructions. Briefly, GH3 cells were seeded in 6-well plates at a density of $6x10^5$ cells/well. After 24h, cells were co-transfected with Lipofectamine 2000 (Invitrogen) as described in section 2.11.1, using 2 µg of the pGL3-Control Vector and 0.2 µg of the *Renilla* Vector (pRL-CMV). In some experiments, the pre-miR-107 precursor or the scrambled miRNA were co-transfected at a final concentration of 50 nM. 24h post-transfection, transfected cells were lysed with 100 µl of 1X passive lysis buffer (PLB) for 10 min at 4℃. 25 µl of cell lysates were transferred to a 96-well luminometer plate and placed into the Omega luminometer (BMG Labtech). Previous to sample measurement, the injector system was primed with the Luciferase Assay Reagent II (LAR II, containing the substrate for firefly) and the Stop & Glo reagent (containing the substrate for *Renilla*). Firefly and *Renilla* luciferase activities were then measured consecutively. Ratios of firefly versus *Renilla* luminescence signals serve as a measure for reporter activity normalised for transfection efficiency.

3.11 Cell cultures (Studies I, III)

The cell lines used in this study were:

- GH3 cells (Study III)

The rat pituitary GH3 cell line was grown in Dulbecco's Modified Eagle Medium (DMEM) (Sigma-Aldrich, UK) supplemented with 10% Fetal Bovine Serum (FBS)

(Biosera), penicillin (100 IU/ml) and streptomycin (100 mg/ml) (Sigma-Aldrich) in a humidified atmosphere, at 37℃ with 5% CO2.

- SH-SY5Y cells (Study III)

The SH-SY5Y human neuroblastoma cell line was cultured in a 1:1 mixture of DMEM and Ham's F-12 medium (Sigma-Aldrich), supplemented and incubated as above.

- HeLa cells (Study I)

The HeLa human cervical carcinoma cell line was cultured as indicated for the GH3 cells.

3.11.1 Transient transfection of cells

GH3, SH-SY5Y and HeLa cells were transiently transfected with plasmid DNA using the Lipofectamine 2000 transfection reagent (Invitrogen), a cationic lipid formulation that confers high transfection efficiency in a wide variety of cell lines. Transfections were carried out following the manufacturer's protocol. Briefly, cells were plated in normal culture medium without antibiotics. Cells were 60-70% confluent at the time of transfection. DNA and Lipofectamine 2000 were diluted in a suitable volume of Opti-MEM I reduced serum medium (Invitrogen) and incubated at room temperature for 5 min. Then, the diluted DNA was mixed with the diluted Lipofectamine and incubated at room temperature for 25 min, to allow complex formation. The complexes were then added to the wells without removing the media. The plates were incubated for 24, 48 or 72h depending on the experiment.

3.12 Cell proliferation assay (Study III)

Cell proliferation of the transiently transfected GH3 and SH-SY5Y cells was measured using [^{3}H] thymidine incorporation as described in (281).

Briefly, cells were seeded in 24-well plates at 1x10^5 cells/well and after 24h transfected with scrambled miRNA (AM17111, Applied Biosystems) and pre-miR-107 precursor (PM10056, Applied Biosystems) at a final concentration of 50 nM.

48 or 72h after transfection, 2 μCi (curie) of [^{3}H]-thymidine (#NET027Z, Perkin-Elmer) were added to the media in each well, and the plates were incubated for a further 6h at 37℃. After removing the media, 1 ml of scintillant fluid (Amersham) was added to each well and the plates were incubated for 5 min at room temperature. The fluid was collected from each well and transferred into separate scintillation vials. Incorporation of thymidine, in units of counts per minute (CPM), was measured using a scintillation counter (Wallac, Turku, Finland).

3.13 Colony formation assay (Study III)

The aim of this assay was to determine the clonogenic ability of transiently transfected GH3 and SH-SY5Y cells. The clonogenic ability is defined as the % of cells in a population that possess the ability to form individual clones when plated alone in culture. A colony is defined as a group of four or more contiguous cells that are judged by their appearance to have arisen from a single cell.

Briefly, cells were seeded in 6-well plates at 6x10^5 cells/well and after 24h transfected with scrambled miRNA, pre-miR-107 precursor or anti-miR-107 (AM10056, Applied Biosystems) at a final concentration of 50 nM. 24h after transfection, cells were trypsinized and seeded in 6-well culture plates at a density of 1500 cells/well to form colonies. Cells were cultured at 37℃ for 7 days. Colony formation was detected by staining the cells with 3 ml of a 0.1% crystal violet solution. Densitometric quantification of the colony formation density was performed with the Odyssey infrared-imaging system (Li-Cor).

3.14 Protein extraction and quantification (Study III)

Protein extraction from cells and quantification was performed as described in (281). Briefly, cell lysis buffer [Cytobuster protein extraction reagent (Novagen, CN Biosciences)] was added to the cells. After an incubation of 20 min, each well was scraped thoroughly and the cell lysates were transferred to 1.5 ml tubes. After a centrifugation step, the supernatants were stored at -80℃.

The Bradford assay (Bio-Rad, UK) was carried out to ensure the protein concentration of the lysates used for Western Blot was normalised. A set of bovine serum albumin (BSA) dilutions was prepared for the calibration curve. 10 μl of

protein samples and standards were transferred into a 96-well plate and then 200 µl of Bradford reagent were added to each well. After an incubation of 5 min, the plate was inserted on the reader and the absorbance was read at 595 nm.

3.15 Western Blot (Study III)

The variation of protein expression after transfection of cells with miR-107 was determined by Western Blot. 10-30 µg of cell culture-lysates were separated by electrophoresis on pre-cast 12% SDS-PAGE gels (Invitrogen) and transferred onto nitrocellulose membranes (Millipore, Billerica, MA, USA) using semi-dry transferring. After a 90 min incubation with blocking buffer, membranes were incubated overnight at 4℃ with mouse monoclonal AIP antibody (ARA9 [35-2], Novus Biologicals, Littleton, CO, USA) at 1:1000 dilution. GAPDH expression was used as endogenous control. Infrared fluorescent-labelled anti-rabbit or anti-mouse secondary antibodies (IRDye 680 and 800) were used at a 1:10000 dilution. Immunoblot detection and density measurements were performed on the Odyssey infrared-imaging system (Li-Cor, UK).

3.16 Bioinformatic analysis (Studies I, III)

- Study I

The possible impact of novel amino acid substitutions on AIP structure and function has been evaluated by the web tool PolyPhen-2 (http://genetics.bwh.harvard.edu/pph2/). The potential effect on splicing of the previously unreported *AIP* variants IVS3+1G>A and c.153C>T was tested *in silico* using Alamut (http://www.interactive-biosoftware.com/alamut.html), a mutation interpretation software integrating the results of four different algorithms (SpliceSiteFinder, MaxEntScan, NNSPLICE, GeneSplicer).

For protein alignments, the human AIP protein sequence and its homologues in other species were retrieved from the UCSC Genome Bioinformatics database and from the Ensembl Genome Browser (http://www.ensembl.org/index.html, version 60, November 2010). Multiple sequence alignment was performed using the ClustalW tool (http://www.ebi.ac.uk/Tools/clustalw).

- Study III

The analysis of miR-107 predicted target genes was done using seven different algorithms: TargetScan v5.1 (http://www.targetscan.org/) (282), microCosm Targets v5.0 (http://www.ebi.ac.uk/enright-srv/microcosm/htdocs/targets/v5/) (283), MicroTar (http://tiger.dbs.nus.edu.sg/microtar/) (284), FindTar v2.0 (http://bio.sz.tsinghua.edu.cn/findtar/) (30), PITA (http://genie.weizmann.ac.il/pubs/mir07/mir07_prediction.html) (285), PicTar (http://www.pictar.org/) (286), and miRanda-September 2008 release (http://www.microrna.org/microrna/home.do) (287).

3.17 Statistical analysis

Statistical analysis was performed with StatsDirect software (Addison-Wesley-Longman, UK). Data are presented as the mean ± standard error of the mean (SEM, Studies III, IV) or mean ± standard deviation (SD, Studies I, II) of 2 to 6 independent experiments each performed in triplicate. Comparisons were calculated using unpaired two-tailed Student's t-test, Mann-Whitney U-test, and Kruskal-Wallis test followed by the Conover-Inman comparison, as appropriate. $P<0.05$ was considered significant.

4 Results

4.1 Study I

4.1.1 Mutation analysis of the *AIP* gene

The patient cohort consisted of 137 cases, including 131 sporadic acromegaly patients (95.6%) and six individuals (4.4%) with a family history of pituitary adenomas. The entire *AIP* gene sequence was analysed in all sporadic patients as well as in probands of FIPA families. Eight SNPs already reported in the literature have been identified in the sporadic and familial cohorts (Table 4.1).

Nucleotide change	Amino acid change	Position	dbSNP ID	Reference
c.47G>A	p.R16H	exon 1	-	(88;94;228;231)
IVS1-18C>T	-	intron 1	-	(231)
IVS3+111C>T	-	intron 3	rs4084113	-
c.516C>T	p.D172D	exon 4	rs2276020	-
c.682C>A	p.Q228K	exon 5	rs641081	-
c.906G>A	p.V302V	exon 6	-	(231)
c.920A>G	p.Q307R	exon 6	rs4930199	-
c.993+60G>C	-	exon 6 (3'UTR)	-	(94;99;228)

Table 4.1 SNPs identified in the *AIP* gene in the 137 patients analysed.

Two sporadic patients (both females), diagnosed with acromegaly at 67 and 38 years of age, were found to harbour the previously reported c.911G>A (p.R304Q) substitution in exon 6 (87;94;201;228). The elder patient had a history of multiple tumours (papillary thyroid carcinoma, colon polyposis, liver, and kidney cysts) and presented a pituitary macroadenoma (18x23 mm). Her daughter died at the age of 40 years from colon carcinoma. The younger *AIP* p.R304Q carrier had a microadenoma (3x2 mm) as the only clinical manifestation. Both patients achieved a good control of disease with SAs, thus did not undergo pituitary surgery or radiotherapy. The *in silico* evaluation by PolyPhen-2 predicted this variant as being benign (Appendix 3, Figure 1).

The second nucleotide change identified in the sporadic cohort was a novel missense substitution in exon 6, c.871G>A (p.V291M) (Figure 4.2), detected in a woman with diagnosis of acromegaly at age 30. As shown in Figure 4.1, this amino acid is highly conserved among species. The PolyPhen-2 web tool analysis

predicted this variant as being damaging (Appendix 3, Figure 2), however, LOH study on tumour DNA conducted by sequencing exon 6, showed the presence of the variant in the heterozygous form, thus excluding the loss of the wt allele. The patient underwent transsphenoidal surgery with a post-operative persistence of disease (IGF-1 556 mg/l and PRL 40.5 mg/l, respectively), and she started pharmacological treatment with SAs with good clinical response. Interestingly, this patient presented also a *MEN1* missense mutation, c.243G>C (p.E45Q) (288), without showing during the clinical history other MEN1-related symptoms.

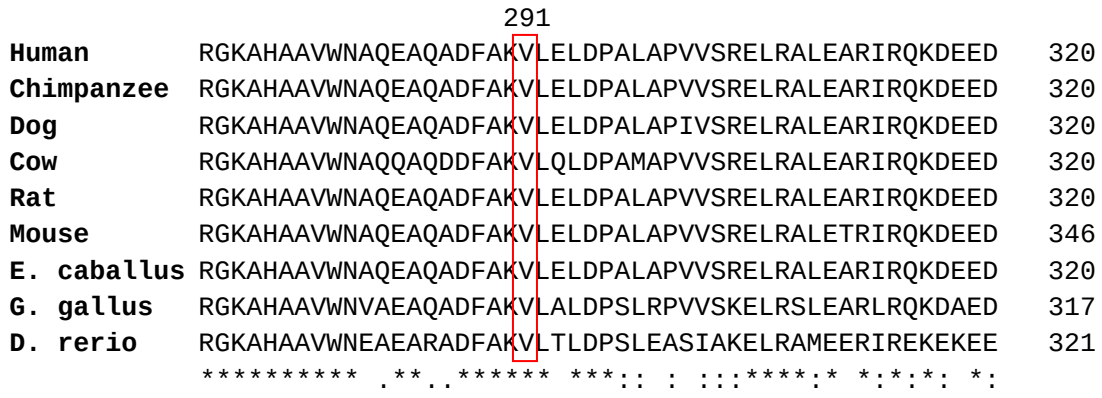

Figure 4.1 Alignment of human AIP amino acid sequence and its homologues among vertebrates. Amino acid sequence homology demonstrates evolutionary conservation of valine 291 and surrounding amino acids in AIP from various species. The multiple sequence alignment was performed using the ClustalW tool. *, amino acidic residues identical in all the aligned sequences; :, conserved amino acids; ., non-conserved amino acids.

A novel nucleotide substitution in the donor splice site of intron 3 (IVS3+1G>A) (Figure 4.2) was identified in a female diagnosed at 62 years of age affected by a microadenoma. A malignant melanoma in her left arm had been surgically removed. The patient presented family history for neoplasias, such as lung carcinoma (father and brother) and breast cancer (mother). All four different algorithms included in Alamut predicted that the IVS3+1G>A substitution is pathogenic because it abolishes the splicing consensus (Appendix 3, Figure 3).

A novel synonymous change in exon 2, c.144G>A (p.T48T) (Figure 4.2), was also detected in a patient diagnosed with acromegaly at age 74 with clinical signs of multiple tumours (benign pancreatic cysts, papillary thyroid carcinoma, tubular adenoma of the colon, and adrenal adenoma) and positive family history of epithelial neoplasia.

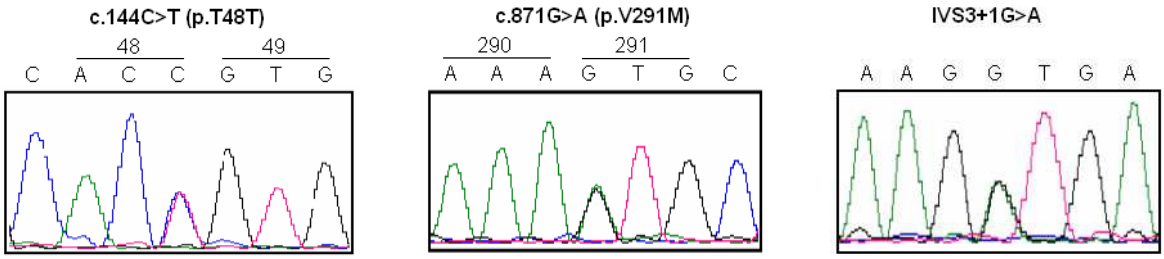

Figure 4.2 Chromatograms showing the three novel *AIP* nucleotide changes, c.144C>T, c.871G>A, and IVS3+1G>A, identified in the cohort of sporadic acromegaly.

Because the bioinformatic prediction was inconclusive (Appendix 3, Figure 4) and the patient's RNA was unavailable, a hybrid minigene was employed to test the pathogenicity of this variant. RT-PCR analysis of mRNA expressed by the *AIP* exon 2 minigene transfected into HeLa cells revealed that the splicing of the hybrid minigene did not differ from that of the wt construct (Figure 4.3). Direct sequencing of the RT-PCR products confirmed correct splicing of both constructs. Taken together, these data suggest that this variant likely represents a rare neutral polymorphism.

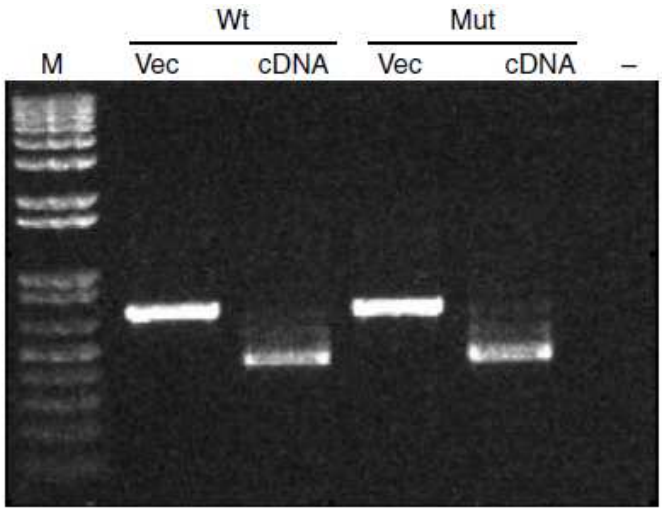

Figure 4.3 RT-PCR analysis of RNA derived from minigene chimeras of *AIP* and *COQ2* expressed in HeLa cells. M, molecular marker; Wt, wild-type construct; Mut, mutant construct; -, negative control. For each vector, plasmid DNA has been amplified as positive control (Vec).

None of the above-reported *AIP* variants was detected in 250 healthy controls. An additional *AIP* sequence change in the 3'UTR (c.993+70C>T) was detected in a sporadic acromegaly patient, and in two out of 90 healthy controls (frequence: 2%), suggesting that this is another neutral polymorphism (Figure 4.4). For all the sporadic cases carrying *AIP* substitutions, relatives were not available for genetic

studies; therefore, it was not possible to perform pedigree analysis. In addition, I could not perform LOH studies in all *AIP* variant carriers either because they did not undergo surgery or because no tumour DNA was available.

AIP germline mutations were not detected in any of the FIPA families investigated.

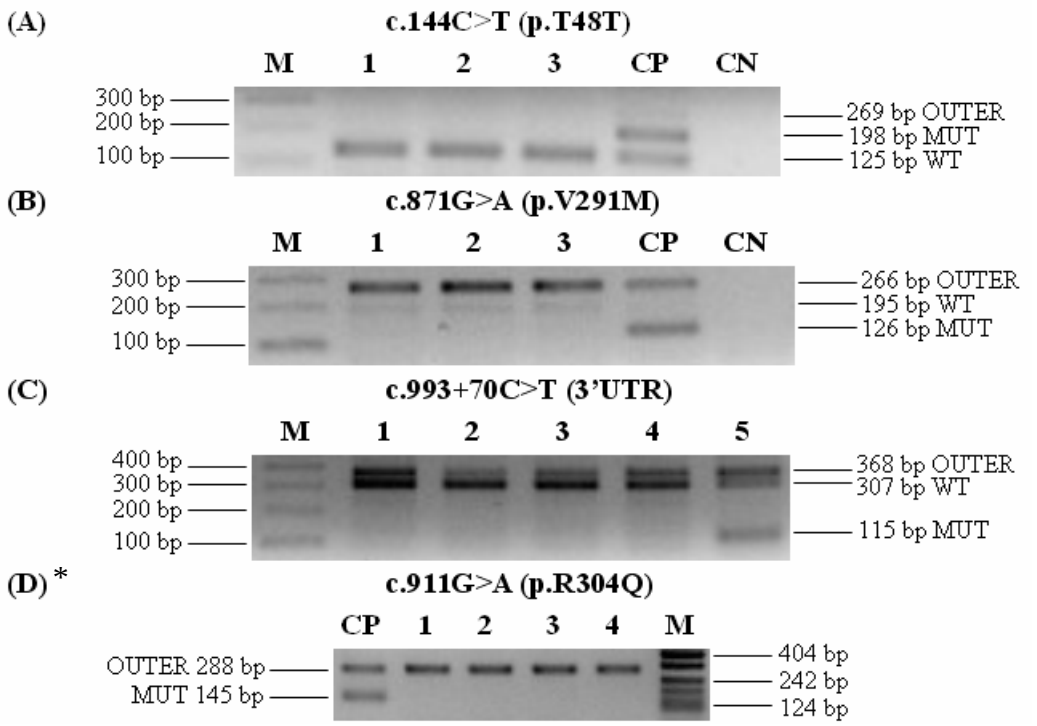

Figure 4.4 Analysis of the *AIP* variants c.144C>T (A), c.871G>A (B), c.993+70C>T (C), and c.911G>A (D) in healthy controls. The Tetra-primer ARMS-PCR system was adopted for the screening. *, for amplification problems the reaction was performed only with the outer primers and the non-wt inner primer. M, molecular weight marker; CP, positive control; CN, negative control; 1-5, healthy subjects.

4.1.2 Mutation analysis of the *CDKN1B* gene

Among the sporadic acromegaly patients, a subgroup of 38 individuals characterized by multiple neoplasia was selected for a mutation screening in the *CDKN1B* gene. A single additional tumour was detected in 24 patients, two tumours in 11 patients, three in two patients, and four in one patient. These other neoplasms affected different tissues: colon (22 cases, 15 with colonic polyposis, six with tubular or villous adenoma with moderate or severe dysplasia, and one with adenocarcinoma), thyroid (nine patients with papillary thyroid carcinoma), adrenal glands (seven patients with adrenal lesions, all without endocrine secretion), liver (five cases of hepatic angioma), uterus (four, fibroadenoma or leiomyoma), intracranial nonpituitary tumours (three meningiomas), stomach (two

patients with gastric leiomyomas), other specific hystotypes were present in single cases (melanoma, lung cancer, breast, and gallbladder). The six *AIP* mutation-negative probands of FIPA families were studied as well for *CDKN1B* germline mutations.

I detected five known SNPs (Table 4.2) and two novel nucleotide substitutions located in the 5'UTR: a c.-202C>T nucleotide change and a c.-452delCCTT 4 bp deletion. The c.-202C>T and c.426G>A (p.T142T) variants were detected by Tetra-primer ARMS-PCR in healthy controls with a frequency of 4.6% and 0.8% respectively, suggesting they are neutral polymorphisms, whereas the c.-452delCCTT variant was not found in the control population.

Nucleotide change	Amino acid change	Position	dbSNP ID	Reference
c.-371C>T	-	exon 1 (5'UTR)	rs11550615	-
c.-79T>C	-	exon 1 (5'UTR)	rs34330	-
c.326T>G	p.V109G	exon 1	rs2066827	(64;67;69;70;73-75)
c.426G>A	p.T142T	exon 1	-	(63;64;70;74;264)
c.596+956C>A	-	exon 3 (3'UTR)	rs7330	-

Table 4.2 SNPs identified in the *CDKN1B* gene in the 38 patients with multiple neoplasia and in the six probands of FIPA families analysed.

4.1.3 *AIP* and *CDKN1B* deletion analysis

I further analysed DNA from the cohort of sporadic and familial cases for *AIP* germline deletions/duplications using the MLPA technique. No evidence of large genomic rearrangements in *AIP* as well as in *MEN1* have been identified neither in the sporadic nor in the familial cases. Analogously, no rearrangements within the *CDKN1B* gene, evaluated both with QMPSF and LR-PCR, have been detected in patients with multiple tumours and in the probands of FIPA families.

4.2 Study II

4.2.1 Patients and tumours characteristics in family 1

The heterogeneous FIPA family identified in Padova, originating from central Italy, is currently composed of an acromegalic male patient and his mother, affected by a prolactinoma.

- *Case1*

The index case (Figure 4.5, subject III-3) was referred to the Endocrinology Unit of Padova in 2007 at the age of 32 years. Age at onset of the first acromegalic features, based on patient interview, was 19 years. Mean GH plasma concentration was 9 µg/L (seven basal determinations, normal range 0-5 µg/L), IGF-1 1008 µg/L (normal range for sex and age 97-306 µg/L) and PRL over 1000 µg/L (normal range 5-15 µg/L), respectively. Hypogonadotropic hypogonadism and impaired glucose tolerance with hyper-insulinemia were also present, and two benign colonic polyps were found by systematic endoscopy. Magnetic resonance imaging (MRI) revealed a pituitary macroadenoma (12x10 mm). Combined medical treatment with SAs (octreotide LAR 30 mg/month) and dopamine agonists (cabergoline up to 2 mg/week) was started, with tumour shrinkage of about 30% and partial biochemical control of the disease. Eight months later, he underwent transsphenoidal surgery, with a post-operative persisting disease (GH nadir after OGTT 3.66 µg/L, IGF-1 896 µg/L and PRL 700 µg/L, respectively) and pharmacological treatment was re-started. A mixed GH/PRL-secreting pituitary adenoma was confirmed by immunohistochemistry and AIP immunostaining was moderately positive. Because partial resistance to the previous treatment was confirmed (IGF-1 814 µg/L, PRL 128 µg/L), pegvisomant (10 mg/day sc) was added with a rapid decrease in IGF-1 levels to 385 µg/L in one month.

- *Case 2*

The 64 years old mother of the index case (Figure 4.5, subject II-5) had a past history of hyperprolactinemia with galactorrhea and menstrual irregularity at age of 30 years, successfully treated with dopamine-agonists until menopause at 53 years. In 2008, she had persisting mild asymptomatic hyperprolactinemia (PRL 50

µg/L) and a 3 mm pituitary microadenoma was present at MRI. Because of type 2 diabetes (HbA_1C 7.2%), a 3h GH profile was performed, with mean plasma GH 0.29 ± 0.14 µg/L. Plasma IGF-1 was normal for age (120 µg/L). Follow-up of the lesion was thus proposed without treatment.

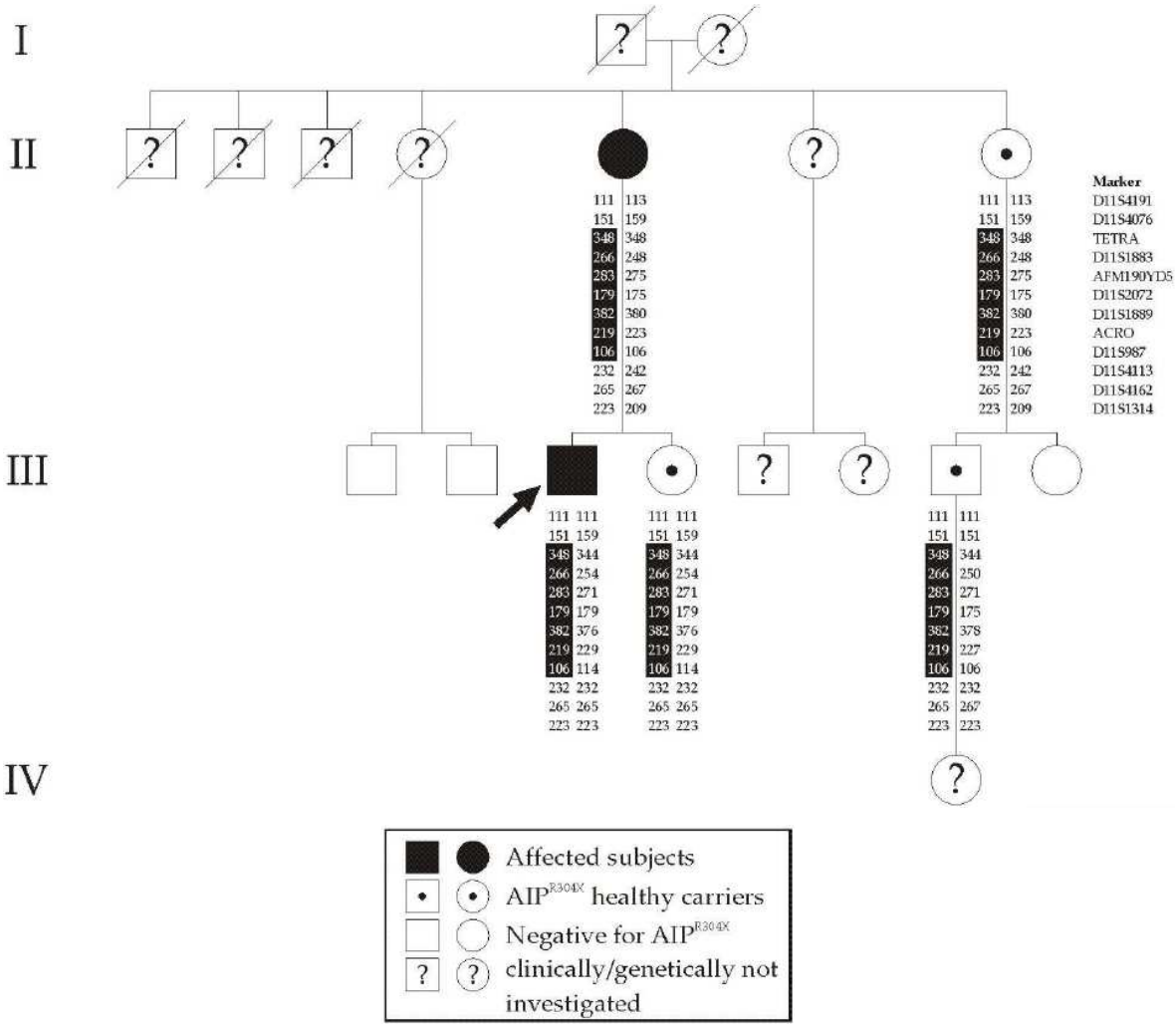

Figure 4.5 Pedigrees structure and haplotype for family 1. Females and males are represented respectively with circles and squares, respectively. Black shadowed boxes represent the shared at-risk haplotype between family 1 and 2. Probands are indicated by a black arrow.

4.2.2 *AIP* sequencing and LOH analysis in family 1

Family 1's proband was first investigated for germline *AIP* mutations and a c.910C>T transition, leading to the truncating p.R304X mutation, was identified. LOH study confirmed the loss of the wt allele (Figure 4.6) at least from markers D11S4076 to D11S987, covering a 6.52 Mb region which includes the *MEN1* gene (Table 4.3). Familial screening further identified the p.R304X mutation in his affected mother and in three relatives (two females and one male, aged 58, 27 and

31 years old, respectively) who had neither clinical, biochemical nor radiological evidence of pituitary disease (Figure 4.5).

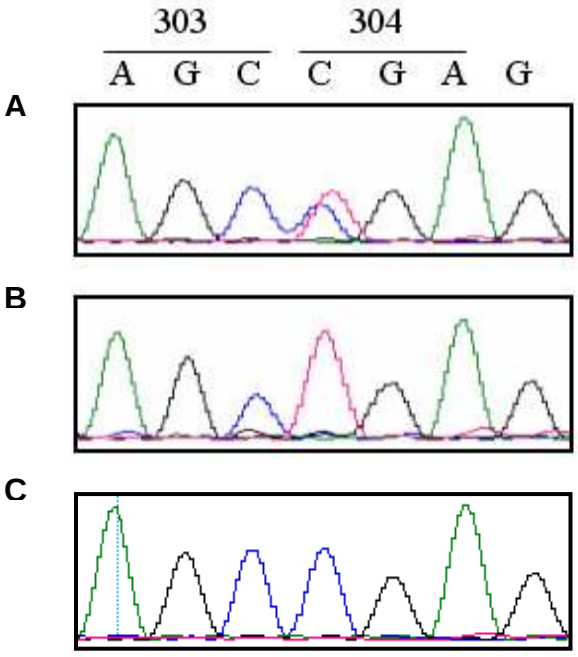

Figure 4.6 Sequence chromatograms showing: A) the heterozygous variant c.910C>T identified in the patient leukocyte DNA, B) the predominant allele in tumour DNA indicating LOH at the *AIP* locus, C) the normal sequence in control DNA.

Marker	Physical Location (Mb)	Leukocyte DNA	Tumour DNA
D11S4191	59.75	NI	NI
D11S4076	61.12	151 159	151
D11S1883	63.13	254 266	266
AFMA190YD5	66.67	271 283	283
D11S1889	67.07	376 382	382
ACRO_CHR11_28	67.21	219 229	219
D11S987	67.64	106 114	106
D11SS4113	68.52	NI	NI
D11S4162	70.65	NI	NI
D11S1314	72.00	NI	NI

Table 4.3 LOH study of proband of family 1. Leukocyte-derived DNA shows the two alleles of the heterozygous markers D11S4076, D11S1883, AFMA190YD5, D11S1889, ACRO_CHR11_28, and D11S987. In the pituitary adenoma-derived DNA one of the two alleles for each heterozygous marker was lost. The more centromeric (D11S4191) and telomeric (D11S4113, D11S4162, D11S1314) markers were non-informative, thus no conclusions can be drawn about their status.

4.2.3 Genotyping

Because the p.R304X mutation was identified in three apparently unrelated Italian FIPA families (88;97;276;277), I wished to find out whether the c.910T mutated

allele had a common origin or was the result of a mutational hot-spot. To address this issue, 12 microsatellite markers around the *AIP* and *MEN1* genes were analysed in all consenting patients and relatives. In family 1, an at-risk haplotype of at least 12 Mb was found to segregate in all mutation carriers. Interestingly, the *AIP* p.R304X mutation carriers in family 2, but not the family 3's proband, shared the same at-risk alleles for seven markers (Table 4.4 , Figure 4.7), strongly arguing for a founder effect common to families 1 and 2. Because the genetic length of the shared region is inversely proportional to the age of the founding event, a SNP (rs4084113) located within *AIP* intron 3 was also genotyped. As showed in Table 4.4, the T allele was associated with the at-risk haplotype in families 1 and 2, whereas family 3's proband is an homozygous carrier of the C allele, further supporting the hypothesis of an independent mutational event occurred in this latter family.

Marker	Physical Location (Mb)	Haplotypes		
		Family 1	Family 2	Family 3
D11S4191[#]	59.75	111	111	NE
D11S4076[#]	61.12	151	159	151 159
m_11TETRA@61.73	61.73	348	348	NE
D11S1883[#]	63.13	266	266	254 260
AFMA190YD5	66.67	283	283	271 271
D11S2072	66.98	179	179	173 173
rs4084113	67.01	T	T	C C
D11S1889[#]	67.07	382	382	378 378
ACRO_CHR11_28[*]	67.21	219	219	229 231
D11S987[#]	67.64	106	106	114 114
D11SS4113[#]	68.52	232	222	NE
D11S4162[#]	70.65	265	267	265 267
D11S1314[#]	72.00	223	217	223 223

Table 4.4 Molecular markers on chromosome 11 and haplotype data in the Italian *AIP* p.R304X families. For families 1 and 2 the at risk-haplotype shared by all mutation carriers is reported and the common disease-associated haplotype is indicated by shadowed boxes. [*], (85); [#], allele size standardized on a known CEPH subject (1347-2); NE, not evaluated.

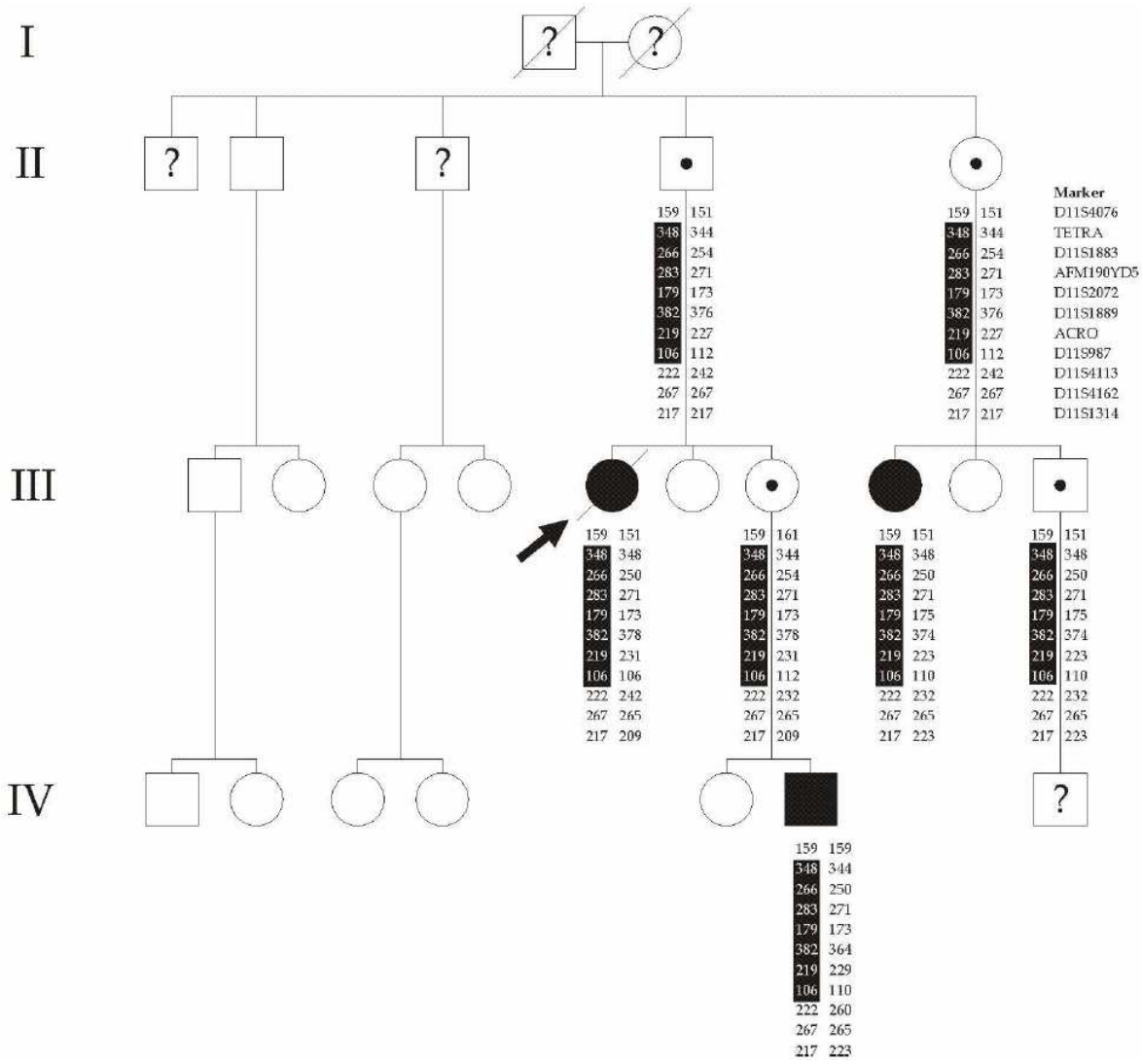

Figure 4.7 Pedigree structure and haplotype for family 2. For the legend refer to Figure 4.5.

4.2.4 Characterization of *AIP* p.R304X mutated subjects

Bio-clinical features of *AIP* p.R304X patients and carriers identified in families 1, 2 and 3 were evaluated comparatively. Family 1 was heterogeneous for somatotropinoma and prolactinoma, whereas families 2 and 3 were homogeneous for somatotropinomas. Overall, among the 17 *AIP* p.R304X genetically confirmed mutation carriers identified so far, seven had developed evidence of pituitary adenoma (4/9 women and 3/8 men, respectively). Penetrance was calculated either with taking into account only affected and obligate carrier subjects or including as well half of the subjects with 50% risk to inherit the mutation (289). Disease penetrance could currently be estimated in this cohort to 41% and 33%, respectively. I am aware that penetrance calculation is subject to bias due to

symptomatic patient referral and due to incomplete genealogical data as well as variable ages of the subjects studied, but this calculation can still provide some useful information.

A consistent variability in clinical disease expressivity was observed in the patients, though age at first symptoms was <30 years in all cases (mean 19.1 ± 6.7, range 8-30) and tended to be younger in male patients (15.0 ± 6.1 vs 22.3 ± 6.0 in females). Accordingly, gigantism was present in two males. Most pituitary adenomas were macroadenomas (71%), including two giant adenomas (277). From a functional point of view, GH- and GH and PRL-secreting tumours were present in 57% (4/7) and in 29% (2/7) of cases, respectively, and confirmed by immunohistochemistry after surgery, the latter case being a non-operated microprolactinoma (14%). From a therapeutic point of view, only one out of six patients who underwent surgical treatment had a successful outcome. Noteworthy, this patient (Figure 4.7, subject IV-6) was the third symptomatic case in a FIPA kindred with aggressive tumours (277). Incipient gigantism could be recognized at the age of 8 years thanks to clinical screening by auxological follow-up, a few months before the *AIP* p.R304X mutation was identified in this kindred.

All patients received pharmacological therapy, and only one out of six patients treated with SAs experienced disease control after six years of exclusive post-operative treatment (octreotide LAR 20 mg/monthly). The remaining patients required combined therapy with dopamine-agonists, pegvisomant and/or radiotherapy for the control of post-operative GH/IGF-1 hypersecretion. Three patients received radiotherapy, resulting in long-term disease control with tumour shrinkage and progressive hypopituitarism, including GH deficit in all cases (follow-up 12 to 13 years). Family 2’s proband recently died at the age of 32 years old from acute polmonitis; she had been suffering in the last years from severe obesity-related respiratory insufficiency and disease-related secondary epilepsy.

4.3 Study III

4.3.1 miR-107 is overexpressed in GH-secreting and NFPA tumours compared to NP

The miRNA expression profiles of pituitary adenomas were determined using TLDA. Out of 738 miR genes available on the TLDA cards, 174 miRs were found expressed in each pool, while the expression of 488 miRs could not be detected in pituitary tissue. Examination of the expression profiles revealed that nine miRNAs (hsa-miR-509-3-5p, hsa-miR-508-5p, hsa-miR-452, hsa-miR-330-5p, hsa-miR-200a*, hsa-miR-503, hsa-miR-424, hsa-miR-449a, hsa-miR-199-5p) were expressed in normal tissues but not in the adenomas, seven miRNAs (hsa-miR-378, hsa-miR-516-3p, hsa-miR-151-3p, hsa-miR-224, hsa-miR-618, hsa-miR-455-3p, hsa-miR-29b) were expressed in the adenomas but not in normal tissue, while 66 miRNAs were differentially expressed in adenomas and normal tissue with a more than 2.5-fold difference. One of these miRNAs, miR-107, is known to be associated with human cancer (290). The TLDA experiment showed a 3.1-fold increase in the expression of miR-107 (Figure 4.8A). In validation studies using qRT-PCR in a separate set of samples, this upregulation was confirmed: in 17 sporadic pituitary adenomas and nine NP tissue miR-107 was found to be overexpressed 3.5±0.97 fold in NFPAs and 2.5±0.39 fold in GH-secreting adenomas ($P<0.05$ for both, Figure 4.8B). These data are compatible with previous data by Bottoni *et al*. (38), although no qRT-PCR validation was performed in that study.

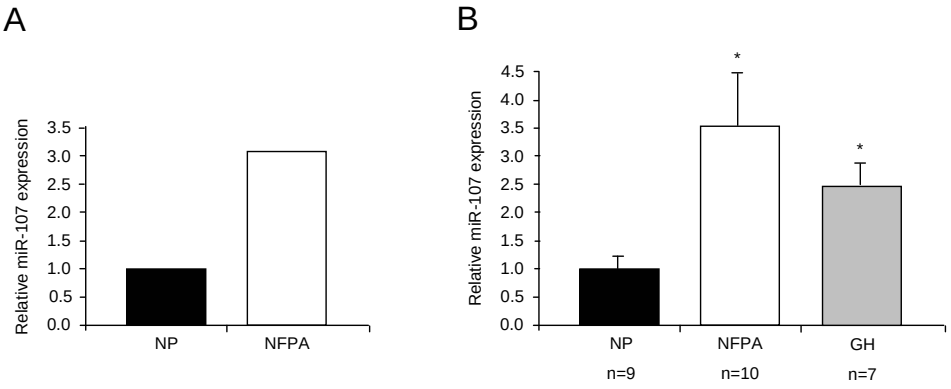

Figure 4.8 miR-107 is abnormally expressed in pituitary tumours. The relative expression levels of miR-107 in NP, NFPA and GH-secreting adenomas were assessed by A) TLDA in two pools of NP and NFPA samples and B) qRT-PCR in NP (n=9), NFPA (n=10) and GH (n=7) samples. Data are expressed as mir-107/RNU6B ratio to NP for both assays. *, $P<0.05$.

4.3.2 miR-107 suppresses cell proliferation and colony formation

To determine the biological functions of miR-107, I investigated its effect on cell proliferation and colony formation in SH-SY5Y and GH3 cells. Using [^{3}H] thymidine incorporation I observed a significant decrease in cell growth in both cell lines at 48 and 72h after transfection with the pre-miR-107 precursor (P<0.05) (Figure 4.9A).

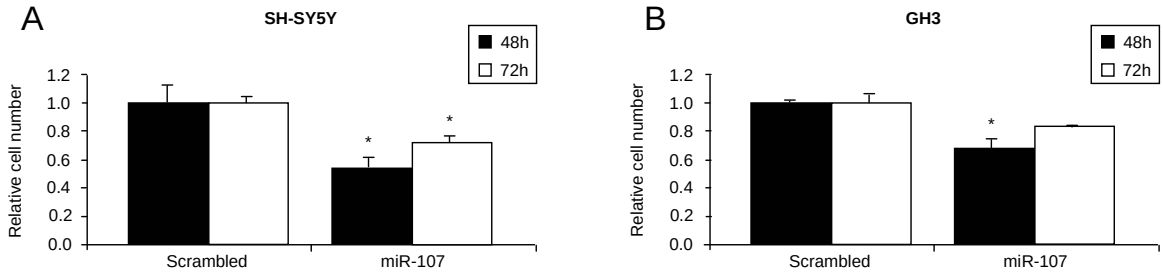

Figure 4.9 The effect of miR-107 on cell proliferation. A) human SH-SY5Y and B) rat GH3 cells were transfected with pre-miR-107 and the proliferation was measured by [^{3}H] thymidine incorporation 48 and 72h after transfection. Data are expressed as ratio to scrambled control transfected cells *, P<0.05.

miR-107 also regulated the clonogenic capacity of SH-SY5Y, since its inhibition increased colony formation by 2.42±0.22 fold (P<0.05; Figure 4.10A). However, I was unable to demonstrate any appreciable effect on the clonogenicty by either overexpressing or suppressing miR-107 in GH3 cells (Figure 4.10B).

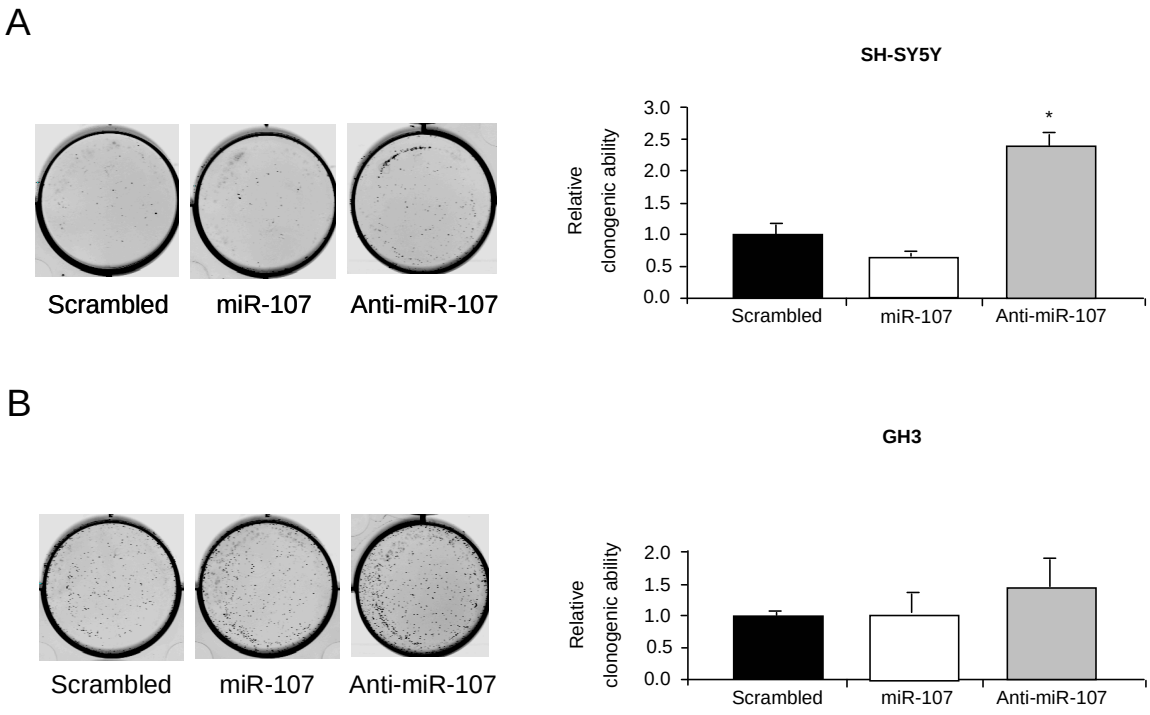

Figure 4.10 The effect of miR-107 on colony formation. A) SH-SY5Y and B) GH3 cells were first transfected with pre-miR-107 or anti-miR-107 for 24h. Thereafter, the cells were trypsinized and 1500 cells were seeded in normal medium. The plates were then incubated for 7 days. Quantitative changes in clonogenicity were determined by densitometric quantification of the colony formation density and expressed as ratio to scrambled control transfected cells. *, P<0.05.

Confirmation of miR-107 overexpression/inhibition after transfection of both GH3 and SH-SY5Y cells with pre-miR-107 precursor and anti-miR-107, was performed by qRT-PCR (Figure 4.11).

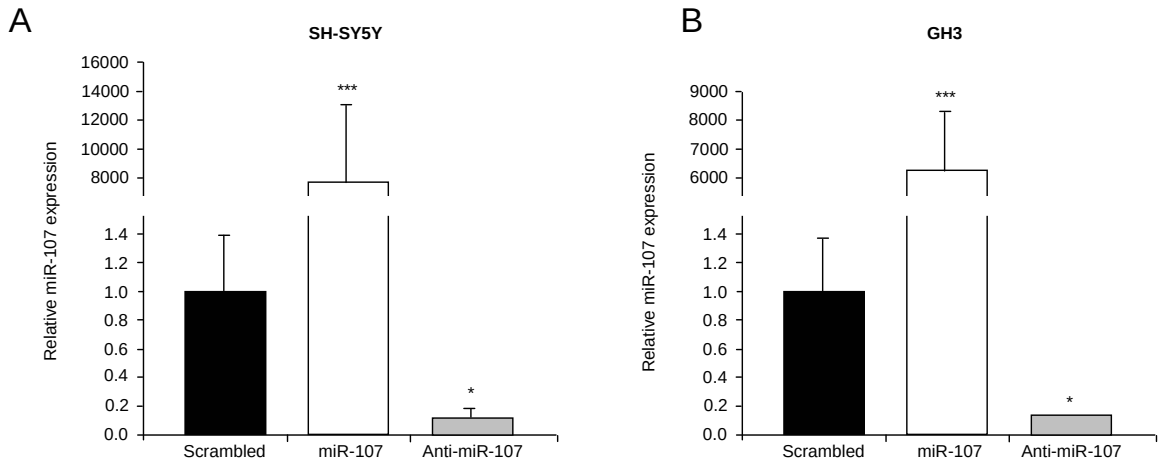

Figure 4.11 Validation of miR-107 overexpression/inhibition in A) SH-SY5Y and B) GH3 cells using a miR-107-specific TaqMan MicroRNA Assay. Data are expressed as AIP/RNU6B (for SH-SY5Y cells) or AIP/GAPDH (for GH3 cells) ratio to scrambled control transfected cells. *, P<0.05; ***, P<0.0001.

4.3.3 miR-107 is predicted to bind the *AIP* 3'UTR at two sites

In order to identify a miR-107 putative target gene that might be involved in pituitary adenoma development, I conducted an *in silico* analysis. Five out of seven target prediction algorithms used in this study predicted miR-107 as possibly targeting the 3'UTR of human *AIP*. A 7mer-A1 site [for the definition of the different types of target sites, see (31)] located 38-44 bp downstream of the stop codon of *AIP* (site 1) was predicted by the TargetScan, FindTar and PITA programs, while a 6mer site at position 65-70 bp (site 2) was predicted by the MicroCosm, MicroTar, FindTar and PITA programs (Figure 4.12 and Appendix, Figure). Site 2 is predicted to have better accessibility than site 1.

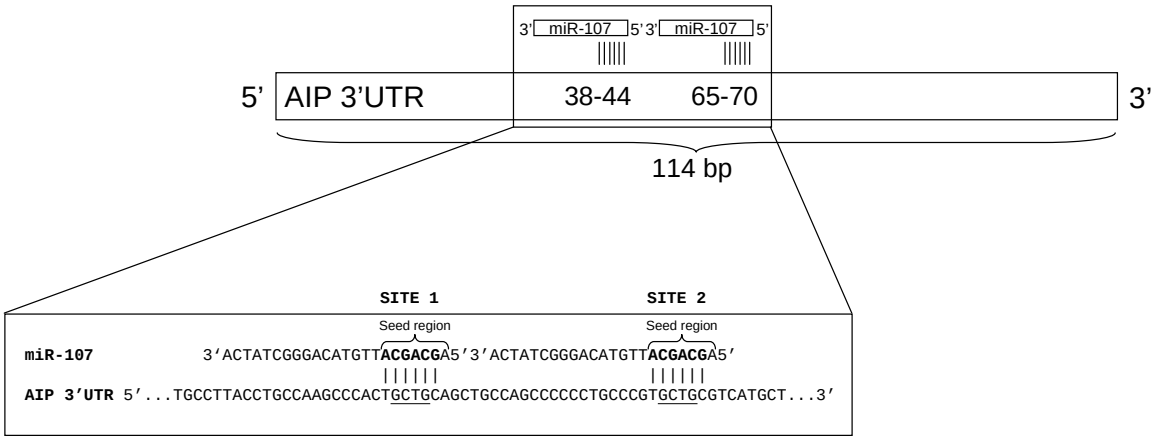

Figure 4.12 Graphic representation of the two predicted miR-107 target sites in *AIP* 3'UTR. The localisation of the seed regions is reported. The underlined sequences represent the four deleted nucleotides in MUT1 and MUT2 *AIP* 3'UTR plasmids.

4.3.4 miR-107 represses AIP through binding at site 2

In order to experimentally verify the *in silico* predicted interaction between miR-107 and AIP, I cloned the human wt *AIP* 3'UTR into a pGL3 reporter vector, downstream to the coding sequence of Firefly luciferase. In this way, the total luciferase output of the *AIP* 3'UTR-Firefly luciferase hybrid transcript depends on the effect of the *AIP* 3´UTR. As shown in Figure 4.13A, the construct containing the wt *AIP* 3'UTR reduced luciferase expression to 14±1% of the empty vector ($P<0.05$). I next assessed if miR-107 *in vitro* binding to the 3'UTR of *AIP* reduces luciferase activity. When the pre-miR-107 precursor was transfected into GH3 cells along with the wt *AIP*-3'UTR, a 50% reduction of luciferase activity was observed compared to the control scrambled miRNA (Figure 4.13C). The choice of GH3 cells as reporter cells was based on the finding that they express relatively low levels of endogenous miR-107. To confirm that the decreased luciferase activity was really caused by miR-107 interaction with the cloned fragment, and not by non-specific binding with the backbone sequence of the pGL3 reporter vector, I compared the effect exerted by the pre-miR-107 precursor and the scrambled miRNA on the empty pGL3 vector. As shown in Figure 4.13B, miR-107 did not change the luciferase activity of the empty vector compared to the scrambled miRNA control. Subsequently, I investigated whether one or both predicted target sites (site 1 and site 2) were functional. For this purpose, two deletion mutants targeting the two putative binding sites were generated. I hereafter refer to them

as MUT1 for the mutated binding site 1, MUT2 for site 2, and MUT1+2 for the sequence carrying both mutations. The luciferase assay demonstrated that miR-107 still inhibits luciferase activity at comparable levels after mutation of site 1, while it loses the inhibitory effect on luciferase activity with MUT2 (Figure 4.13C).

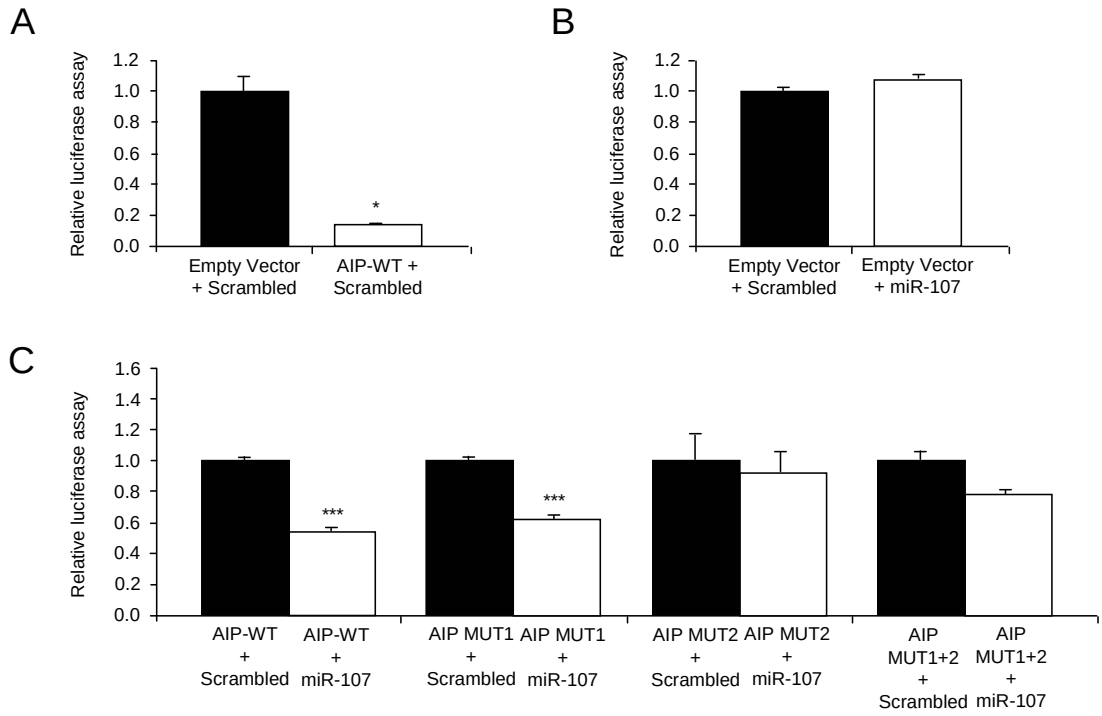

Figure 4.13 miR-107 interacts *in vitro* with AIP. The full-length *AIP* 3'UTR segment harbouring the target sites for miR-107 was cloned into the pGL3 Control Vector. A) the wt *AIP* 3'UTR significantly reduces luciferase activity compared to the insertion-less reporter vector. B) miR-107 does not interact with the backbone vector sequence. C) miR-107 mediates AIP repression via binding at predicted site 2. The results are shown as a relative change of the miR-107 + pGL3–*AIP* WT and mutated *AIP* Firefly/*Renilla* activity ratios with respect to that of the scrambled control transfected cells. *, P<0.05; ***, P<0.0001.

To verify the reliability of the assay I included in each experiment a reporter vector containing the 3'UTR of the *NFI-A* gene (Figure 4.14), which had previously been demonstrated to be targeted by miR-107 using the same technique (291).

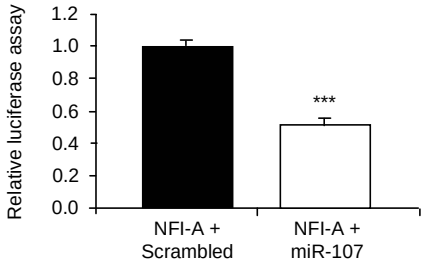

Figure 4.14 miRNA reporter assay of *NFI-A*-miR-107 interaction. The *NFI-A* 3'UTR segment harboring the target site for miR-107 was cloned into the pGL3 Control Vector (291). ***, P<0.0001.

4.3.5 Regulation of endogenous AIP expression by miR-107

It is accepted that miRNAs are able to downregulate mRNA and/or the protein levels of target genes (27). Therefore, to further characterize the interaction between miR-107 and AIP, I measured mRNA and protein levels of endogenous AIP after miR-107 overexpression in human SH-SY5Y and rat GH3 cells. These cell lines were chosen since previous studies had demonstrated relatively high expression levels of AIP in them (87;201). The GH3 cell line was investigated because it represents the most relevant available model for GH- and PRL-secreting adenomas, the diseases caused by inactivating mutations in the *AIP* gene. However, it should be noted that miR-107 was not predicted to bind the rat *AIP* 3'UTR by any of the predictions tools used in this study.

As shown in Figure 4.15A, miR-107 overexpression, but not the scrambled miRNA, caused endogenous human AIP expression to decrease both at the mRNA and protein level in SH-SY5Y cells. The decrease of AIP protein expression was already detectable at 24h post-transfection and became more pronounced at 48h, reaching statistical significance ($P<0.0001$). At the mRNA level, miR-107 decreased AIP expression to 53±2% of the scrambled miRNA control ($P<0.05$). On the contrary, transient transfection of pre-miR-107 precursor triggered only a negligible change in AIP expression at either the mRNA or protein level in GH3 cells (Figure 4.15B), supporting the bioinformatic prediction suggesting there were no target sites in the rat *AIP* 3'UTR.

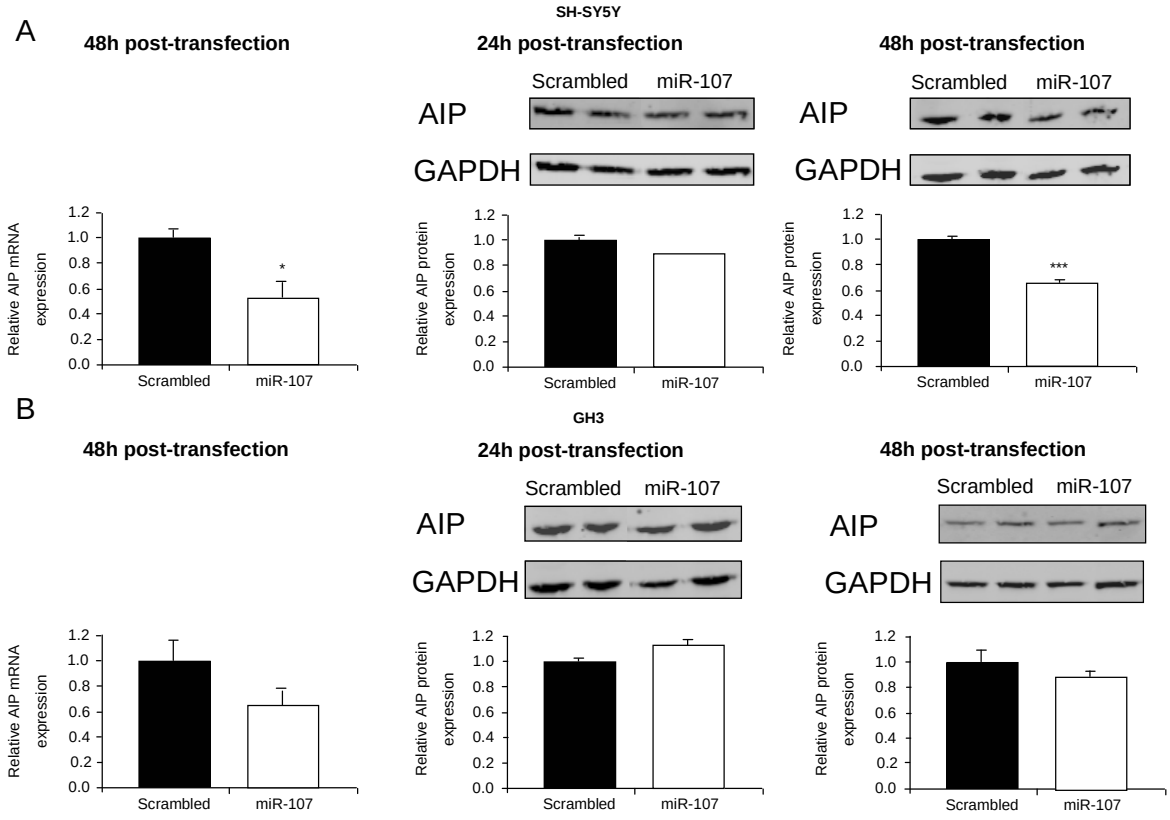

Figure 4.15 Effect of miR-107 on endogenous AIP mRNA and protein expression in A) SH-SY5Y and B) GH3 cells. Data are expressed as AIP/GAPDH ratio to scrambled control transfected cells. *, P<0.05; ***, P<0.0001.

I also demonstrated the reliability of GAPDH as an endogenous control since its levels were proven to be unaffected by miR-107 in both human and rat cell lines (Figure 4.16). This result confirms the *in silico* predicted absence of miR-107 target sites on the *GAPDH* gene, in agreement with a previous study (292).

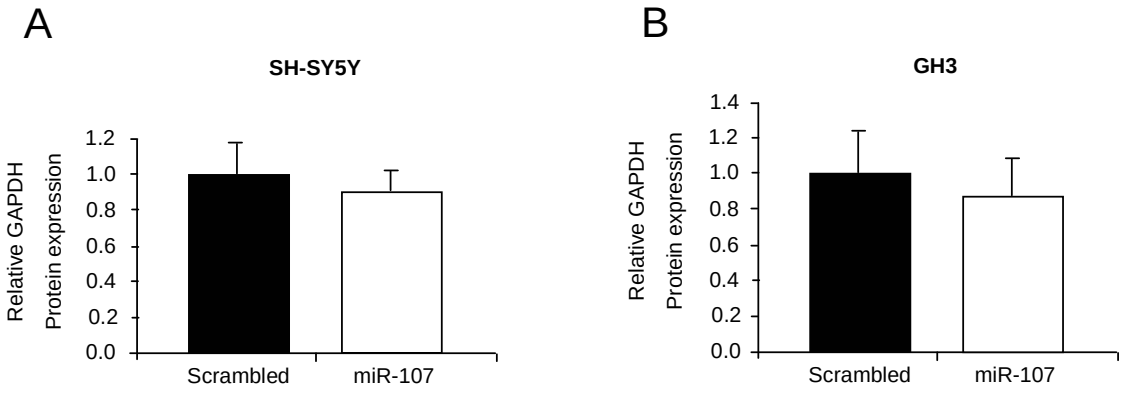

Figure 4.16 Effect of miR-107 on endogenous GAPDH protein expression in A) SH-SY5Y and B) GH3 cells. Data are expressed as ratio to scrambled control transfected cells.

To verify whether AIP can counteract miR-107 repression via a negative feedback mechanism, I compared miR-107 expression levels in untransfected and AIP-overexpressing GH3 cells. I did not see any significant difference between the two conditions (Figure 4.17).

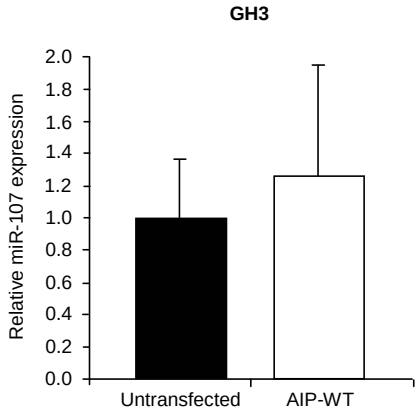

Figure 4.17 miR-107 expression levels in untransfected and AIP-WT-overexpressing GH3 cells (87) measured by a miR-107-specific TaqMan MicroRNA Assay. Data are expressed as mir-107/GAPDH ratio to untransfected cells.

4.4 Study IV

The mRNA expression of 23 GH-secreting tumours and 11 normal pituitaries was evaluated by qRT-PCR. AHRR mRNA levels were found significantly higher in somatotropinomas, ranging from 0.09 to 66.21 (mean 7.71 ± 3.04), than in normal pituitaries, ranging from 0.27 to 4.38 (mean 1.00 ± 0.37) (P=0.003) (Table 4.5, Figure 4.18A).

Sample	AHRR expression	Age (year)	Sex	Adenoma size
1	0.09	39	F	Macro
2	0.31	27	M	Macro
3	0.49	55	F	Macro
4	0.68	59	F	Macro
5	0.94	76	F	NA
6	1.16	32	M	NA
7	1.19	33	F	NA
8	1.29	34	M	Macro
9	1.67	43	F	Macro
10	1.76	65	F	Macro
11	1.97	45	F	NA
12	2.41	52	F	NA
13	3.32	43	F	Macro
14	4.30	42	F	Macro
15	4.72	56	F	Macro
16	5.09	53	F	Micro
17	5.51	36	F	Macro
18	8.02	39	M	Macro
19	9.18	44	F	Macro
20	10.92	43	F	Macro
21	13.29	57	F	Micro
22	32.92	50	M	Macro
23	66.21	26	M	Macro

Sample	AHRR expression
NPit1	0.27
NPit2	0.28
NPit3	0.42
NPit4	0.42
NPit5	0.53
NPit6	0.54
NPit7	0.55
NPit8	0.55
NPit9	1.03
NPit10	2.03
NPit11	4.38

Table 4.5 AHRR mRNA expression levels in the somatotropinoma and normal pituitary samples analysed. Age, sex and adenoma size of each sample are reported. Npit, normal pituitary; macro/micro, macroadenoma/microadenoma; NA, not available.

Among the GH-secreting tumours, five samples showed very high AHRR expression levels (selected as displaying AHRR expression levels at least 2X higher than the normal pituitary sample with the highest AHRR expression), ranging from 9.18 to 66.21 (mean 26.51 ± 10.81), compared to the remaining 18 (P<0.0001) (Figure 4.18B). No significant differences in age, sex or tumour size were found between the two somatotropinomas subgroups.

Interestingly, if I excluded the five AHRR overexpressing adenomas from the analysis, the difference between the GH-secreting tumours and the normal pituitaries was still significant (P=0.02).

A

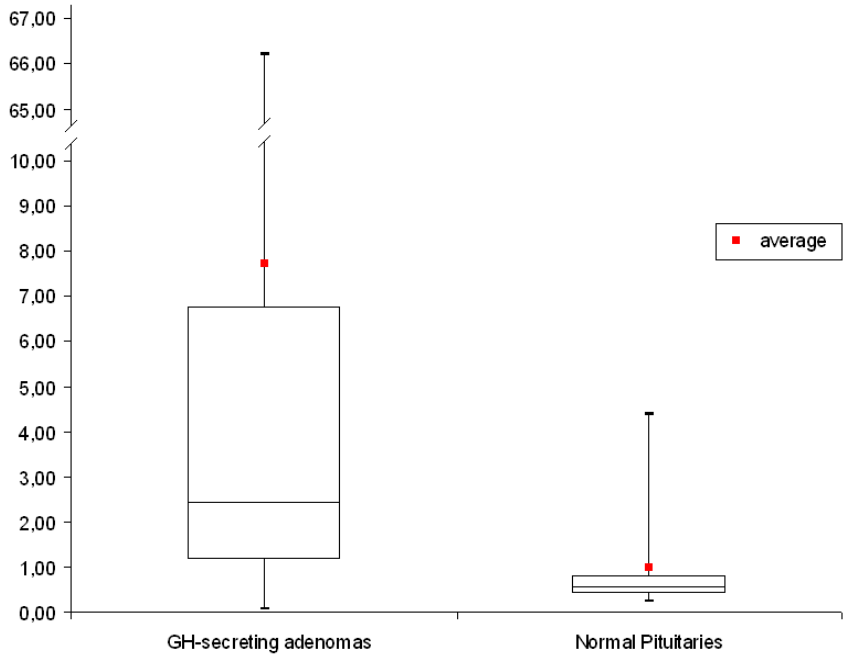

B

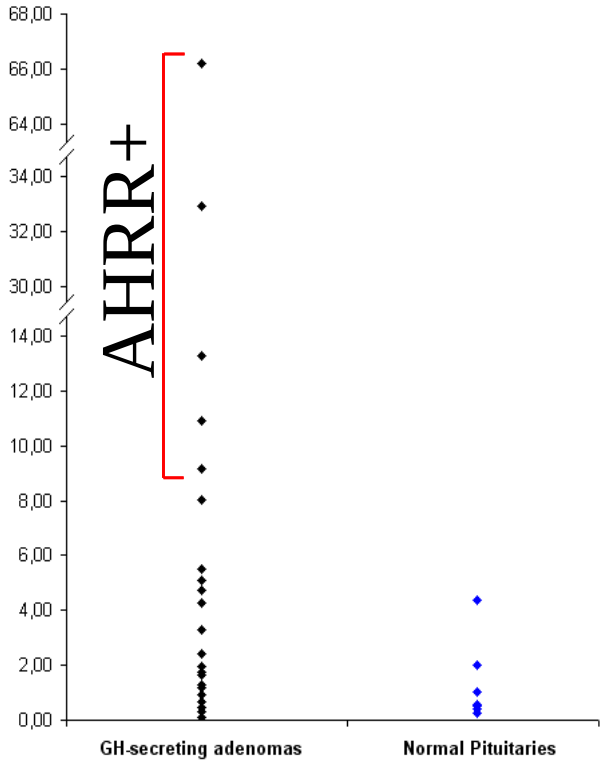

Figure 4.18 A) Boxplot representation showing the minimum, maximum, median, average and the 1st and 3rd quartile values for both groups. B) Data distribution within each group. AHRR+: five somatotropinomas overexpressing AHRR.

5 Discussion

5.1 Study I

In this study I determined the prevalence of *AIP* and *CDKN1B* mutations/rearrangements in a homogeneous cohort of Italian patients with either sporadic acromegaly or FIPA.

I detected three presumably pathogenic *AIP* mutations in four apparently sporadic cases (3.1%), confirming the prevalence data reported in other cohorts (71;87;94;99;225-228;230). The age at diagnosis in *AIP*-mutated subjects ranged from 30 to 67 years and is relatively high compared with those reported in other nonselected cohorts of sporadic acromegaly patients. According to previous data (293), this might be a consequence of the nature of the mutations: missense, with possibly a reduced pathogenicity in three out of four cases in this work, versus nonsense, frameshift or affecting splice sites, hence with a strong effect on AIP function, in other series (71;94;225;226;228). The majority of apparently sporadic *AIP*-mutated acromegaly patients reported so far (71;87;94;99;225-228;230) were diagnosed at an age younger than 40 years (14 out of 16, excluding the sporadic acromegaly patients from Finland known to harbour a founder mutation). Therefore, although an age at diagnosis <40 may be considered a good selection criteria for *AIP* screening in apparently sporadic acromegaly patients, it must be considered that about 10% of patients, carrying milder *AIP* mutations, would be missed with such inclusion criteria.

I detected the c.911G>A (p.R304Q) missense mutation in two sporadic patients diagnosed with acromegaly at 67 and 38 years of age. The R304Q locus is part of a CpG island mutational hot-spot. This amino acid change is relatively conservative changing a longer side chain positively charged amino acid to a slightly shorter, uncharged, hydrophilic residue in the a-7 helix. The amino acid is conserved in mammals, but not in lower species, where it is usually replaced by another basic amino acid, lysine. Notably, this variant has never been detected in control populations in different studies [(87;94;228), this study]. Even if *in silico* (Appendix 3, Figure 1) and *in vitro* data (96) suggests this variant as being non-deleterious, the pathogenic role of R304Q is supported by the fact that it has been identified in several independent FIPA families as well as in sporadic patients

(87;94;96;201;228). Clearly further data are needed to understand the real role of this variant.

The identification of the novel missense p.V291M variant is of great interest. This change affects a very well conserved residue located in the third TPR motif (Figure 4.1), which mediates the interaction of AIP with several proteins. It is thus likely that this variant might interfere with AIP function. In addition, it was not detected in the control population. However, it should be stated that LOH study on tumour DNA excluded the loss of the wt allele. Only functional studies could thus establish the real role of this variant. Interestingly, the patient harbouring this substitution, presented also the already described *MEN1* p.E45Q mutation (288), suggesting that this might be a compound heterozygote. The patient was not diagnosed with a severe phenotype and she did not present any symptom of MEN1, beside the pituitary tumour. The reason of a mild phenotype may be due to different reasons. *MEN1* and *AIP* mutations exhibit both a reduced penetrance (about 30–40% for pituitary tumours in both cases (224;294)), so I cannot exclude that only one of them is fully penetrant. Although it is apparently a rare event, other cases in which *MEN1* germline mutations are associated with mutations in a second TSG in the same patient have been described (295;296). In those cases, the coexistence of *BRCA1*/*BRCA2* mutations in *MEN1*-mutated patients did not lead to a more severe clinical phenotype as is observed in some oligogenic disorders such as Kallmann syndrome (involving *FGFR1* and *NELF* genes) or normosmic idiopathic hypogonadotropic hypogonadism (involving *FGFR1* and *GNRHR* genes) (297). On the other hand, a high phenotypic variability could be observed in patients with multiple mutations affecting the same TSGs: simultaneous deletion of *BMPR1a* and *PTEN* may be associated with severe polyposis in some patients (298), but not in others (299). Neither information on relatives' health condition nor on the segregation of *AIP*/*MEN1* variants in the patient's family were available; therefore, functional studies are mandatory to understand the possible combined effects of *MEN1* and *AIP* mutations in determining the pituitary phenotype.

Regarding the novel silent substitution c.144C>T (p.T48T), albeit in principle I cannot exclude an effect on other cellular processes besides splicing of exon 2, the functional study (Figure 4.3) strongly suggests that this variant should be considered a rare polymorphism.

A novel nucleotide substitution in the donor splice site of intron 3 (IVS3+1G>A) was identified in a 62 years old patient affected by a GH-secreting microadenoma. The *in silico* analysis predicted this variant as being pathogenic because it abolishes the splicing consensus. This nucleotide change can lead to either retention of intron 3 or to skipping of exon 3. In the first case, the presence of intron 3 after the splice site generates a frameshift and the consequent introduction of a premature stop-codon, which results in a truncated protein or in an unstable RNA transcript. In the other scenario, the lack of exon 3 will not alter the reading frame since that exon is a multiple of three nucleotides in lenght, but it will cause the loss of a critical group of amino acids involved in the interaction of AIP with other proteins. Since this variant has been detected in a sporadic patient, the latter outcome is the most likely because the protein, even if not complete, is still present. In order to establish the real impact of the variant on the splicing mechanism, a minigene study similar to that employed to study the p.T48T variant will be performed in the laboratory of Adrenal and Pituitary Physiopathology of the University of Padova.

Although the conventional approach of direct sequencing of germline DNA identified the vast majority of *AIP* mutations, five out of 56 investigated FIPA families who had tested negative for *AIP* point mutations harboured large genomic deletions probably due to Alu-mediated recombination (95;96). Thus, in order to study in a more complete manner the *AIP* gene, I employed the MLPA technique to identify possible rearrangements. I did not detect gross *AIP* rearrangements in the cohort, confirming that these are relatively rare events in familial cases and are even more uncommon in sporadic acromegaly patients (only one in 245 patients analysed so far) [(95;96), this study]. Therefore, this type of mutational event should be only marginally considered for molecular analysis in sporadic cases.

Six FIPA families either homogeneous for prolactinomas or heterogeneous with PRL-secreting/NFPA tumours were also evaluated for *AIP* germline mutations/rearrangements without finding any causative nucleotide change. Thus, in accordance with prevalence data reported previously (88), among the seven FIPA families collected at the Endocrinology Division of Padova Hospital/University (one heterogeneous with PRL- and GH-secreting tumours is described in Study II) *AIP* mutations have been detected in a single kindred. This data further support the observation that *AIP* mutations play a primary role almost

exclusively in families with at least one member affected with somatotropinoma (293).

So far, only few *CDKN1B*-mutated MEN4 patients have been detected, thus a genotype–phenotype correlation is not univocally established. Although the frequency of pituitary tumours did not differ significantly from that described in MEN1-mutated patients (37.5% vs 42%) (71), among the few *CDKN1B*-mutated subjects with a pituitary adenoma, a higher prevalence of acromegalic patients was observed (67% vs 10%) (294). Although *in vitro* and *in vivo* studies clearly support a role for the GH/IGF-1 axis in tumour development, as a consequence of the mitogenic and anti-apoptotic actions it exerted in many tissues (300), the existence of genetic and epigenetic factors predisposing to the development of both GH-secreting tumours and different cancers was recently proposed (301). Using the Swedish Family-Cancer database to analyse familial risk for pituitary adenomas and associated tumours, Hemminki *et al.* (301) demonstrated a significant association between GH-secreting pituitary adenomas and the presence of different tumour types in first and second degree relatives and in the acromegaly patients themselves. Based on the role of $p27^{Kip1}$ loss in several human malignancies (258) and the increased risk of developing extrapituitary tumours in patients with acromegaly (300), I hypothesized that *CDKN1B* mutations could represent the common unifying nonendocrine etiology for acromegaly and cancer.

No known mutations were found in *CDKN1B*. I detected the silent c.426G>A (p.T142T) substitution in a 55-year-old patient affected by thyroid carcinoma, adrenal, and colon adenomas. This variant was already described in a MEN1-like patient with tumours of both the parathyroids and pituitary gland, renal angiomyolipoma, and thyroid tumour (70), in a subject with secondary hyperparathyroidism (74), in one sporadic acromegaly patient (64) and also in one case of breast carcinoma (264). Based on such observations, it was proposed that p.T142T might be a rare hyperparathyroidism-predisposing allele (74). In the present study, I detected the p.T142T allele, albeit with a low frequency (0.8%), in the control population. Based on this and the *in silico* data that excludes its possible effect on splicing (64), it is very likely that it represents a neutral polymorphism. A case–control association study on c.426G>A, as well as

functional studies, are mandatory to better understand the role of this variant in predisposing subjects to multiple cancers.

The identification of the novel c.-452delCCTT variant is of great interest. Indeed, it is located in a region that has been demonstrated to possess sequences which regulate the translation of $p27^{Kip1}$ (302). To determine if this variant negatively affects $p27^{Kip1}$ expression levels, functional studies are now in progress in the laboratory of Adrenal and Pituitary Physiopathology of the University of Padova.

The presence of gross deletions/duplications in the *CDKN1B* gene was also excluded in both the sporadic and familial cases by the homemade QMPSF assay and by LR-PCR. It should be noted that this kind of analysis for the *CDKN1B* gene is here reported for the first time.

The absence of either germline or somatic mutations in *CDKN1B* observed in sporadic GH-secreting pituitary tumours [(64;271;274), this study] suggests that their contribution to tumour pathogenesis is probably limited. However, there is considerable evidence that during the progression from normal to neoplastic pituitary, $p27^{Kip1}$ levels are decreased as a probable consequence of an impaired translational and/or post-translational mechanisms (66).

In conclusion, *AIP* germline mutations play a minor role in sporadic acromegaly patients, as well as in FIPA families without any evidence of acromegaly. In addition, mutations in *CDKN1B* are unlikely the genetic cause predisposing to the higher extrapituitary cancer risk observed in patients with acromegaly.

5.2 Study II

In the present study, genetic and bio-clinical features of a novel Italian FIPA family carrying an *AIP* p.R304X mutation have been described and compared with the two *AIP* p.R304X unrelated Italian kindreds previously reported (85;88;276;277). The p.R304X mutation leads to the premature termination of translation resulting in a loss of 26 amino acids at the end of the α-7 helix and consequent impairment of protein-protein interactions. In particular, integrity of the α-7 helix is essential for AIP to stabilise the AhR in a multimeric cytoplasmic complex (123;303) and, though AIP is generally expressed in R304X pituitary adenomas (87;145), AhR is destabilised in the corresponding tumours (145). Indeed, in agreement with LOH in 11q13 in most *AIP*-mutated pituitary adenomas (85;87;94;225;226), and as further demonstrated in this study, only the truncated R304X protein is expressed at a somatic level (145).

Together with the Finnish founder mutation *AIP* p.Q14X which, similarly to other disorders, is likely to reflect a founder effect in this population (85;304), the R304X currently represents the most frequently reported *AIP* mutation in FIPA. Yet, it has been reported in nine European FIPA kindreds (85;87;88;96;100), including two unrelated Italian families (85;88), as well as in two young patients with apparently sporadic acromegaly from France (228) and India (100). Thus, the family reported in this study is the third apparently unrelated Italian *AIP* p.R304X kindred, and a collaborative study was thought in order to look for a potential common ancestor. Data obtained on haplotyping around the *AIP* gene revealed that the two kindreds, who probably originated from the same region of central Italy (the oldest male subject in family 2 was adopted in this region), shared about 6 Mb on chromosome 11q (Table 4.4), supporting the presence of a founder effect in this region – namely Lazio -. Conversely, the nucleotide substitution observed in family 3 could be ascribed to an independent mutational event.

Because *AIP* p.R304Q mutations have also been described in three sporadic patients with acromegaly (94;201;228), one with Cushing's disease (94), and in two FIPA families (87;96), originating from at least four different countries, the presence of a mutational hot-spot at codon 304 is likely. From a genetic point of view, this could be related to the presence of two CpG dinucleotides located within a CG-rich region. Indeed, DNA methylation of intragenic CpGs followed by

deamination of 5-methylcytosine to thymine, is the most frequent cause of point mutations in humans, accounting for about 20% of all base substitutions causing genetic diseases (305). Of note, a second mutational hot spot, *AIP* p.R271W, has been recently identified in five FIPA kindreds (88;233). Because of the small size of FIPA families and the number of *AIP* mutations reported so far, potential genotype-phenotype correlations have been rarely addressed (102;233;293). In this study the clinical presentation of seven *AIP* p.R304X patients have been compared and the penetrance of the disease has been evaluated among R304X carriers according to familial screening. Depending on the type of calculation used, the penetrance of pituitary adenomas in R304X carriers observed in the three families was either slightly higher or the same as that reported by Naves *et al*. (102) in a large Brazilian family carrying the *AIP* p.E174fsX47 mutation (41 or 33% vs 33%, respectively). Actually, these values might be underrated since one healthy carrier is younger than 30 years of age (the age at first symptoms in the oldest affected patient) and therefore could theoretically develop a pituitary tumour. Taking into account data reported on R304X obligated mutation carriers [(87;96;100), this study], up to 35 out of 86 carriers identified so far have developed clinical evidence of pituitary adenomas (41%). However, there is an ascertainment bias for the presentation of affected subjects; thus, the true penetrance is probably lower than that predicted from the available data. In any case, further studies both in high-risk families and in a general population are mandatory for a more reliable penetrance estimation.

Differences in *AIP*-related disease penetrance or expressivity may in part depend on the functional consequences of the mutation itself (i.e. localisation and type of missense mutation, length of the truncated protein). Interestingly, significant phenotypic variability could be observed even among *AIP* p.R304X kindreds, as illustrated herein by the severe phenotype observed in family 2 as compared to family 1, despite a common genetic background was assessed by haplotyping. Intrafamilial variability can also be present, with an heterogeneous FIPA pattern observed in family 1 and in two previously reported kindreds (87), and an homogeneous pattern for somatotropinomas in families 2 and 3, respectively. Disease variability points out the role of additional factors, such as environmental factors or genetic modifiers, in determining the clinical phenotype (306). However, all *AIP* p.R304X patients reported so far [(85;87;88;96;100;228;276;277), this

study] had GH and/or PRL-secreting adenomas, with a large predominance of somatotropinomas and a young age at disease onset (46.7% and 93.3% under 20 and 30 years old, respectively, vs 6.7% over 40 years old). Although the frequent male predominance reported in patients with *AIP* mutations has not been observed in *AIP* p.R304X patients taken as a whole [16 males/17 females vs 41 males/16 females as reported in (293)], the mean age at diagnosis tends to be lower in males (17.4 ± 6.1 vs 24.9 ± 7.4 years old in female patients, P=0.10). Accordingly, gigantism is rare in females (87). It is remarkable that, in the present series, only the young boy diagnosed with pre-pubertal incipient gigantism could be successfully operated by transsphenoidal surgery. This strongly supports early genetic testing in these kindreds (224), as already proposed for MEN1, where pituitary evaluation is advised since early childhood (307).

Another important point is the potential resistance to pharmacological therapy. In fact, somatotropinoma resistance to SAs, has already been reported in acromegalic patients carrying different *AIP* mutations (225), suggesting that an altered AIP function and/or expression might in some way influence somatostatin receptor signalling.

In conclusion, while further supporting the presence of a mutational hot-spot at *AIP* codon 304, my data also provide the first genetic evidence for a founder effect of the *AIP* p.R304X mutation in a region of central Italy [a second founder effect for this mutation has been very recently described also in four families originating from Northern Ireland (100)]. In order to further define its magnitude and favour precocious diagnosis in potentially affected carriers, I suggest that special attention should be paid to young acromegalics in this region. The potential severity and common pharmacological resistance of R304X-related somatotropinomas further supports *AIP* mutational screening in such patients.

5.3 Study III

The main focus of this study is the evaluation of the involvement of miR-107 in the pathogenesis of pituitary tumours and its interaction with AIP. miR-107 is a member of the miR-15/107 gene superfamily and has known association with human cancer (290). Members of this family have previously been found to be altered in pituitary adenomas (36-38), suggesting they may play a role in the pathogenesis of pituitary tumours. The expression of miR-107 has been observed in many mammalian tissues, with the highest concentration found in the brain (308;309), and miR-107 has also been found to be overexpressed in several tumour types (33;310;311). In this study I showed, using miR array and qRT-PCR on normal human pituitaries and pituitary adenomas, that miR-107 is significantly upregulated in both sporadic GH-secreting pituitary adenomas and NFPAs, compared to normal pituitary tissues. In addition, I showed that miR-107 regulates the expression of the pituitary TSG *AIP*.

The biological functions exerted by miR-107 have only recently started to be unraveled. miR-107 is a conserved miRNA located within an intron of the gene encoding the pantothenate kinase enzyme 1 (PANK1), an enzyme involved in the regulation of cellular Co-enzyme A (CoA) levels. Although miR-107 was predicted to act synergistically with the *PANK1* gene in pathways involving acetyl-CoA and lipid levels (312), miR-107 and PANK1 expression have been experimentally proven to be uncorrelated (308;313). The reason for this discrepancy may be due to the fact that miR-107 is transcribed independently from the host mRNA, since it has been demonstrated to possess its own promoter within the intron of the *PANK1* gene (28;314). Experimental evidence supports a role for miR-107 in cell cycle arrest and growth suppression in lung and pancreatic cancers (309;311). Its involvement in the attenuation of tumour progression was also demonstrated to occur in colon cancer through a mechanism related to angiogenesis (292). In contrast, in breast and gastric cancer cells, high levels of miR-107 have been shown to promote invasivness and metastatic dissemination (310;315). Thus, it is apparent that miR-107 can act as a TSG or as an oncogene depending on the cell type, similarly to other miRNAs (316-319). In the present study I showed that miR-107 decreases both cell proliferation and colony formation efficiency in human SH-SY5Y cells. The inhibitory effect exerted by miR-107 is limited to cell growth in the

rat GH3 cell line. These results clearly demonstrate that miR-107 behaves as a TSG in neuroblastoma and pituitary adenoma cell lines.

Several direct miR-107 target genes have been identified and experimentally confirmed in various studies, including *NFI-A*, *BACE1*, *ARNT*, *PLAG1*, *CDK6*, *RBL2*, *GRN*, *INSIG1*, *PPIB and Dicer* (291;292;310;320-325). I decided to identify potential miR-107 target genes that could be involved in pituitary adenoma pathogenesis using various *in silico* software programs. Several bioinformatic algorithms have been developed so far to predict transcripts targeted by miRNAs (30;31;282-287). They are generally based on the assumption that the “seed” region of the miRNA forms perfect Watson–Crick pairing with the target sites, and is usually conserved between species. However, there is considerable evidence suggesting that the miRNA-mRNA interaction is much more complicated than simple base pairing. The secondary structure, as well as the whole 3’UTR sequence, may indeed contribute to miRNA function (285;326;327). For instance, the presence of RNA-binding proteins in the 3’UTR could physically prevent the interaction of miRNAs with nearby target sites (328). At present, each algorithm has a high false positive rate, and there are differences in these algorithms that often lead to variable predictions. These considerations imply the need to combine and weigh the information gathered from different *in silico* prediction programs in order to obtain confident predictions and underscore the limits of pure *in silico* approaches alone, which therefore require experimental validation.

Bearing this in mind, I ran several prediction programs. Combining all the outputs, two predicted target sites were repeatedly detected in the 3’UTR of *AIP*. Interestingly, both miR-107 and AIP have previously been demonstrated to regulate ARNT levels, a molecule which participates in one of the AIP-related pathways potentially involved in pituitary tumorigenesis (161;292). To determine whether miR-107 binds *in vitro* to AIP, I fused the entire human *AIP* 3′UTR containing the predicted miR-107 target sites to a luciferase reporter plasmid. As shown in Figure 4.13A, the luciferase activity of the hybrid transcript was markedly lower as compared with the luciferase vector without the insert. The 3’UTR of *AIP* could be thus considered a potent regulator of gene expression. The luciferase assay was then performed with different *AIP* 3’UTR mutants for the two putative miR-107 binding sites. These data suggest that only site 2 is responsible for miR-107-mediated *AIP* repression. This result indicates that binding site 1 has a lower

miR-binding ability under experimental conditions, probably because of a poor site accessibility that impedes the miRNA-mRNA duplex formation. Furthermore, if I applied the most stringent criteria for miR-binding predictions (30), only one program out of seven would predict site 1.

Site 2 is a non-conserved site, meaning that its sequence is not preserved across species. It is generally believed that 3'UTRs are under evolutionary pressure to maintain miRNA interactions, thus conservation is usually interpreted as an indication of functional or highly effective sites, whereas targets that do not possess evolutionary conserved complementarity to their counterparts may constitute either biologically important but species-specific targets or non-functional targets (329). Although proven to be functional, the non-conservation of site 2 may indicate that miR-107 is not the major determinant of the regulation of AIP expression. According to the classification made by Ye *et al*. (30), the miR-107-*AIP* duplex forming at site 2 possesses a type I decenter loop, which was shown to decrease the repressive efficiency of miRNAs. It is thus likely that miR-107 can act cooperatively with other negative and positive regulators to fine-tuning global AIP expression. Whatever the precise mechanism, I demonstrated that miR-107 overexpression alone is sufficient to significantly inhibit endogenous AIP mRNA and protein levels in human, but not in rat, cell lines (Figure 4.15). Taken together, these results suggest that the endogenous miR-107 can bind to the 3'UTR of the human AIP mRNA and inhibit protein synthesis by RNA degradation.

Since miR-107 was found to be upregulated in sporadic pituitary adenomas and shown to negatively regulate AIP expression, one would expect to find low AIP levels in such tumours. Low AIP expression was indeed observed in a subgroup of GH-secreting adenomas characterized by aggressive features (145;242), whereas high AIP expression was described in NFPAs (87;145;242), which are adenomas arising from a cell type normally not expressing AIP (87). I speculated that miR-107 overexpression might be due to an AIP-induced negative feedback mechanism on miR-107 expression, but this was shown not to be the case (Figure 4.17). In addition, the finding that both miR-107 and AIP are overexpressed in NFPAs corresponds with a previous observation made in pancreatic tumours that the predicted target genes of miR-107 are overexpressed more frequently than expected (311). An explanation for the elevated concomitant miR-107 and AIP levels could lie in other positive regulators of AIP which may provide a

compensatory mechanism able to restore AIP levels. In addition, the presence of potential competing binding sites for miR-107 on other mRNAs could contribute to our findings (330). Another plausible explanation is that the upregulation of miR-107 seen in sporadic pituitary adenomas (2/3-fold higher levels than that present in normal pituitary tissues) is not sufficient to suppress AIP expression as demonstrated by artificially overexpressing miR-107 in SH-SY5Y cells (8000-fold rise compared to untransfected cells) (Figure 4.11). Taking all these data together, I believe that AIP is differentially regulated in various pituitary cell types, as supported by 1) the different expression in normal pituitary cells (87); 2) the clinical data from AIP mutant patients having primarily somatotroph adenomas (224;331); 3) the aberrant emergence of AIP expression in sporadic non-GH/PRL adenomas (87); and 4) the aberrant subcellular localisation of AIP in sporadic non-GH-secreting adenomas (87;145). My data on miR-107 inhibiting AIP expression could play a role in aggressive somatotroph adenomas, a cell type where AIP is physiologically expressed, and therefore sensitive to normal regulators, while miR-107's effect may not be able to act on the abberantly expressed AIP in NFPAs.

In conclusion, miR-107 is overexpressed in pituitary adenomas and may act as a TSG. I have identified and experimentally validated *AIP* as an miR-107 target gene, and suggest that both AIP and miR-107 interact and may play roles in pituitary adenoma pathogenesis.

5.4 Study IV

In the present study I identified an increased expression of AHRR mRNA in somatotropinomas compared to normal pituitaries, with these levels particularly high in about 25% of cases (Figure 4.18). The biological functions of AHRR are not well understood, but recent findings suggest that AHRR is involved in the regulation of cell growth: AHRR overexpression inhibits *in vitro* the growth of human tumour cells (332-334), whereas knockdown of AHRR enhances cell growth and confers resistance to apoptosis (335). Consistent with this, the *AHRR* gene, which in humans maps to the short arm of chromosome 5 (5p15), has been found to be silenced by hypermethylation in a variety of human cancers (335). Absence of AHRR eliminates competition for binding to ARNT and AHREs, which results in an imbalance between positive and negative transactivation signals, thereby causing the induction of a series of genes related to tumorigenesis and cancer progression (335). Based on these and other findings, *AHRR* has been proposed to function as a TSG in cancers from different tissue origins (335;336).

An explanation for the observed overexpression of AHRR in GH-secreting adenomas is not immediately clear but the involvement of AHRR in the cellular senescence pathway may be proposed. This process presents a barrier for the development of true malignancies through the inhibition of cell cycle progression (48). Interestingly, AHRR overexpression has been shown to slow tumour growth by disturbing the transcriptional and/or post-translational regulation of cell cycle-related genes (332). In addition, some evidences point out the involvement of the AHRR target, AhR, in the inhibition of senescence (47). Cellular senescence is also known to occur in pituitary adenoma cells as a mechanism to escape from the deleterious consequences that the proliferative pressure of oncogenes, hormones and transformation factors could exert on their crucial control of homeostasis (48). Studies on the expression of a senescence marker (i.e. β-galactosidase), as well as of AHRR protein levels in the tumours examined, integrated by functional studies, such as AHRR overexpression/knockdown in GH3 cells, are mandatory to support this hypothesis and shed light on the AHRR pathway.

Appendix 1

Table 1 Summary of studies regarding screening for germline *CDKN1B* ($p27^{Kip1}$) mutations since its identification as a MEN predisposing gene. NA, not available.

N° of patients tested	Familial cases	Sporadic cases	Mutation	LOH	Phenotype of mutation-positive patients (age of onset/diagnosis)	Family history (age of onset/diagnosis)	Reference
1	1 family with MEN1 syndrome	-	c.G692A (p.W76X)	No	GH-secreting adenoma (30), primary HPT (46) (familial)	Father with acromegaly (NA); one mutation-positive sister with renal angiomyolipoma (55); the sister's son with testicular cancer (28), but unknown mutation status; two asymptomatic mutation-positive relatives (sister and niece)	(62)
106	34: 19 familial acromegaly/pituitary adenoma cases, 15 familial suspected MEN1 cases	72: 50 sporadic acromegaly cases, 22 sporadic suspected MEN1 cases	c.59_77dup19 (p.P26fsX103)	Yes (cervical carcinoma)	Small-cell neuroendocrine cervical carcinoma (45), ACTH-secreting adenoma (46), hyperparathyroidism (47) (apparently sporadic)	-	(64)
34	18: 11 familial cases with MEN1 variant (defined as pituitary tumour and parathyroid tumour without pancreas involvement), 5 cases diagnosed with FIPA, 2 cases diagnosed with familial hyperparathyroidism and renal angiomyolipoma	16 sporadic cases with MEN1 variant	None detected	-	-	-	(70)
27	-	27 cases with sporadic pancreatic endocrine tumours	None detected	-	-	-	(73)
35	-	35 cases with chronic kidney disease and refractory secondary or tertiary hyperparathyroidism	None detected	-	-	-	(74)
69	16 familial MEN1 cases	53 sporadic MEN1 cases	None detected	-	-	-	(69)
21	3 familial MEN1 cases	18 sporadic MEN1 cases	None detected	-	-	-	(67)

196	7% familial MEN1 cases, 17% familial primary hyperparathyroidism cases; 4% FIPA cases	35% sporadic MEN1 cases, 11% sporadic primary hyperparathyroidism cases, 8% multigland primary hyperparathyroidism cases, 7% hyperparathyroidism-jaw tumour syndrome or parathyroid cancer cases, 1% sporadic pituitary tumour cases, 10% other cases	c.-7G>C c.283C>T (p.P95S) c.595T>C (p.X199Q)	No NA NA	Primary hyperparathyroidism (1 tumour) (61), bilateral adrenal non-functioning mass (63), uterine fibroids Primary hyperparathyroidism (2 tumours) (50), Zollinger-Ellison syndrome (50), duodenal and pancreatic masses (50) Primary hyperparathyroidism (3 tumours) (50) (familial)	Two asymptomatic mutation-positive daughters (one with stomach problems) NA Monozygotic twin mutation-positive sister with primary HPT (66), aunt (52) and cousin (NA) with primary HPT, but unknown mutation status	(63)
27	-	27 MEN1 sporadic cases	c.678C>T (p.P69L)	Yes (carcinoid), No (parathyroid adenoma)	Bilateral multiple lung metastases of bronchial carcinoid, type 2 diabetes mellitus, non functioning pituitary microadenoma. History of endocrine and non-endocrine malignancies: papillary thyroid carcinoma with neck lymphnode metastases (64), multiple typical bronchial carcinoids, subcutaneous epigastric lipoma, parathyroid adenoma (67)	NA	(65)
29	6: 3 cases with family history of primary hyperparathyroidism, 3 cases with suspected MEN1 lesions in the family	23 cases with sporadic primary hyperparathyroidism	None detected	-	-	-	(72)
44	6 cases diagnosed with FIPA	38 sporadic acromegalic cases characterized by multiple neoplasia	None detected	-	-	-	(68)
91	12: 2 pediatric familial/syndromic Cushing's disease, 10 pediatric (n=3) and adult (n=7) familial/syndromic GH- and PRL-secreting adenomas	79: 74 cases with sporadic, isolated Cushing's disease, 5 pediatric isolated GH- and PRL-secreting adenomas	None detected	-	-	-	(71)

Table 2 Interacting partners of AIP. The techniques used to identify the various interactions, the functions of the different AIP partners and the organisms/cell types where the interactions have been proved are reported.

Partner	Y2H	co-IP	Pull-down	Other	Confirmed interaction	Function	Organism and/or cell type(s)	Reference
HBV X	✓			✓	Yes	transcriptional activator	human lymphoma, HeLa cells	(103)
EBNA-3	✓		✓		Yes	immortalization and transformation of B-cells	EBV-immortalized lymphoblastoid cells, human lymphocytes and fetal brain	(120)
AhR	✓	✓	✓	✓	Yes	adaptive and toxic responses, development	HeLa, Hepa1c1c7, COS-1, B-cells	(104;115;117)
Hsp90		✓	✓	✓	Yes	protein folding, mitochondrial protein import	HeLa, HEK, COS-1, COS-7, bacterial cells	(107;108;118;123-126)
Hsc70			✓		Yes	protein folding, mitochondrial protein import, disassembly of clathrin-coated vesicles	HeLa cells	(118)
Actin		✓			No	cytoskeletal component	COS-7 cells	(171)
PDE4A5	✓	✓	✓		Yes	cAMP degradation	rat brain, COS-7 cells	(177)
PDE2A3	✓	✓	✓		Yes	cAMP and cGMP degradation	human brain, COS-1, HeLa cells	(190)
PPARα		✓		✓	Yes	regulation of energy homeostasis	mouse liver	(194)
TRβ1	✓	✓			Yes	activation of TRH transcription	mouse paraventricular nucleus of the hypothalamus	(196)
RET	✓	✓			Yes	development, maturation, survival	human fetal brain, rat pituitary, neuroblastoma and HEK293 cells	(201)
EGFR	✓				No	cellular proliferation, survival, adhesion, migration, differentiation	human fetal brain	(204)
Gα13	✓		✓		Yes	mediates receptor-stimulated signalling pathways	HEK293T, Hepa1c1c7, COS-7 cells	(208)
Gαq			✓		Yes	mediates receptor-stimulated signalling pathways	HEK293T, Hepa1c1c7 cells	(208)
TOMM20	✓		✓		Yes	mitochondrial import receptor	human fetal liver, COS-7, HeLa cells	(118)
Survivin		✓	✓	✓	Yes	suppression of apoptosis	HeLa, MCF-7, Raji cells	(221)
TNNI3K	✓				No	promotes cardiomyogenesis, enhances cardiac performance, protects the myocardium from ischemic injury	human hearth	(223)

Table 3 SNPs and mutations reported in the *AIP* gene to date.

Region	Chr. Position	dbSNP rs#/Genbank ref	Heterozygosity	dbSNP allele	Codon position	DNA level	Protein level	Amino acid position	Mutation type	Patogenicity	Reference
5' near gene	67248532	rs1638579	N.D.	G/T	-		-	-	promoter	no	
5' near gene	67248638	rs11828274	0.5	A/C	-		-	-	promoter	no	
5' near gene	67248677	rs1638580	0.5	-/A/T	-		-	-	promoter	no	
5' near gene	67248677	rs77347124	0.278	A/T	-		-	-	promoter	no	
5' near gene	67248898	rs1790743	N.D.	A/G	-		-	-	promoter	no	
5' near gene	67249057	rs71058704	N.D.	-/C	-		-	-	promoter	no	
5' near gene	67249057	rs76325437	N.D.	-/G	-		-	-	promoter	no	
5' near gene	67249058	rs67365326	N.D.	-/G	-		-	-	promoter	no	
5' near gene	67249397	rs1638581	0.176	C/T	-		-	-	promoter	no	
5' near gene	67249694	rs71457777	0.5	C/T	-	c.-936T>C	-	-	promoter	no	
5' near gene	67249760	rs1638582	N.D.	A/C	-	c.-870A>C	-	-	promoter	no	
5' near gene	67249778	rs1638583	N.D.	A/C	-	c.-852A>C	-	-	promoter	no	
5' near gene	67249827			-/G	-	c.-802	-	-	promoter	no	
5' near gene					-	c.-270_269CG>AA	-	-	promoter	yes	(87)
5' near gene					-	c.-262G>A	-	-	promoter	no	(87)
5' near gene					-	c.-220G>A	-	-	promoter	no	(87)
5' near gene	67250464	rs12271280	N.D.	A/G	-	c.-166G>A	-	-	promoter	no	
5'UTR	67250544	rs1049506	N.D.	A/G	-	c.-86G>A	-	-		no	
5'UTR					-	c.-5G>C	-	-		?	(231)
exon 1	67250665	rs79662690	0.027	A/G	3	c.36G>A	p.=	12	synonymous	no	(87;228;230;231)
exon 1				G/A	2	c.47G>A	p.R16H	16	missense	no	
exon 1					2	c.68G>A	p.G23E	23	missense	no	(228;231)
exon 1					1	c.70G>T	p.E24X	24	nonsense	yes	(83;87)
exon 1					-	c.74_81delins7	p.L25PfsX130	25	in-frame	yes	(67)

									deletion		
intron 1	67250738	rs78579534	0.054	C/T	-	IVS1+10T>C	-	-	intronic	no	
intron 1	67251035	rs12272798	0.449	C/T	-	IVS1+307C>T	-	-	intronic	no	
intron 1	67251108	rs35392564	N.D.	-/TT	-	IVS1+380_99+381del2	-	-	intronic	no	
intron 1	67251108	rs76839115	0.219	A/T	-	IVS1+380T>A	-	-	intronic	no	
intron 1	67251109	rs74364031	0.219		-	IVS1+381T>C	-	-	intronic	no	
intron 1	67251254	rs1638584	0.234	C/T	-	IVS1+526T>C	-	-	intronic	no	
intron 1	67251302	rs1638585	0.244	C/G	-	IVS1+574G>C	-	-	intronic	no	
intron 1	67251855	rs79806126	0.153	A/G	-	IVS1+1127A>G	-	-	intronic	no	
intron 1	67251932	rs79124300	0.105	G/T	-	IVS1+1204T>G	-	-	intronic	no	
intron 1	67252177	rs1618605	0.235	G/T	-	IVS1+1449G>T	-	-	intronic	no	
intron 1	67252400	rs1620333	N.D.	C/T	-	IVS1+1672C>T	-	-	intronic	no	
intron 1	67252631	rs35670062	N.D.	-/G	-	IVS1-1846_100-1845insG	-	-	intronic	no	
intron 1	67252989	rs595130	N.D.	A/T	-	IVS1-1488T>A	-	-	intronic	no	
intron 1	67253136	rs57126355	N.D.	-/A	-	IVS1-1341_100-1340insA	-	-	intronic	no	
intron 1	67253215	rs57783261	N.D.	-/TT	-		-	-	intronic	no	
intron 1	67253215	rs68156813		-/T	-	IVS1-1262delT	-	-	intronic	no	
intron 1	67253382	rs59524104	N.D.	A/G	-	IVS1-1095G>A	-	-	intronic	no	
intron 1	67253564	rs7110021	0.278	C/T	-	IVS1-913T>C	-	-	intronic	no	
intron 1	67253673	rs630172	0.5	A/C	-	IVS1-804C>A	-	-	intronic	no	
intron 1	67253919	rs76605055	N.D.	C/G	-	IVS1-558C>G	-	-	intronic	no	
intron 1	67253921	rs75081450	N.D.	C/G	-	IVS1-556C>G	-	-	intronic	no	
intron 1					-	IVS1-18C>T	-	-	intronic	no	(94)
					-	c.1104-1109_279+578 (ex1_ex2del)	-	-	large genomic deletions	yes	(95)
					-	c.100-1025_279+357 (ex2del)	p.A34_K93	-	large genomic deletions	yes	(95)
exon 2						novel frameshift mutation			frameshift	?	(337)
exon 2	67254509	rs11822907	0.095	C/T	3	c.132C>T	p.=	44	synonymous	no	(228)
exon 2					3	c.135C>T	p.=	45	synonymous	?	(99)
exon 2					-	c.138_161del24	p.G47_R54del	-	in-frame deletion	?	(88)
exon 2					3	c.144C>T	p.=	48	synonymous	no	(68)
exon 2	67254522	rs1063385	N.D.	G/T	1	c.145G>T	p.V49L	49	missense	no	
exon 2					1	c.145G>A	p.V49M	49	missense	?	(99)
exon 2					1	c.241C>T	p.R81X	81	nonsense	yes	(87;92;93;338)
exon 2					3	c.249G>T	p.G83AfsX15	83	splice site	yes	(67)
intron 2	67255056	rs10896176	0.5	A/G	-	IVS2+400G>A	-	-	intronic	no	
intron 2	67255156	rs1790745	N.D.	A/G	-	IVS2+500T>C	-	-	intronic	no	
intron 2	67255170	rs581525	0.089	A/G	-	IVS2+514T>C	-	-	intronic	no	
intron 2	67255312	rs75859562	0.176	C/G	-	IVS2+656G>C	-	-	intronic	no	
intron 2	67255343	rs75105505	0.027	C/T	-	IVS2+687T>C	-	-	intronic	no	
intron 2	67255636	rs604540	0.239	C/T	-	IVS2+980T>C	-	-	intronic	no	
intron 2	67255855	rs11823597	0.18	C/T	-	IVS2-883C>T	-	-	intronic	no	
intron 2	67255877	rs35787427	0.278	C/T	-	IVS2-861C>T	-	-	intronic	no	

intron 2	67255953	rs595490	0.444	G/T	-	IVS2-785G>T	-	-	intronic	no	
intron 2	67256047	rs602720	N.D.	A/G	-	IVS2-691G>A	-	-	intronic	no	
intron 2	67256111	rs596431	N.D.	A/C	-	IVS2-627C>A	-	-	intronic	no	
intron 2	67256191	rs602220	N.D.	T/C	-	IVS2-547C>T	-	-	intronic	no	
intron 2	67256241	rs596944	N.D.	C/G	-	IVS2-497G>C	-	-	intronic	no	
intron 2	67256351	rs35286380	N.D.	-/C	-	IVS2-387_280-386insC	-	-	intronic	no	
intron 2	67256355	rs71461650	0.5	-/C	-	IVS2-383_280-382insC	-	-	intronic	no	
intron 2	67256369	rs601363	0.239	A/G	-	IVS2-369G>A	-	-	intronic	no	
intron 2					-	IVS2-81G>A	-	-	intronic	?	(228)
intron 2					-	c.280-1G>A	IVS2-1G>C	-	splice site	?	(94)
exon 3					-	c.286_287delGT	p.V96PfsX32	96	frameshift	yes	(84;99)
exon 3					2	c.308A>G	p.K103R	103	missense	?	(71;339)
exon 3					-	-	p.P114fs	114	frameshift	yes	(339)
exon 3		EF553637			2	c.404delA	p.H135LfsX20	135	frameshift	yes	(228)
exon 3					1	c.424C>T	p.Q142X	142	nonsense	yes	(88)
intron 3						IVS3+1G>A	-	-	intronic	yes	(68)
intron 3					-	IVS3+15C>T	-	-	intronic	?	(84;231)
intron 3	67257037	rs4084113	0.347	T/C	-	IVS3+111C>T	-	-	intronic	no	(228)
intron 3	67257062	rs79270719	0.077	A/G	-	IVS3+136A>G	-	-	intronic	no	(340)
intron 3	67257273	rs611697	0.202	A/C	-	IVS3-236G>T	-	-	intronic	no	
intron 3	67257294	rs75842186	0.077	G/T	-	IVS3-215G>T	-	-	intronic	no	
intron 3	67257359	rs5792416	N.D.	(>6bp)	-	IVS3-150_469-149ins4	-	-	intronic	no	
intron 3	67257360	rs33941803	N.D.	(>6bp)	-	IVS3-149_469-148ins4	-	-	intronic	no	
intron 3	67257365	rs10625132	N.D.	(>6bp)	-	IVS3-144_469-143ins4	-	-	intronic	no	
intron 3	67257366	rs33961879	N.D.	(>6bp)	-	IVS3-143_469-142ins4	-	-	intronic	no	
intron 3	67257366	rs76392311	0.147	A/T	-	IVS3-143A>T	-	-	intronic	no	
intron 3		EF553638			-	IVS3-2A>G	-	-	splice site	?	(228)
intron 3					-	IVS3-1G>A	-	-	splice site	yes	(85)
exon 4					1	c.490C>T	p.Q164X	164	nonsense	yes	(341)
exon 4	67257556	rs2276020	0.195	A/G	3	c.516C>T	p.=	172	synonymous	no	(99;225;228)
exon 4					-	c.500delC	p.P167HfsX3	167	frameshift	yes	(306)
exon 4					-	c.517_521delGAAGA	p.E174fsX47	174	frameshift	yes	(88;102)
exon 4					2	c.542delT	p.L181fsX13	181	frameshift	yes	(94)
exon 4		EF553639			1	c.601A>T	p.K201X	201	nonsense	yes	(228)
exon 4					-	c.622dupC	p.C208LfsX15	208	frameshift	yes	(67)
exon 4	67257680	rs3210041	N.D.	A/C	1	c.640A>C	p.M214L	214	missense	no	
intron 4					-	IVS4+37G>A	-	-	intronic	?	(228)
exon 5					1	c.649C>T	p.Q217X	217	nonsense	yes	(88)
exon 5					-	c.662dupC	p.E222X	222	nonsense	yes	(67)
exon 5	67257823	rs641081	0.308	G/T	1	c.682C>A	p.Q228K	228	missense	no	(225;228)
exon 5					3	c.696G>C	p.=	232	synonymous	?	(94)
exon 5					2	c.713G>A	p.C238Y	238	missense	yes	(87)
exon 5					3	c.714C>T	p.=	238	synonymous	?	(231)
exon 5					1	c.715C>T	p.Q239X	239	nonsense	yes	(88)
exon 5					3	c.720C>T	p.=	240	synonymous	no	(228)

exon 5					1	c.721A>G	p.K241E	241	missense	?	(88)
exon 5					1	c.721A>T	p.K241X	241	nonsense	yes	(71;339)
exon 5					-	c.742_744delTAC	p.Y248del	248	in-frame deletion	yes	(226)
exon 5					1	c.769A>G	p.I257V	257	missense	?	(342)
exon 5					3	c.783C>T	p.=	261	synonymous	no	(228)
exon 5	67257928	rs71679836	N.D.	LARGE DELETION	1			263	frameshift	no	
intron 5					-	IVS5+24C>T	-	-	intronic	no	(228)
exon 6					3	c.804A>C	p.Y268X	268	nonsense	yes	(98)
exon 6					-	c.805_825dup	p.F269_H275dup	-	in-frame insertion	yes	(87;93)
exon 6					3	c.807C>T	p.=	269	splice site	?	(87;228)
exon 6					1	c.811C>T	p.R271W	271	missense	yes	(88;233)
exon 6					-	c.824_825insA	p.H275QfsX12	275	frameshift	yes	(94)
exon 6	67258298	rs61741147	N.D.	C/T	2	c.827C>T	p.A276V	276	missense	no	
exon 6					3	c.831C>T	p.=	277	synonymous	?	unpublished
exon 6					-	c.854_857delAGGC	p.Q285fsX16	285	frameshift	yes	(88)
exon 6					1	c.871G>A	p.V291M	291	missense	?	(68)
exon 6					-	c.880_891delCTGGACCCAGCC	p.L294_A297del	294	in-frame deletion	?	(94)
						And	and				
exon 6					-	c.878_879AG>GT	p.E293G	293			
exon 6	67258362	rs35665586	0.027	A/C	3	c.891C>A	p.=	297	synonymous	no	(228)
exon 6		EF203235			2	c.896C>T	p.A299V	229	missense	?	(94;228)
exon 6					3	c.906G>A	p.=	302	synonymous	?	(94)
exon 6		AM236344			1	c.910C>T	p.R304X	304	nonsense	yes	(85;87;88;97;228)
exon 6		EF203236			2	c.911G>A	p.R304Q	304	missense	?	(68;87;94;228)
exon 6					1	c.919insC	p.Q307fsX103	307	frameshift	yes	(339)
exon 6	67258391	rs4930199	N.D.	A/G	2	c.920A>G	p.Q307R	307	missense	no	
exon 6					2	c.965C>T	p.A322V	322	missense	no	(228)
exon 6	67258452	rs1049565	N.D.	C/T	3	c.981C>T	p.=	327	synonymous	no	
exon 6					3	c.987C>T	p.=	329	synonymous	no	(228)
3'UTR					-	c.993+34C>G	-	-		?	(228)
3'UTR					-	c.993+56C>G	-	-		no	(228)
3'UTR					-	c.993+60G>C	-	-		no	(94;99;228)
3'UTR					-	c.993+70C>T	-	-		no	(68)
3'UTR					-	c.993+77C>A	-	-		?	(87)
3' near gene	67258720	rs12361982	N.D.	C/G	-	c.993+256G>C	-	-		no	
3' near gene	67258798	rs75044644	0.18	G/T	-	c.993+334T>G	-	-		no	
3' near gene	67258805	rs751567	0.425	C/G	-	c.993+341G>C	-	-		no	

					-	whole gene deletion	-	-	large genomic deletions	yes	(67)
					-	c.1-?_993+?del-	-	-	large genomic deletions	yes	(67)

Appendix 2

Figure 1 Pedigree structures for the 6 FIPA families analysed in study I. Families 1–4 were homogeneous for PRL-secreting adenomas, while families 5 and 6 were heterogeneous for PRL/NFPA (subjects III3 and I2 in families 5 and 6, respectively, carry a NFPA). Females and males are represented respectively with circles and squares. Probands are indicated by a black arrow. Below each subject the age at diagnosis is reported. NA, not available.

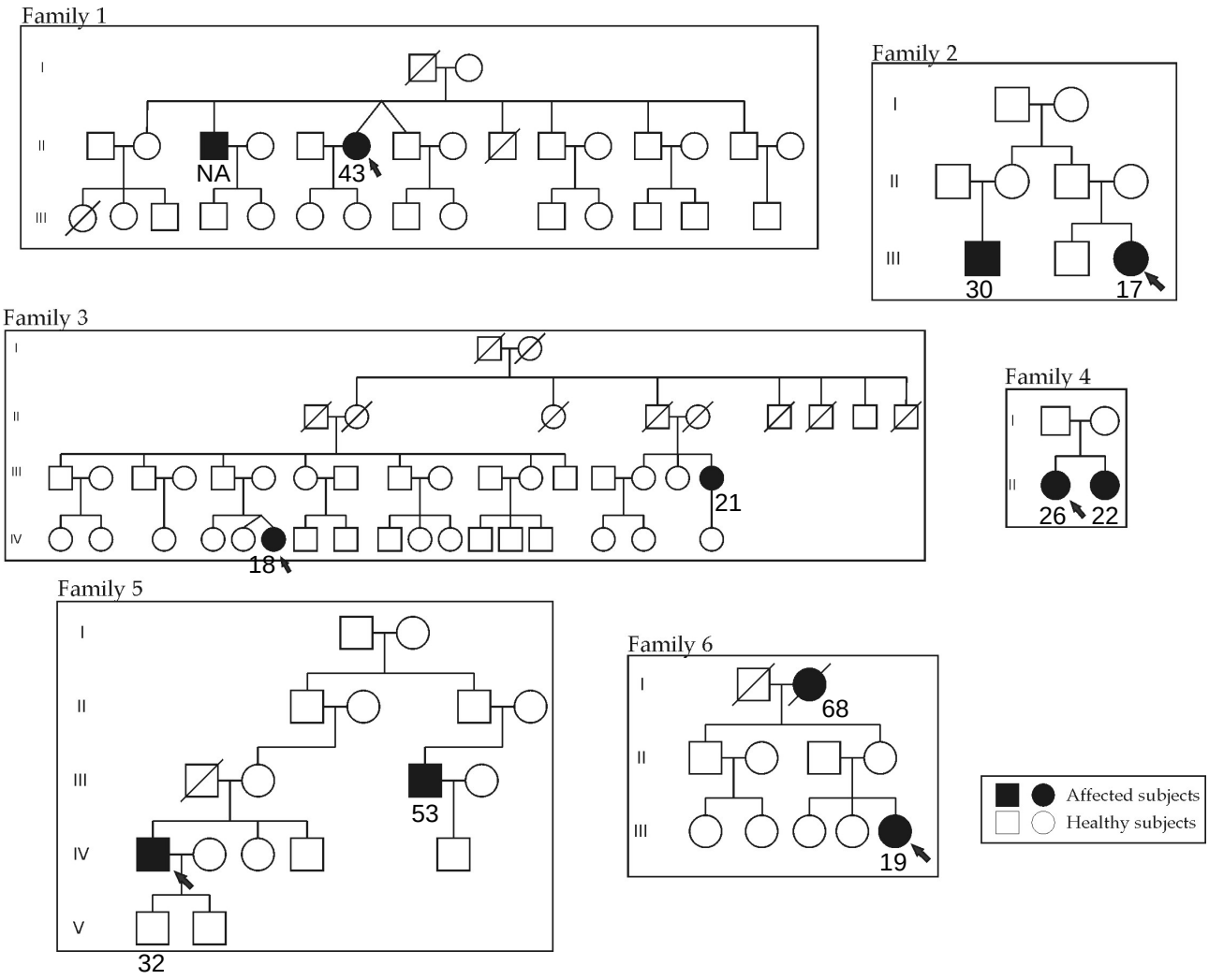

Table 1 Primers used to detect germline *AIP* and *CDKN1B* variants. Primers were tailed with an M13 forward or reverse primer sequence on the 5'-end. This allowed the use of universal M13 primers in the sequencing reaction.

Gene	Exon	Primer	Sequence (5'-3')	Product size (bp)
AIP	1	Forward	AACCAATCACCATCCGTTTC	397
		Reverse	GTCGAGTTCTGCATGTGAGC	
	2	Forward	GACTTCTCCTTGGGGGTCAG	311
		Reverse	CCTGGGGATAGGGAATAGGA	
	3	Forward	CAGCCCACGGTGACAGAG	377
		Reverse	AAGGGTCCTGCACAGGTTTT	
	4	Forward	AGATGTGGGTCAGGTCTGCT	337
		Reverse	GCGGGGAGAAGCTGTAGAC	
	5	Forward	CCTCAAGAACCTGCAGATGA	349
		Reverse	CTAGGTCTTGACCCCAGCAG	
	6	Forward	ATGGTGCCAGGAGACATGA	477
		Reverse	AACAGCCACCCAAGTACCAG	
CDKN1B	1a	Forward	CCAATGGATCTCCTCCTCTG	407
		Reverse	GGAGCCAAAAGACACAGACC	
	1b	Forward	CCATTTGATCAGCGGAGACT	438
		Reverse	GCCCTCTAGGGGTTTGTGAT	
	1c	Forward	GAGTTAACCCGGGACTTGGAG	445
		Reverse	ATACGCCGAAAAGCAAGCTA	
	2	Forward	TGACTATGGGGCCAACTTCT	296
		Reverse	TTTGCCAGCAACCAGTAAGA	
	3a	Forward	CCCCATCAAGTATTTCCAAGC	406
		Reverse	CCTCCCTTCCCCAAAGTTTA	
	3b	Forward	TGCCTCTAAAAGCGTTGGAT	542
		Reverse	TTTTTGCCCCAAACTACCTG	
	3c	Forward	GCCCTCCCCAGTCTCTCTTA	414
		Reverse	GGTTTTTCCATACACAGGCAAT	
	3d	Forward	TCTGTCCATTTATCCACAGGAA	474
		Reverse	TGCCAGGTCAAATACCTTGTT	

Table 2 Primers used in Tetra-primer ARMS-PCR experiments. The optimal conditions were experimentally determined for each reaction.

Variant	Primer	Sequence (5'-3')
c.144C>T	INNER Forward	GACGCTGCACAGTGACGACGAGGGCCCT
	OUTER Reverse	TGGACAGCCACCGCAGACAGGTACAGGA
	OUTER Forward	TGGGGGTCAGGGTGAGGGTTTGTGCCTTTG
	INNER Reverse	CCACGAGCCCGGCTGTCGTCCAGCCCG
c.871G>A	INNER Forward	CAGGAGGCCCAGGCTGACTTTGCCACAA
	OUTER Reverse	CCGGGCTTTGTCCTCTTCGTCCTTCTGC
	OUTER Forward	TGCCAGGAGACATGAGGGCAGGCAGCTG
	INNER Reverse	GCGCCAGGGCTGGGTCCAGCTCCAGAAC
c.911G>A	INNER Forward	ACCCAGCCCTGGCGCCTGTGGTGAGACA
	OUTER Reverse	GGGCTTGGCAGGTAAGGCAGGGCCAAGTGC
	OUTER Forward	CCCCCTCATGCCCTTGCATGCCCACT
	INNER Reverse	ATCCGTGCCTCCAGGGCCTGCAGCTATC
c.993+70C>T	INNER Forward	AGCTGCCAGCCCCCCTGCCCGTGCGGT
	OUTER Reverse	CCAGGTGATGACCCGGCTCTCCCAGTGGA
	OUTER Forward	GCAGACAACGTCAAGGCCTACTTCAA
	INNER Reverse	AGGCCTTTATATACACAGAAGCATGCCG

Table 3 Primers used for *CDKN1B* deletion analysis.

Amplicon	Primer	Sequence (5'-3')	Product size (bp)
CTRL -	Forward	TGTCTGTGACGCCGTTGTCT	276
	Reverse	AAGGGTTTTCTAGCACACATAGGAA	
p27_EX1_I	Forward	GCCGCAACCAATGGATCTC	115
	Reverse	ACGAGCCCCCTTTTTTTAGTG	
p27_EX1_II	Forward	CTCTGAGGACACGCATTTGGT	200
	Reverse	AAATCAGAATACGCCGAAAAGC	
p27_EX2	Forward	TTTCCCCTGCGCTTAGATTC	150
	Reverse	CCACCGAGCTGTTTACGTTTG	
p27_EX3_I	Forward	CCCCATCAAGTATTTCCAAGCT	256
	Reverse	GTTATTGTGTTGTTGTTTTTCAGTGCTTA	
p27_EX3_II	Forward	AACTTCCATAGCTATTCATTGAGTCAAA	173
	Reverse	AACTGCTAACTACATTCGGACTACATAAA	

Table 4 Primers used for haplotype analysis. *, primer sequences obtained from the UCSC Genome Browser website; †, primers designed with Primer3; #, (85).

D11S4076*	Forward	CATGAATGCTCTTGTCCC
	Reverse	AACCCCCTGGAAAATAGACT
m_11TETRA@61,73†	Forward	TGCAACTGCCATTTATTCAG
	Reverse	TGGCGTGATCTCAACTCA
D11S1883*	Forward	TTCAGTAACAGGAGACAAAAGG
	Reverse	TGGTTTCGGATCTCTTCTCA
AFMA190YD5*	Forward	GACATACCATGAACACTATAAGAGG
	Reverse	CAACCCATACCAGGGATAAG
D11S2072*	Forward	ATGGCTTCTGTTAAAAAAATAAAG
	Reverse	TCTCAGTGTTACATTATAAGTGA
D11S1889†	Forward	TGAACCTGTCGCAATCTCTTT
	Reverse	GAGCAGAGTCGAGCTTATCAGA
ACRO_CHR11_28#	Forward	GCTTTGGTGCATGGTATGTG
	Reverse	TCCACGCTTCCTTCAGAAAC
D11S987*	Forward	ACTCCAGTCTGGGCAATAAAAGC
	Reverse	GGTGGCAGCATGACCTCTAAAG
D11S4162†	Forward	GCACTGTTGACAGGCTTTTG
	Reverse	TCCAATTCCCATAACGAAGC
D11S1314†	Forward	CCCATCTACACATGCCACAC
	Reverse	GCGGCTCTTTTCTACACACC

Table 5 Primers used in cloning experiments.

Study I	Forward	GAGTCTCGAGCGTCCCTTATGCCGTCTG
	Reverse	AGAGAAGCTTGCAGTCTAGCAGAGGGTGGA
Study III	Forward	GGGTCTAGACGTCAAGGCCTACTTCAAGC
	Reverse	GGGTCTAGACCAGTTCAACAGGGGACACT

Table 6 Site-directed mutagenesis primers. Primers were designed using the Stratagene's QuickChange primer design program.

Site 1	Forward	GCCAAGCCCACTCAGCTGCCAGCC
	Reverse	GGCTGGCAGCTGAGTGGGCTTGGC
Site 2	Forward	CCCCCCTGCCCGTCGTCATGCTTC
	Reverse	GAAGCATGACGACGGGCAGGGGGG

Appendix 3

Figure 1 PolyPhen-2 report for *AIP* p.R304Q.

Query

Protein Acc	Position	AA_1	AA_2	Description
AIP	304	R	Q	N/A

Results

Prediction/Confidence

HumDiv

This mutation is predicted to be benign with a score of **0.011** (sensitivity: **0.96**; specificity: **0.73**)

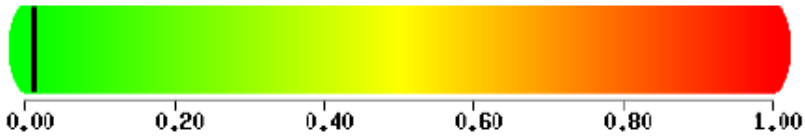

Figure 2 PolyPhen-2 report for *AIP* p.V291M.

Query

Protein Acc	Position	AA_1	AA_2	Description
AIP	291	V	M	N/A

Results

Prediction/Confidence *PolyPhen-2 v2.0.23r349*

HumDiv

This mutation is predicted to be probably damaging with a score of **0.903** (sensitivity: **0.78**; specificity: **0.91**)

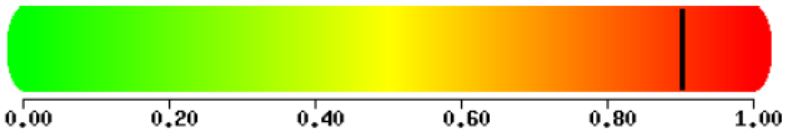

Figure 3 Alamut output for *AIP* IVS3+1G>A.

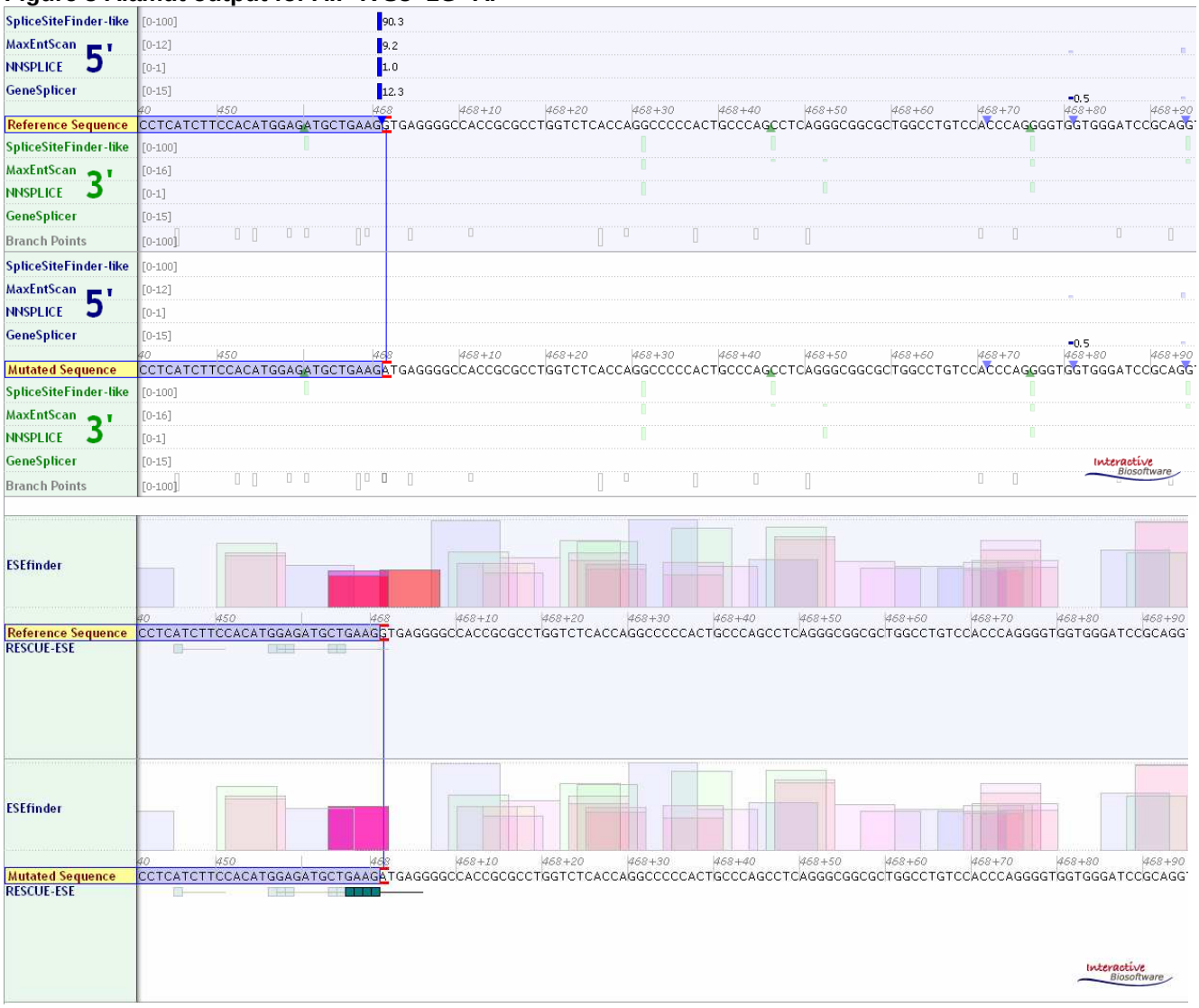

Figure 4 Alamut output for *AIP* p.T48T.

Figure 5 Putative miR-107 target sites in the 3'UTR of *AIP* predicted by five different programs. The outputs of A) TargetScan, B) MicroCosm, C) FindTar, D) MicroTar, E) PITA are shown. The miRNA prediction tools MicroTar and PITA calculate also miR-107 target sites accessibility as measured by the energetic scores "Dimer-Monomer Difference" and "ΔΔG", respectively. The lower the values, the stronger the binding of the miRNA is expected to be to the given site.

A

Poorly conserved

	predicted consequential pairing of target region (top) and miRNA (bottom)	seed match
Position 38-44 of AIP 3' UTR	5' ...ACCUGCCAAGCCCACUGCUGCAG...	7mer-1A
hsa-miR-107	3' ACUAUCGGGACAUGUUACGACGA	

B

Rfam ID	Score	Energy	Base P	Poisson P	Org P	Start	End	Alignment
hsa-miR-107	15.8384	-19.77	7.497160e-02	7.223020e-02	7.460080e-03	50	71	GGGACAUGUUACGACG ||||| | :|||||| CCCTG-CCCGTGCTGC

C

```
Find Targets of hsa-miR-107 Position 17-44. Loop Score 20, ΔG -23, Tail Score 13

hsa-miR-107     3' ACTATCGGGACATGTTACGACGA 5'
                   *****|||**|**||*******
AIP             5' TACCTGCCAAGCCCACTGCTGCA 3'
Find Targets of hsa-miR-107 Position 47-71. Loop Score 20, ΔG -26.5, Tail Score 18
hsa-miR-107     3' ACTATCGGG-ACATG-TTACGACGA 5'
                   ****|||||***|:|**:|******
AIP             5' TGCCAGCCCCCCTGCCCGTGCTGCG 3'
```

D

```
          70
          |
mRNA    3'  CGTCGTG  5'
miRNA   5'  GCAGCAT  3'
          |
          2
mRNA Monomer Energy       : -27.60
mRNA::miRNA Dimer Energy  : -36.40
Dimer-Monomer Difference  : -8.80
-ve Normalized Free Energy : 1.123026
```

E

Sites	ΔGduplex	ΔGopen	ΔΔG
Site 1	-22.7	-12.62	-10.14
Site 2	-22.4	-10.76	-11.63

Acknowledgements

This work was carried out during the years 2008-2010 at the Department of Medical and Surgical Sciences, University of Padova, and at the Department of Endocrinology, William Harvey Research Institute, Queen Mary University of London. I would like to express my deepest gratitude to all those who partecipated in this study:

My supervisor Professor Carla Scaroni, and my co-supervisor Dr Gianluca Occhi for their guidance, support and encouragement throughout the three years of my PhD.

The head of the Endocrinology Division of Padova Hospital, Professor Franco Mantero, for giving me the opportunity to work in the laboratory of Adrenal and Pituitary Physiopathology.

Professor Márta Korbonits and Professor Ashley Grossman for accepting me in their group during the last year of my PhD. Their profound knowledge on endocrinology and genetics has been essential to complete this work.

All friends and colleagues from the Department of Medical and Surgical Sciences in Padova and from the Department of Endocrinology in London for their friendship and technical assistance.

My family and friends, especially my parents Sebastiano and Lionella, for their support and practical help during all these years.

My girlfriend Clara. I am grateful beyond words for her many wonderful qualities, but above all for her love, trust, patience and support.

Padova, January 2011

Reference List

1. **DeGroot LJ, Jameson J** 2006 Endocrinology, 5th edition., Elsevier Saunders edn

2. **Yeung CM, Chan CB, Leung PS, Cheng CH** 2006 Cells of the anterior pituitary. Int J Biochem Cell Biol 38:1441-1449

3. **Ooi GT, Tawadros N, Escalona RM** 2004 Pituitary cell lines and their endocrine applications. Mol Cell Endocrinol 228:1-21

4. **Nussey S, Whitehead S** 2001 Endocrinology: An Integrated Approach., London:Taylor & Francis edn

5. **Asa SL, Ezzat S** 2009 The pathogenesis of pituitary tumors. Annu Rev Pathol 4:97-126

6. **Herman V, Fagin J, Gonsky R, Kovacs K, Melmed S** 1990 Clonal origin of pituitary adenomas. J Clin Endocrinol Metab 71:1427-1433

7. **DeLellis RA, Lloyd RV, Heitz PU, Eng C** 2004 WHO Pathology and genetics of tumours of endocrine organs., IARC Press, Lyon edn

8. **Yamada S** 2001 Epidemiology of pituitary tumors. In: Thapar K, Kovacs K, Scheithauer BW, Lloyd RV (eds). Diagnosis and management of pituitary tumors.Humana Press, Totawa:57-69

9. **Fernandez A, Karavitaki N, Wass JA** 2010 Prevalence of pituitary adenomas: a community-based, cross-sectional study in Banbury (Oxfordshire, UK). Clin Endocrinol (Oxf) 72:377-382

10. **Chacko G, Chacko AG, Lombardero M, Mani S, Seshadri MS, Kovacs K, Scheithauer BW** 2009 Clinicopathologic correlates of giant pituitary adenomas. J Clin Neurosci 16:660-665

11. **Marie P** 1886 Sur deux cas d'acromegalie. Hyperthrophe singuliere no congénitale des extrémités supérieuses et cephalique. Revue Médicale Française 6:297-333

12. **de Herder WW** 2009 Acromegaly and gigantism in the medical literature. Case descriptions in the era before and the early years after the initial publication of Pierre Marie (1886). Pituitary 12:236-244

13. **Melmed S** 2006 Medical progress: Acromegaly. N Eng J Med 355:2558-2573

14. **Colao A, Ferone D, Marzullo P, Lombardi G** 2004 Systemic complications of acromegaly: epidemiology, pathogenesis, and management. Endocrine Rev 25:102-152

15. **Cordero RA, Barkan AL** 2008 Current diagnosis of acromegaly. Rev Endocr Metab Disord 9:13-19

16. **Bertagna X, Guignat L, Groussin L, Bertherat J** 2009 Cushing's disease. Best Pract Res Clin Endocrinol Metab 23:607-623

17. **Knudson AG, Jr.** 1971 Mutation and cancer: statistical study of retinoblastoma. Proc Natl Acad Sci USA 68:820-823

18. **Weinberg RA** 2007 The biology of cancer, 1st edition.Taylor & Francis Group, 1st edn

19. **Lania A, Mantovani G, Spada A** 2003 Genetics of pituitary tumors: Focus on G-protein mutations. Exp Biol Med (Maywood) 228:1004-1017

20. **Boikos SA, Stratakis CA** 2007 Molecular genetics of the cAMP-dependent protein kinase pathway and of sporadic pituitary tumorigenesis. Hum Mol Genet 16 Spec No 1:R80-R87

21. **Malumbres M, Barbacid M** 2005 Mammalian cyclin-dependent kinases. Trends Biochem Sci 30:630-641

22. **Quereda V, Malumbres M** 2009 Cell cycle control of pituitary development and disease. J Mol Endocrinol 42:75-86

23. **Franklin DS, Godfrey VL, Lee H, Kovalev GI, Schoonhoven R, Chen-Kiang S, Su L, Xiong Y** 1998 CDK inhibitors p18(INK4c) and p27(Kip1) mediate two separate pathways to collaboratively suppress pituitary tumorigenesis. Genes Dev 12:2899-2911

24. **Fero ML, Rivkin M, Tasch M, Porter P, Carow CE, Firpo E, Polyak K, Tsai LH, Broudy V, Perlmutter RM, Kaushansky K, Roberts JM** 1996 A syndrome of multiorgan hyperplasia with features of gigantism, tumorigenesis, and female sterility in p27(Kip1)-deficient mice. Cell 85:733-744

25. **Kiyokawa H, Kineman RD, Manova-Todorova KO, Soares VC, Hoffman ES, Ono M, Khanam D, Hayday AC, Frohman LA, Koff A** 1996 Enhanced growth of mice lacking the cyclin-dependent kinase inhibitor function of p27(Kip1). Cell 85:721-732

26. **Nakayama K, Ishida N, Shirane M, Inomata A, Inoue T, Shishido N, Horii I, Loh DY, Nakayama K** 1996 Mice lacking p27(Kip1) display increased body size, multiple organ hyperplasia, retinal dysplasia, and pituitary tumors. Cell 85:707-720

27. **Fabian MR, Sonenberg N, Filipowicz W** 2010 Regulation of mRNA translation and stability by microRNAs. Annu Rev Biochem 79:351-379

28. **Monteys AM, Spengler RM, Wan J, Tecedor L, Lennox KA, Xing Y, Davidson BL** 2010 Structure and activity of putative intronic miRNA promoters. RNA 16:495-505

29. **Kim VN** 2005 MicroRNA biogenesis: coordinated cropping and dicing. Nat Rev Mol Cell Biol 6:376-385

30. **Ye W, Lv Q, Wong CK, Hu S, Fu C, Hua Z, Cai G, Li G, Yang BB, Zhang Y** 2008 The effect of central loops in miRNA:MRE duplexes on the efficiency of miRNA-mediated gene regulation. PLoS One 3:e1719

31. **Bartel DP** 2009 MicroRNAs: target recognition and regulatory functions. Cell 136:215-233

32. **Jeffrey SS** 2008 Cancer biomarker profiling with microRNAs. Nat Biotechnol 26:400-401

33. **Volinia S, Calin GA, Liu CG, Ambs S, Cimmino A, Petrocca F, Visone R, Iorio M, Roldo C, Ferracin M, Prueitt RL, Yanaihara N, Lanza G, Scarpa A, Vecchione A, Negrini M, Harris CC, Croce CM** 2006 A microRNA expression signature of human solid tumors defines cancer gene targets. Proc Natl Acad Sci USA 103:2257-2261

34. **Garzon R, Calin GA, Croce CM** 2009 MicroRNAs in Cancer. Annu Rev Med 60:167-179

35. **Voorhoeve PM** 2010 MicroRNAs: Oncogenes, tumor suppressors or master regulators of cancer heterogeneity? Biochim Biophys Acta 1805:72-86

36. **Amaral FC, Torres N, Saggioro F, Neder L, Machado HR, Silva WA, Jr., Moreira AC, Castro M** 2009 MicroRNAs differentially expressed in ACTH-secreting pituitary tumors. J Clin Endocrinol Metab 94:320-323

37. **Bottoni A, Piccin D, Tagliati F, Luchin A, Zatelli MC, Degli Uberti EC** 2005 miR-15a and miR-16-1 down-regulation in pituitary adenomas. J Cell Physiol 204:280-285

38. **Bottoni A, Zatelli MC, Ferracin M, Tagliati F, Piccin D, Vignali C, Calin GA, Negrini M, Croce CM, Degli Uberti EC** 2007 Identification of differentially expressed microRNAs by microarray: a possible role for microRNA genes in pituitary adenomas. J Cell Physiol 210:370-377

39. **Butz H, Liko I, Czirjak S, Igaz P, Korbonits M, Racz K, Patocs A** 2010 MicroRNA profile indicates downregulation of the TGFbeta pathway in sporadic non-functioning pituitary adenomas. Pituitary (Epub ahead of print)

40. **Butz H, Liko I, Czirjak S, Igaz P, Munayem KM, Zivkovic V, Balint K, Korbonits M, Racz K, Patocs A** 2010 Down-regulation of Wee1 kinase by a specific subset of microRNA in human sporadic pituitary adenomas. J Clin Endocrinol Metab 95:E181-E191

41. **Qian ZR, Asa SL, Siomi H, Siomi MC, Yoshimoto K, Yamada S, Wang EL, Rahman MM, Inoue H, Itakura M, Kudo E, Sano T** 2009 Overexpression of HMGA2 relates to reduction of the let-7 and its

relationship to clinicopathological features in pituitary adenomas. Mod Pathol 22:431-441

42. **Stilling G, Sun ZF, Zhang SY, Jin L, Righi A, Gabor K, Korbonits M, Scheithauer BW, Kovacs K, Lloyd RV** 2010 MicroRNA expression in ACTH-producing pituitary tumors: up-regulation of microRNA-122 and-493 in pituitary carcinomas. Endocrine 38:67-75

43. **Cheung HH, Lee TL, Rennert OM, Chan WY** 2009 DNA methylation of cancer genome. Birth Defects Res C Embryo Today 87:335-350

44. **Dudley KJ, Revill K, Clayton RN, Farrell WE** 2009 Pituitary tumours: all silent on the epigenetics front. J Mol Endocrinol 42:461-468

45. **Korbonits M, Morris DG, Nanzer A, Kola B, Grossman AB** 2004 Role of regulatory factors in pituitary tumour formation. Front Horm Res 32:63-95

46. **Kuilman T, Michaloglou C, Vredeveld LC, Douma S, van DR, Desmet CJ, Aarden LA, Mooi WJ, Peeper DS** 2008 Oncogene-induced senescence relayed by an interleukin-dependent inflammatory network. Cell 133:1019-1031

47. **Ray S, Swanson HI** 2009 Activation of the aryl hydrocarbon receptor by TCDD inhibits senescence: a tumor promoting event? Biochem Pharmacol 77:681-688

48. **Chesnokova V, Melmed S** 2010 Pituitary senescence: the evolving role of Pttg. Mol Cell Endocrinol 326:55-59

49. **Chesnokova V, Zonis S, Kovacs K, Ben-Shlomo A, Wawrowsky K, Bannykh S, Melmed S** 2008 p21(Cip1) restrains pituitary tumor growth. Proc Natl Acad Sci USA 105:17498-17503

50. **Landis CA, Masters SB, Spada A, Pace AM, Bourne HR, Vallar L** 1989 GTPase inhibiting mutations activate the alpha chain of Gs and stimulate adenylyl cyclase in human pituitary tumours. Nature 340:692-696

51. **Lania A, Spada A** 2009 G-protein and signalling in pituitary tumours. Horm Res 71 Suppl 2:95-100

52. **Vallar L, Spada A, Giannattasio G** 1987 Altered Gs and adenylate cyclase activity in human GH-secreting pituitary adenomas. Nature 330:566-568

53. **Stork PJ, Schmitt JM** 2002 Crosstalk between cAMP and MAP kinase signaling in the regulation of cell proliferation. Trends Cell Biol 12:258-266

54. **Ham J, Ivan M, Wynford-Thomas D, Scanlon MF** 1997 GH3 cells expressing constitutively active Gs alpha (Q227L) show enhanced hormone secretion and proliferation. Mol Cell Endocrinol 127:41-47

55. **Weinstein LS, Shenker A, Gejman PV, Merino MJ, Friedman E, Spiegel AM** 1991 Activating mutations of the stimulatory G protein in the McCune-Albright syndrome. N Eng J Med 325:1688-1695

56. **Thakker RV** 2010 Multiple endocrine neoplasia type 1 (MEN1). Best Pract Res Clin Endocrinol Metab 24:355-370

57. **Agarwal SK, Ozawa A, Mateo CM, Marx SJ** 2009 The MEN1 gene and pituitary tumours. Horm Res 71 Suppl 2:131-138

58. **Lemos MC, Thakker RV** 2008 Multiple endocrine neoplasia type 1 (MEN1): analysis of 1336 mutations reported in the first decade following identification of the gene. Hum Mutat 29:22-32

59. **Elston MS, McDonald KL, Clifton-Bligh RJ, Robinson BG** 2009 Familial pituitary tumor syndromes. Nat Rev Endocrinol 5:453-461

60. **Burgess JR, Nord B, David R, Greenaway TM, Parameswaran V, Larsson C, Shepherd JJ, Teh BT** 2000 Phenotype and phenocopy: the relationship between genotype and clinical phenotype in a single large family with multiple endocrine neoplasia type 1 (MEN 1). Clin Endocrinol (Oxf) 53:205-211

61. **Hai N, Aoki N, Shimatsu A, Mori T, Kosugi S** 2000 Clinical features of multiple endocrine neoplasia type 1 (MEN1) phenocopy without germline MEN1 gene mutations: analysis of 20 Japanese sporadic cases with MEN1. Clin Endocrinol (Oxf) 52:509-518

62. **Pellegata NS, Quintanilla-Martinez L, Siggelkow H, Samson E, Bink K, Hofler H, Fend F, Graw J, Atkinson MJ** 2006 Germ-line mutations in p27Kip1 cause a multiple endocrine neoplasia syndrome in rats and humans. Proc Natl Acad Sci USA 103:15558-15563

63. **Agarwal SK, Mateo CM, Marx SJ** 2009 Rare germline mutations in cyclin-dependent kinase inhibitor genes in multiple endocrine neoplasia type 1 and related states. J Clin Endocrinol Metab 94:1826-1834

64. **Georgitsi M, Raitila A, Karhu A, van der Luijt RB, Aalfs CM, Sane T, Vierimaa O, Makinen MJ, Tuppurainen K, Paschke R, Gimm O, Koch CA, Gundogdu S, Lucassen A, Tischkowitz M, Izatt L, Aylwin S, Bano G, Hodgson S, De ME, Launonen V, Vahteristo P, Aaltonen LA** 2007 Germline CDKN1B/p27Kip1 mutation in multiple endocrine neoplasia. J Clin Endocrinol Metab 92:3321-3325

65. **Molatore S, Marinoni I, Lee M, Pulz E, Ambrosio MR, Uberti EC, Zatelli MC, Pellegata NS** 2010 A novel germline CDKN1B mutation causing multiple endocrine tumors: clinical, genetic and functional characterization. Hum Mutat 31:E1825-E1835

66. **Marinoni I, Pellegata NS** 2010 p27kip1: A New Multiple Endocrine Neoplasia Gene? Neuroendocrinology (Epub ahead of print)

67. **Igreja S, Chahal HS, Akker SA, Gueorguiev M, Popovic V, Damjanovic S, Burman P, Wass JA, Quinton R, Grossman AB, Korbonits M** 2009 Assessment of p27 (cyclin-dependent kinase inhibitor 1B) and aryl hydrocarbon receptor-interacting protein (AIP) genes in multiple endocrine neoplasia (MEN1) syndrome patients without any detectable MEN1 gene mutations. Clin Endocrinol (Oxf) 70:259-264

68. **Occhi G, Trivellin G, Ceccato F, De LP, Giorgi G, Dematte S, Grimaldi F, Castello R, Davi MV, Arnaldi G, Salviati L, Opocher G, Mantero F, Scaroni C** 2010 Prevalence of AIP mutations in a large series of sporadic Italian acromegalic patients and evaluation of CDKN1B status in acromegalic patients with multiple endocrine neoplasia. Eur J Endocrinol 163:369-376

69. **Owens M, Stals K, Ellard S, Vaidya B** 2009 Germline mutations in the CDKN1B gene encoding p27Kip1 are a rare cause of multiple endocrine neoplasia type 1. Clin Endocrinol (Oxf) 70:499-500

70. **Ozawa A, Agarwal SK, Mateo CM, Burns AL, Rice TS, Kennedy PA, Quigley CM, Simonds WF, Weinstein LS, Chandrasekharappa SC, Collins FS, Spiegel AM, Marx SJ** 2007 The parathyroid/pituitary variant of multiple endocrine neoplasia type 1 usually has causes other than p27Kip1 mutations. J Clin Endocrinol Metab 92:1948-1951

71. **Stratakis CA, Tichomirowa MA, Boikos S, Azevedo MF, Lodish M, Martari M, Verma S, Daly AF, Raygada M, Keil MF, Papademetriou J, Drori-Herishanu L, Horvath A, Tsang KM, Nesterova M, Franklin S, Vanbellinghen JF, Bours V, Salvatori R, Beckers A** 2010 The role of germline AIP, MEN1, PRKAR1A, CDKN1B and CDKN2C mutations in causing pituitary adenomas in a large cohort of children, adolescents, and patients with genetic syndromes. Clin Genet 78:457-463

72. **Vierimaa O, Villablanca A, Alimov A, Georgitsi M, Raitila A, Vahteristo P, Larsson C, Ruokonen A, Eloranta E, Ebeling TM, Ignatius J, Aaltonen LA, Leisti J, Salmela PI** 2009 Mutation analysis of MEN1, HRPT2, CASR, CDKN1B and AIP genes in primary hyperparathyroidism patients with features of genetic predisposition. J Endocrinol Invest 32:512-518

73. **Lindberg D, Akerstrom G, Westin G** 2007 Mutational analysis of p27 (CDKN1B) and p18 (CDKN2C) in sporadic pancreatic endocrine tumors argues against tumor-suppressor function. Neoplasia 9:533-535

74. **Lauter KB, Arnold A** 2008 Mutational analysis of CDKN1B, a candidate tumor-suppressor gene, in refractory secondary/tertiary hyperparathyroidism. Kidney Int 73:1137-1140

75. **Pellegata NS, Quintanilla-Martinez L, Keller G, Liyanarachchi S, Hofler H, Atkinson MJ, Fend F** 2007 Human pheochromocytomas show reduced p27Kip1 expression that is not associated with somatic gene mutations and rarely with deletions. Virchows Arch 451:37-46

76. **Boikos SA, Stratakis CA** 2007 Carney complex: the first 20 years. Curr Opin Oncol 19:24-29

77. **Carney JA, Gordon H, Carpenter PC, Shenoy BV, Go VL** 1985 The complex of myxomas, spotty pigmentation, and endocrine overactivity. Medicine (Baltimore) 64:270-283

78. **Horvath A, Stratakis CA** 2008 Clinical and molecular genetics of acromegaly: MEN1, Carney complex, McCune-Albright syndrome, familial acromegaly and genetic defects in sporadic tumors. Rev Endocr Metab Disord 9:1-11

79. **Stratakis CA, Carney JA, Lin JP, Papanicolaou DA, Karl M, Kastner DL, Pras E, Chrousos GP** 1996 Carney complex, a familial multiple neoplasia and lentiginosis syndrome. Analysis of 11 kindreds and linkage to the short arm of chromosome 2. J Clin Invest 97:699-705

80. **Kirschner LS, Sandrini F, Monbo J, Lin JP, Carney JA, Stratakis CA** 2000 Genetic heterogeneity and spectrum of mutations of the PRKAR1A gene in patients with the carney complex. Hum Mol Genet 9:3037-3046

81. **Groussin L, Kirschner LS, Vincent-Dejean C, Perlemoine K, Jullian E, Delemer B, Zacharieva S, Pignatelli D, Carney JA, Luton JP, Bertagna X, Stratakis CA, Bertherat J** 2002 Molecular analysis of the cyclic AMP-dependent protein kinase A (PKA) regulatory subunit 1A (PRKAR1A) gene in patients with Carney complex and primary pigmented nodular adrenocortical disease (PPNAD) reveals novel mutations and clues for pathophysiology: augmented PKA signaling is associated with adrenal tumorigenesis in PPNAD. Am J Hum Genet 71:1433-1442

82. **Valdes-Socin H, Betea V, Stevenaert A, Beckers A** 2000 Familial isolated pituitary adenomas not related to the MEN-1 syndrome: A study of 27 patients. 10th Meeting of the Belgian Endocrine Society. Abstract. 10th Meeting of the Belgian Endocrine Society

83. **Gadelha MR, Prezant TR, Une KN, Glick RP, Moskal SF, Vaisman M, Melmed S, Kineman RD, Frohman LA** 1999 Loss of heterozygosity on chromosome 11q13 in two families with acromegaly/gigantism is independent of mutations of the multiple endocrine neoplasia type I gene. J Clin Endocrinol Metab 84:249-256

84. **Yamada S, Yoshimoto K, Sano T, Takada K, Itakura M, Usui M, Teramoto A** 1997 Inactivation of the tumor suppressor gene on 11q13 in brothers with familial acrogigantism without multiple endocrine neoplasia type 1. J Clin Endocrinol Metab 82:239-242

85. **Vierimaa O, Georgitsi M, Lehtonen R, Vahteristo P, Kokko A, Raitila A, Tuppurainen K, Ebeling TM, Salmela PI, Paschke R, Gundogdu S, De ME, Makinen MJ, Launonen V, Karhu A, Aaltonen LA** 2006 Pituitary adenoma predisposition caused by germline mutations in the AIP gene. Science 312:1228-1230

86. **Beckers A, Daly AF** 2007 The clinical, pathological, and genetic features of familial isolated pituitary adenomas. Eur J Endocrinol 157:371-382

87. **Leontiou CA, Gueorguiev M, van der SJ, Quinton R, Lolli F, Hassan S, Chahal HS, Igreja SC, Jordan S, Rowe J, Stolbrink M, Christian HC, Wray J, Bishop-Bailey D, Berney DM, Wass JA, Popovic V, Ribeiro-Oliveira A, Jr., Gadelha MR, Monson JP, Akker SA, Davis JR, Clayton RN, Yoshimoto K, Iwata T, Matsuno A, Eguchi K, Musat M, Flanagan D, Peters G, Bolger GB, Chapple JP, Frohman LA, Grossman AB, Korbonits M** 2008 The role of the aryl hydrocarbon receptor-interacting protein gene in familial and sporadic pituitary adenomas. J Clin Endocrinol Metab 93:2390-2401

88. **Daly AF, Vanbellinghen JF, Khoo SK, Jaffrain-Rea ML, Naves LA, Guitelman MA, Murat A, Emy P, Gimenez-Roqueplo AP, Tamburrano G, Raverot G, Barlier A, De HW, Penfornis A, Ciccarelli E, Estour B, Lecomte P, Gatta B, Chabre O, Sabate MI, Bertagna X, Garcia BN, Stalldecker G, Colao A, Ferolla P, Wemeau JL, Caron P, Sadoul JL, Oneto A, Archambeaud F, Calender A, Sinilnikova O, Montanana CF, Cavagnini F, Hana V, Solano A, Delettieres D, Luccio-Camelo DC, Basso A, Rohmer V, Brue T, Bours V, Teh BT, Beckers A** 2007 Aryl hydrocarbon receptor-interacting protein gene mutations in familial isolated pituitary adenomas: analysis in 73 families. J Clin Endocrinol Metab 92:1891-1896

89. **Daly AF, Jaffrain-Rea ML, Ciccarelli A, Valdes-Socin H, Rohmer V, Tamburrano G, Borson-Chazot C, Estour B, Ciccarelli E, Brue T, Ferolla P, Emy P, Colao A, De ME, Lecomte P, Penfornis F, Delemer B, Bertherat J, Wemeau JL, De HW, Archambeaud F, Stevenaert A, Calender A, Murat A, Cavagnini F, Beckers A** 2006 Clinical characterization of familial isolated pituitary adenomas. J Clin Endocrinol Metab 91:3316-3323

90. **Benlian P, Giraud S, Lahlou N, Roger M, Blin C, Holler C, Lenoir G, Sallandre J, Calender A, Turpin G** 1995 Familial acromegaly: a specific clinical entity--further evidence from the genetic study of a three-generation family. Eur J Endocrinol 133:451-456

91. **Gadelha MR, Une KN, Rohde K, Vaisman M, Kineman RD, Frohman LA** 2000 Isolated familial somatotropinomas: establishment of linkage to chromosome 11q13.1-11q13.3 and evidence for a potential second locus at chromosome 2p16-12. J Clin Endocrinol Metab 85:707-714

92. **Luccio-Camelo DC, Une KN, Ferreira RE, Khoo SK, Nickolov R, Bronstein MD, Vaisman M, Teh BT, Frohman LA, Mendonca BB, Gadelha MR** 2004 A meiotic recombination in a new isolated familial somatotropinoma kindred. Eur J Endocrinol 150:643-648

93. **Soares BS, Eguchi K, Frohman LA** 2005 Tumor deletion mapping on chromosome 11q13 in eight families with isolated familial somatotropinoma

and in 15 sporadic somatotropinomas. J Clin Endocrinol Metab 90:6580-6587

94. **Georgitsi M, Raitila A, Karhu A, Tuppurainen K, Makinen MJ, Vierimaa O, Paschke R, Saeger W, van der Luijt RB, Sane T, Robledo M, De ME, Weil RJ, Wasik A, Zielinski G, Lucewicz O, Lubinski J, Launonen V, Vahteristo P, Aaltonen LA** 2007 Molecular diagnosis of pituitary adenoma predisposition caused by aryl hydrocarbon receptor-interacting protein gene mutations. Proc Natl Acad Sci USA 104:4101-4105

95. **Georgitsi M, Heliovaara E, Paschke R, Kumar AV, Tischkowitz M, Vierimaa O, Salmela P, Sane T, De ME, Cannavo S, Gundogdu S, Lucassen A, Izatt L, Aylwin S, Bano G, Hodgson S, Koch CA, Karhu A, Aaltonen LA** 2008 Large genomic deletions of aryl hydrocarbon receptor interacting protein (AIP) gene in pituitary adenoma predisposition. J Clin Endocrinol Metab 93:4146-4151

96. **Igreja S, Chahal HS, King P, Bolger GB, Srirangalingam U, Guasti L, Chapple JP, Trivellin G, Gueorguiev M, Guegan K, Stals K, Khoo B, Kumar AV, Ellard S, Grossman AB, Korbonits M** 2010 Characterization of aryl hydrocarbon receptor interacting protein (AIP) mutations in familial isolated pituitary adenoma families. Hum Mutat 31:950-960

97. **Occhi G, Jaffrain-Rea ML, Trivellin G, Albiger N, Ceccato F, De ME, Angelini M, Ferasin S, Beckers A, Mantero F, Scaroni C** 2010 The R304X mutation of the Aryl hydrocarbon receptor Interacting Protein gene in familial isolated pituitary adenomas: mutational Hot-Spot or founder effect? J Endocrinol Invest (Epub ahead of print)

98. **Toledo RA, Lourenco DM, Jr., Liberman B, Cunha-Neto MB, Cavalcanti MG, Moyses CB, Toledo SP, Dahia PL** 2007 Germline mutation in the aryl hydrocarbon receptor interacting protein gene in familial somatotropinoma. J Clin Endocrinol Metab 92:1934-1937

99. **Iwata T, Yamada S, Mizusawa N, Golam HM, Sano T, Yoshimoto K** 2007 The aryl hydrocarbon receptor-interacting protein gene is rarely mutated in sporadic GH-secreting adenomas. Clin Endocrinol (Oxf) 66:499-502

100. **Chahal HS, Stals K, Unterlander M, Balding DJ, Thomas MG, Kumar AV, Besser GM, Atkinson AB, Morrison PJ, Howlett TA, Levy MJ, Orme SM, Akker SA, Abel RL, Grossman AB, Burger J, Ellard S, Korbonits M** 2011 AIP mutation in pituitary adenomas in the 18th century and today. N Eng J Med 364:43-50

101. **Daly AF, Tichomirowa MA, Beckers A** 2009 Genetic, molecular and clinical features of familial isolated pituitary adenomas. Horm Res 71 Suppl 2:116-122

102. **Naves LA, Daly AF, Vanbellinghen JF, Casulari LA, Spilioti C, Magalhaes AV, Azevedo MF, Giacomini LA, Nascimento PP, Nunes RO, Rosa JW, Jaffrain-Rea ML, Bours V, Beckers A** 2007 Variable

pathological and clinical features of a large Brazilian family harboring a mutation in the aryl hydrocarbon receptor-interacting protein gene. Eur J Endocrinol 157:383-391

103. **Kuzhandaivelu N, Cong YS, Inouye C, Yang WM, Seto E** 1996 XAP2, a novel hepatitis B virus X-associated protein that inhibits X transactivation. Nucleic Acids Res 24:4741-4750

104. **Carver LA, Bradfield CA** 1997 Ligand-dependent interaction of the aryl hydrocarbon receptor with a novel immunophilin homolog in vivo. J Biol Chem 272:11452-11456

105. **Blatch GL, Cox MB, Smith DF** 2006 Functions of the Hsp90-Binding FKBP Immunophilins. Networking of Chaperones by Co-Chaperones.:13-25

106. **Galat A, Metcalfe SM** 1995 Peptidylproline cis/trans isomerases. Prog Biophys Mol Biol 63:67-118

107. **Laenger A, Lang-Rollin I, Kozany C, Zschocke J, Zimmermann N, Ruegg J, Holsboer F, Hausch F, Rein T** 2009 XAP2 inhibits glucocorticoid receptor activity in mammalian cells. FEBS Lett 583:1493-1498

108. **Carver LA, LaPres JJ, Jain S, Dunham EE, Bradfield CA** 1998 Characterization of the Ah receptor-associated protein, ARA9. J Biol Chem 273:33580-33587

109. **D'Andrea LD, Regan L** 2003 TPR proteins: the versatile helix. Trends Biochem Sci 28:655-662

110. **Goebl M, Yanagida M** 1991 The TPR snap helix: a novel protein repeat motif from mitosis to transcription. Trends Biochem Sci 16:173-177

111. **Lovell SC, Li X, Weerasinghe NR, Hentges KE** 2009 Correlation of microsynteny conservation and disease gene distribution in mammalian genomes. BMC Genomics 10:521

112. **Lin BC, Sullivan R, Lee Y, Moran S, Glover E, Bradfield CA** 2007 Deletion of the aryl hydrocarbon receptor-associated protein 9 leads to cardiac malformation and embryonic lethality. J Biol Chem 282:35924-35932

113. **Brown KR, Otasek D, Ali M, McGuffin MJ, Xie W, Devani B, Toch IL, Jurisica I** 2009 NAViGaTOR: Network Analysis, Visualization and Graphing Toronto. Bioinformatics 25:3327-3329

114. **Koike K** 2009 Hepatitis B virus X gene is implicated in liver carcinogenesis. Cancer Lett 286:60-68

115. **Ma Q, Whitlock JP, Jr.** 1997 A novel cytoplasmic protein that interacts with the Ah receptor, contains tetratricopeptide repeat motifs, and augments the transcriptional response to 2,3,7,8-tetrachlorodibenzo-p-dioxin. J Biol Chem 272:8878-8884

116. **Meyer BK, Petrulis JR, Perdew GH** 2000 Aryl hydrocarbon (Ah) receptor levels are selectively modulated by hsp90-associated immunophilin homolog XAP2. Cell Stress Chaperones 5:243-254

117. **Meyer BK, Pray-Grant MG, Vanden Heuvel JP, Perdew GH** 1998 Hepatitis B virus X-associated protein 2 is a subunit of the unliganded aryl hydrocarbon receptor core complex and exhibits transcriptional enhancer activity. Mol Cell Biol 18:978-988

118. **Yano M, Terada K, Mori M** 2003 AIP is a mitochondrial import mediator that binds to both import receptor Tom20 and preproteins. J Cell Biol 163:45-56

119. **Tomkinson B, Robertson E, Kieff E** 1993 Epstein-Barr virus nuclear proteins EBNA-3A and EBNA-3C are essential for B-lymphocyte growth transformation. J Virol 67:2014-2025

120. **Kashuba E, Kashuba V, Pokrovskaja K, Klein G, Szekely L** 2000 Epstein-Barr virus encoded nuclear protein EBNA-3 binds XAP-2, a protein associated with Hepatitis B virus X antigen. Oncogene 19:1801-1806

121. **Hahn ME** 2002 Aryl hydrocarbon receptors: diversity and evolution. Chem Biol Interact 141:131-160

122. **Kashuba EV, Gradin K, Isaguliants M, Szekely L, Poellinger L, Klein G, Kazlauskas A** 2006 Regulation of transactivation function of the aryl hydrocarbon receptor by the Epstein-Barr virus-encoded EBNA-3 protein. J Biol Chem 281:1215-1223

123. **Bell DR, Poland A** 2000 Binding of aryl hydrocarbon receptor (AhR) to AhR-interacting protein. The role of hsp90. J Biol Chem 275:36407-36414

124. **Kazlauskas A, Poellinger L, Pongratz I** 2002 Two distinct regions of the immunophilin-like protein XAP2 regulate dioxin receptor function and interaction with hsp90. J Biol Chem 277:11795-11801

125. **Meyer BK, Perdew GH** 1999 Characterization of the AhR-hsp90-XAP2 core complex and the role of the immunophilin-related protein XAP2 in AhR stabilization. Biochemistry 38:8907-8917

126. **Schulke JP, Wochnik GM, Lang-Rollin I, Gassen NC, Knapp RT, Berning B, Yassouridis A, Rein T** 2010 Differential impact of tetratricopeptide repeat proteins on the steroid hormone receptors. PLoS One 5:e11717

127. **Denison MS, Nagy SR** 2003 Activation of the aryl hydrocarbon receptor by structurally diverse exogenous and endogenous chemicals. Annu Rev Pharmacol Toxicol 43:309-334

128. **Nguyen LP, Bradfield CA** 2008 The search for endogenous activators of the aryl hydrocarbon receptor. Chem Res Toxicol 21:102-116

129. **Oesch-Bartlomowicz B, Huelster A, Wiss O, ntoniou-Lipfert P, Dietrich C, Arand M, Weiss C, Bockamp E, Oesch F** 2005 Aryl hydrocarbon receptor activation by cAMP vs. dioxin: divergent signaling pathways. Proc Natl Acad Sci USA 102:9218-9223

130. **Perdew GH** 1988 Association of the Ah receptor with the 90-kDa heat shock protein. J Biol Chem 263:13802-13805

131. **Nair SC, Toran EJ, Rimerman RA, Hjermstad S, Smithgall TE, Smith DF** 1996 A pathway of multi-chaperone interactions common to diverse regulatory proteins: estrogen receptor, Fes tyrosine kinase, heat shock transcription factor Hsf1, and the aryl hydrocarbon receptor. Cell Stress Chaperones 1:237-250

132. **Beischlag TV, Luis MJ, Hollingshead BD, Perdew GH** 2008 The aryl hydrocarbon receptor complex and the control of gene expression. Crit Rev Eukaryot Gene Expr 18:207-250

133. **Kazlauskas A, Poellinger L, Pongratz I** 1999 Evidence that the co-chaperone p23 regulates ligand responsiveness of the dioxin (Aryl hydrocarbon) receptor. J Biol Chem 274:13519-13524

134. **Kazlauskas A, Sundstrom S, Poellinger L, Pongratz I** 2001 The hsp90 chaperone complex regulates intracellular localization of the dioxin receptor. Mol Cell Biol 21:2594-2607

135. **Cox MB, Miller CA, III** 2004 Cooperation of heat shock protein 90 and p23 in aryl hydrocarbon receptor signaling. Cell Stress Chaperones 9:4-20

136. **Flaveny C, Perdew GH, Miller CA, III** 2009 The Aryl-hydrocarbon receptor does not require the p23 co-chaperone for ligand binding and target gene expression in vivo. Toxicol Lett 189:57-62

137. **Chen HS, Perdew GH** 1994 Subunit composition of the heteromeric cytosolic aryl hydrocarbon receptor complex. J Biol Chem 269:27554-27558

138. **LaPres JJ, Glover E, Dunham EE, Bunger MK, Bradfield CA** 2000 ARA9 modifies agonist signaling through an increase in cytosolic aryl hydrocarbon receptor. J Biol Chem 275:6153-6159

139. **Nukaya M, Lin BC, Glover E, Moran SM, Kennedy GD, Bradfield CA** 2010 The aryl hydrocarbon receptor-interacting protein (AIP) is required for dioxin-induced hepatotoxicity but not for the induction of the Cyp1a1 and Cyp1a2 genes. J Biol Chem 285:35599-35605

140. **Hollingshead BD, Petrulis JR, Perdew GH** 2004 The aryl hydrocarbon (Ah) receptor transcriptional regulator hepatitis B virus X-associated protein 2 antagonizes p23 binding to Ah receptor-Hsp90 complexes and is dispensable for receptor function. J Biol Chem 279:45652-45661

141. **Pollenz RS, Dougherty EJ** 2005 Redefining the role of the endogenous XAP2 and C-terminal hsp70-interacting protein on the endogenous Ah

receptors expressed in mouse and rat cell lines. J Biol Chem 280:33346-33356

142. **Pollenz RS, Wilson SE, Dougherty EJ** 2006 Role of endogenous XAP2 protein on the localization and nucleocytoplasmic shuttling of the endogenous mouse Ahb-1 receptor in the presence and absence of ligand. Mol Pharmacol 70:1369-1379

143. **Kazlauskas A, Poellinger L, Pongratz I** 2000 The immunophilin-like protein XAP2 regulates ubiquitination and subcellular localization of the dioxin receptor. J Biol Chem 275:41317-41324

144. **Morales JL, Perdew GH** 2007 Carboxyl terminus of hsc70-interacting protein (CHIP) can remodel mature aryl hydrocarbon receptor (AhR) complexes and mediate ubiquitination of both the AhR and the 90 kDa heat-shock protein (hsp90) in vitro. Biochemistry 46:610-621

145. **Jaffrain-Rea ML, Angelini M, Gargano D, Tichomirowa MA, Daly AF, Vanbellinghen JF, D'Innocenzo E, Barlier A, Giangaspero F, Esposito V, Ventura L, Arcella A, Theodoropoulou M, Naves LA, Fajardo C, Zacharieva S, Rohmer V, Brue T, Gulino A, Cantore G, Alesse E, Beckers A** 2009 Expression of aryl hydrocarbon receptor (AHR) and AHR-interacting protein in pituitary adenomas: pathological and clinical implications. Endocr Relat Cancer 16:1029-1043

146. **Ramadoss P, Petrulis JR, Hollingshead BD, Kusnadi A, Perdew GH** 2004 Divergent roles of hepatitis B virus X-associated protein 2 (XAP2) in human versus mouse Ah receptor complexes. Biochemistry 43:700-709

147. **Karchner SI, Franks DG, Powell WH, Hahn ME** 2002 Regulatory interactions among three members of the vertebrate aryl hydrocarbon receptor family: AHR repressor, AHR1, and AHR2. J Biol Chem 277:6949-6959

148. **Baba T, Mimura J, Gradin K, Kuroiwa A, Watanabe T, Matsuda Y, Inazawa J, Sogawa K, Fujii-Kuriyama Y** 2001 Structure and expression of the Ah receptor repressor gene. J Biol Chem 276:33101-33110

149. **Mimura J, Ema M, Sogawa K, Fujii-Kuriyama Y** 1999 Identification of a novel mechanism of regulation of Ah (dioxin) receptor function. Genes Dev 13:20-25

150. **Hoffman EC, Reyes H, Chu FF, Sander F, Conley LH, Brooks BA, Hankinson O** 1991 Cloning of a factor required for activity of the Ah (dioxin) receptor. Science 252:954-958

151. **Evans BR, Karchner SI, Allan LL, Pollenz RS, Tanguay RL, Jenny MJ, Sherr DH, Hahn ME** 2008 Repression of aryl hydrocarbon receptor (AHR) signaling by AHR repressor: role of DNA binding and competition for AHR nuclear translocator. Mol Pharmacol 73:387-398

152. **Huang P, Ceccatelli S, Hoegberg P, Sten Shi TJ, Hakansson H, Rannug A** 2003 TCDD-induced expression of Ah receptor responsive genes in the pituitary and brain of cellular retinol-binding protein (CRBP-I) knockout mice. Toxicol Appl Pharmacol 192:262-274

153. **Korkalainen M, Tuomisto J, Pohjanvirta R** 2004 Primary structure and inducibility by 2,3,7,8-tetrachlorodibenzo-p-dioxin (TCDD) of aryl hydrocarbon receptor repressor in a TCDD-sensitive and a TCDD-resistant rat strain. Biochem Biophys Res Commun 315:123-131

154. **Huang P, Ceccatelli S, Hakansson H, Grandison L, Rannug A** 2002 Constitutive and TCDD-induced expression of Ah receptor-responsive genes in the pituitary. Neurotoxicology 23:783-793

155. **Pearl LH, Prodromou C** 2006 Structure and mechanism of the Hsp90 molecular chaperone machinery. Annu Rev Biochem 75:271-294

156. **Kekatpure VD, Dannenberg AJ, Subbaramaiah K** 2009 HDAC6 modulates Hsp90 chaperone activity and regulates activation of aryl hydrocarbon receptor signaling. J Biol Chem 284:7436-7445

157. **Young JC, Hoogenraad NJ, Hartl FU** 2003 Molecular chaperones Hsp90 and Hsp70 deliver preproteins to the mitochondrial import receptor Tom70. Cell 112:41-50

158. **Alberts B, Johnson A, Lewis J, Raff M, Roberts K, Walter P** 2002 The Molecular Mechanisms of Vesicular Transport and the Maintenance of Compartmental Diversity. Molecular Biology of the Cell 4th edition.:New York: Garland Science

159. **Gething MJ, Sambrook J** 1992 Protein folding in the cell. Nature 355:33-45

160. **Goldfarb SB, Kashlan OB, Watkins JN, Suaud L, Yan W, Kleyman TR, Rubenstein RC** 2006 Differential effects of Hsc70 and Hsp70 on the intracellular trafficking and functional expression of epithelial sodium channels. Proc Natl Acad Sci USA 103:5817-5822

161. **Heliovaara E, Raitila A, Launonen V, Paetau A, Arola J, Lehtonen H, Sane T, Weil RJ, Vierimaa O, Salmela P, Tuppurainen K, Makinen M, Aaltonen LA, Karhu A** 2009 The expression of AIP-related molecules in elucidation of cellular pathways in pituitary adenomas. Am J Pathol 175:2501-2507

162. **Raitila A, Lehtonen HJ, Arola J, Heliovaara E, Ahlsten M, Georgitsi M, Jalanko A, Paetau A, Aaltonen LA, Karhu A** 2010 Mice with Inactivation of Aryl Hydrocarbon Receptor-Interacting Protein (Aip) Display Complete Penetrance of Pituitary Adenomas with Aberrant ARNT Expression. Am J Pathol 177:1969-1976

163. **Das AK, Cohen PW, Barford D** 1998 The structure of the tetratricopeptide repeats of protein phosphatase 5: implications for TPR-mediated protein-protein interactions. EMBO J 17:1192-1199

164. **Nyarko A, Mosbahi K, Rowe AJ, Leech A, Boter M, Shirasu K, Kleanthous C** 2007 TPR-Mediated self-association of plant SGT1. Biochemistry 46:11331-11341

165. **Taylor P, Dornan J, Carrello A, Minchin RF, Ratajczak T, Walkinshaw MD** 2001 Two structures of cyclophilin 40: folding and fidelity in the TPR domains. Structure 9:431-438

166. **Petrulis JR, Hord NG, Perdew GH** 2000 Subcellular localization of the aryl hydrocarbon receptor is modulated by the immunophilin homolog hepatitis B virus X-associated protein 2. J Biol Chem 275:37448-37453

167. **Yang J, Roe SM, Cliff MJ, Williams MA, Ladbury JE, Cohen PT, Barford D** 2005 Molecular basis for TPR domain-mediated regulation of protein phosphatase 5. EMBO J 24:1-10

168. **Antonsson C, Whitelaw ML, McGuire J, Gustafsson JA, Poellinger L** 1995 Distinct roles of the molecular chaperone hsp90 in modulating dioxin receptor function via the basic helix-loop-helix and PAS domains. Mol Cell Biol 15:756-765

169. **Pratt WB, Galigniana MD, Harrell JM, DeFranco DB** 2004 Role of hsp90 and the hsp90-binding immunophilins in signalling protein movement. Cell Signal 16:857-872

170. **Galigniana MD, Harrell JM, Murphy PJ, Chinkers M, Radanyi C, Renoir JM, Zhang M, Pratt WB** 2002 Binding of hsp90-associated immunophilins to cytoplasmic dynein: direct binding and in vivo evidence that the peptidylprolyl isomerase domain is a dynein interaction domain. Biochemistry 41:13602-13610

171. **Berg P, Pongratz I** 2002 Two parallel pathways mediate cytoplasmic localization of the dioxin (aryl hydrocarbon) receptor. J Biol Chem 277:32310-32319

172. **Petrulis JR, Kusnadi A, Ramadoss P, Hollingshead B, Perdew GH** 2003 The hsp90 Co-chaperone XAP2 alters importin beta recognition of the bipartite nuclear localization signal of the Ah receptor and represses transcriptional activity. J Biol Chem 278:2677-2685

173. **Bender AT, Beavo JA** 2006 Cyclic nucleotide phosphodiesterases: molecular regulation to clinical use. Pharmacol Rev 58:488-520

174. **Zaccolo M, Movsesian MA** 2007 cAMP and cGMP signaling cross-talk: role of phosphodiesterases and implications for cardiac pathophysiology. Circ Res 100:1569-1578

175. **Conti M, Beavo J** 2007 Biochemistry and physiology of cyclic nucleotide phosphodiesterases: essential components in cyclic nucleotide signaling. Annu Rev Biochem 76:481-511

176. **Lugnier C** 2006 Cyclic nucleotide phosphodiesterase (PDE) superfamily: a new target for the development of specific therapeutic agents. Pharmacol Ther 109:366-398

177. **Bolger GB, Peden AH, Steele MR, MacKenzie C, McEwan DG, Wallace DA, Huston E, Baillie GS, Houslay MD** 2003 Attenuation of the activity of the cAMP-specific phosphodiesterase PDE4A5 by interaction with the immunophilin XAP2. J Biol Chem 278:33351-33363

178. **de Oliveira SK, Smolenski A** 2009 Phosphodiesterases link the aryl hydrocarbon receptor complex to cyclic nucleotide signaling. Biochem Pharmacol 77:723-733

179. **Mackenzie KF, Topping EC, Bugaj-Gaweda B, Deng C, Cheung YF, Olsen AE, Stockard CR, High ML, Baillie GS, Grizzle WE, De VM, Houslay MD, Wang D, Bolger GB** 2008 Human PDE4A8, a novel brain-expressed PDE4 cAMP-specific phosphodiesterase that has undergone rapid evolutionary change. Biochem J 411:361-369

180. **Lennox CA, Trivellin G, Korbonits M** 2011 Evaluation of the interaction of phosphodiesterases 2A and 4A5 with the aryl hydrocarbon receptor interacting protein in pituitary cells. Endocrine Abstracts P281

181. **Huston E, Beard M, McCallum F, Pyne NJ, Vandenabeele P, Scotland G, Houslay MD** 2000 The cAMP-specific phosphodiesterase PDE4A5 is cleaved downstream of its SH3 interaction domain by caspase-3. Consequences for altered intracellular distribution. J Biol Chem 275:28063-28074

182. **Beard MB, Huston E, Campbell L, Gall I, McPhee I, Yarwood S, Scotland G, Houslay MD** 2002 In addition to the SH3 binding region, multiple regions within the N-terminal noncatalytic portion of the cAMP-specific phosphodiesterase, PDE4A5, contribute to its intracellular targeting. Cell Signal 14:453-465

183. **O'Connell JC, McCallum JF, McPhee I, Wakefield J, Houslay ES, Wishart W, Bolger G, Frame M, Houslay MD** 1996 The SH3 domain of Src tyrosyl protein kinase interacts with the N-terminal splice region of the PDE4A cAMP-specific phosphodiesterase RPDE-6 (RNPDE4A5). Biochem J 318 (Pt 1):255-261

184. **Bajpai M, Fiedler SE, Huang Z, Vijayaraghavan S, Olson GE, Livera G, Conti M, Carr DW** 2006 AKAP3 selectively binds PDE4A isoforms in bovine spermatozoa. Biol Reprod 74:109-118

185. **Stephenson DT, Coskran TM, Wilhelms MB, Adamowicz WO, O'Donnell MM, Muravnick KB, Menniti FS, Kleiman RJ, Morton D** 2009

Immunohistochemical localization of phosphodiesterase 2A in multiple mammalian species. J Histochem Cytochem 57:933-949

186. **Lin DT, Fretier P, Jiang C, Vincent SR** 2010 Nitric oxide signaling via cGMP-stimulated phosphodiesterase in striatal neurons. Synapse 64:460-466

187. **Rosman GJ, Martins TJ, Sonnenburg WK, Beavo JA, Ferguson K, Loughney K** 1997 Isolation and characterization of human cDNAs encoding a cGMP-stimulated 3',5'-cyclic nucleotide phosphodiesterase. Gene 191:89-95

188. **Sadhu K, Hensley K, Florio VA, Wolda SL** 1999 Differential expression of the cyclic GMP-stimulated phosphodiesterase PDE2A in human venous and capillary endothelial cells. J Histochem Cytochem 47:895-906

189. **Velardez MO, De LA, del Carmen DM, Lasaga M, Pisera D, Seilicovich A, Duvilanski BH** 2000 Role of phosphodiesterase and protein kinase G on nitric oxide-induced inhibition of prolactin release from the rat anterior pituitary. Eur J Endocrinol 143:279-284

190. **de Oliveira SK, Hoffmeister M, Gambaryan S, Muller-Esterl W, Guimaraes JA, Smolenski AP** 2007 Phosphodiesterase 2A forms a complex with the co-chaperone XAP2 and regulates nuclear translocation of the aryl hydrocarbon receptor. J Biol Chem 282:13656-13663

191. **Grad I, Picard D** 2007 The glucocorticoid responses are shaped by molecular chaperones. Mol Cell Endocrinol 275:2-12

192. **Heitzer MD, Wolf IM, Sanchez ER, Witchel SF, DeFranco DB** 2007 Glucocorticoid receptor physiology. Rev Endocr Metab Disord 8:321-330

193. **Yoon M** 2009 The role of PPARalpha in lipid metabolism and obesity: focusing on the effects of estrogen on PPARalpha actions. Pharmacol Res 60:151-159

194. **Sumanasekera WK, Tien ES, Turpey R, Vanden Heuvel JP, Perdew GH** 2003 Evidence that peroxisome proliferator-activated receptor alpha is complexed with the 90-kDa heat shock protein and the hepatitis virus B X-associated protein 2. J Biol Chem 278:4467-4473

195. **Cheng SY, Leonard JL, Davis PJ** 2010 Molecular aspects of thyroid hormone actions. Endocrine Rev 31:139-170

196. **Froidevaux MS, Berg P, Seugnet I, Decherf S, Becker N, Sachs LM, Bilesimo P, Nygard M, Pongratz I, Demeneix BA** 2006 The co-chaperone XAP2 is required for activation of hypothalamic thyrotropin-releasing hormone transcription in vivo. EMBO Rep 7:1035-1039

197. **Lai AZ, Gujral TS, Mulligan LM** 2007 RET signaling in endocrine tumors: delving deeper into molecular mechanisms. Endocr Pathol 18:57-67

198. **Tahira T, Ishizaka Y, Itoh F, Sugimura T, Nagao M** 1990 Characterization of ret proto-oncogene mRNAs encoding two isoforms of the protein product in a human neuroblastoma cell line. Oncogene 5:97-102

199. **Canibano C, Rodriguez NL, Saez C, Tovar S, Garcia-Lavandeira M, Borrello MG, Vidal A, Costantini F, Japon M, Dieguez C, Alvarez CV** 2007 The dependence receptor Ret induces apoptosis in somatotrophs through a Pit-1/p53 pathway, preventing tumor growth. EMBO J 26:2015-2028

200. **Heliovaara E, Tuupanen S, Ahlsten M, Hodgson S, De ME, Kuismin O, Izatt L, McKinlay Gardner RJ, Gundogdu S, Lucassen A, Arola J, Tuomisto A, Makinen MJ, Karhu A, Aaltonen LA** 2010 No evidence of RET germline mutations in familial pituitary adenoma. J Mol Endocrinol 46:1-8

201. **Vargiolu M, Fusco D, Kurelac I, Dirnberger D, Baumeister R, Morra I, Melcarne A, Rimondini R, Romeo G, Bonora E** 2009 The tyrosine kinase receptor RET interacts in vivo with aryl hydrocarbon receptor-interacting protein to alter survivin availability. J Clin Endocrinol Metab 94:2571-2578

202. **Dirnberger D, Messerschmid M, Baumeister R** 2008 An optimized split-ubiquitin cDNA-library screening system to identify novel interactors of the human Frizzled 1 receptor. Nucleic Acids Res 36:e37

203. **Harari PM, Allen GW, Bonner JA** 2007 Biology of interactions: antiepidermal growth factor receptor agents. J Clin Oncol 25:4057-4065

204. **Deribe YL, Wild P, Chandrashaker A, Curak J, Schmidt MH, Kalaidzidis Y, Milutinovic N, Kratchmarova I, Buerkle L, Fetchko MJ, Schmidt P, Kittanakom S, Brown KR, Jurisica I, Blagoev B, Zerial M, Stagljar I, Dikic I** 2009 Regulation of epidermal growth factor receptor trafficking by lysine deacetylase HDAC6. Sci Signal 2:ra84

205. **Snider J, Kittanakom S, Curak J, Stagljar I** 2010 Split-ubiquitin based membrane yeast two-hybrid (MYTH) system: a powerful tool for identifying protein-protein interactions. J Vis Exp 36:pii: 1698

206. **Fields S** 2005 High-throughput two-hybrid analysis. The promise and the peril. FEBS J 272:5391-5399

207. **Worzfeld T, Wettschureck N, Offermanns S** 2008 G(12)/G(13)-mediated signalling in mammalian physiology and disease. Trends Pharmacol Sci 29:582-589

208. **Nakata A, Urano D, Fujii-Kuriyama Y, Mizuno N, Tago K, Itoh H** 2009 G-protein signalling negatively regulates the stability of aryl hydrocarbon receptor. EMBO Rep 10:622-628

209. **Yamaguchi Y, Katoh H, Mori K, Negishi M** 2002 Galpha(12) and Galpha(13) interact with Ser/Thr protein phosphatase type 5 and stimulate its phosphatase activity. Curr Biol 12:1353-1358

210. **Jiang LI, Collins J, Davis R, Lin KM, DeCamp D, Roach T, Hsueh R, Rebres RA, Ross EM, Taussig R, Fraser I, Sternweis PC** 2007 Use of a cAMP BRET sensor to characterize a novel regulation of cAMP by the sphingosine 1-phosphate/G13 pathway. J Biol Chem 282:10576-10584

211. **Jiang LI, Collins J, Davis R, Fraser ID, Sternweis PC** 2008 Regulation of cAMP responses by the G12/13 pathway converges on adenylyl cyclase VII. J Biol Chem 283:23429-23439

212. **Baker MJ, Frazier AE, Gulbis JM, Ryan MT** 2007 Mitochondrial protein-import machinery: correlating structure with function. Trends Cell Biol 17:456-464

213. **Abe Y, Shodai T, Muto T, Mihara K, Torii H, Nishikawa S, Endo T, Kohda D** 2000 Structural basis of presequence recognition by the mitochondrial protein import receptor Tom20. Cell 100:551-560

214. **Smith DF** 2004 Tetratricopeptide repeat cochaperones in steroid receptor complexes. Cell Stress Chaperones 9:109-121

215. **Wei Y, Fan T, Yu M** 2008 Inhibitor of apoptosis proteins and apoptosis. Acta Biochim Biophys Sin (Shanghai) 40:278-288

216. **Dohi T, Beltrami E, Wall NR, Plescia J, Altieri DC** 2004 Mitochondrial survivin inhibits apoptosis and promotes tumorigenesis. J Clin Invest 114:1117-1127

217. **Fortugno P, Beltrami E, Plescia J, Fontana J, Pradhan D, Marchisio PC, Sessa WC, Altieri DC** 2003 Regulation of survivin function by Hsp90. Proc Natl Acad Sci USA 100:13791-13796

218. **Yang D, Welm A, Bishop JM** 2004 Cell division and cell survival in the absence of survivin. Proc Natl Acad Sci USA 101:15100-15105

219. **Verdecia MA, Huang H, Dutil E, Kaiser DA, Hunter T, Noel JP** 2000 Structure of the human anti-apoptotic protein survivin reveals a dimeric arrangement. Nat Struct Biol 7:602-608

220. **Chantalat L, Skoufias DA, Kleman JP, Jung B, Dideberg O, Margolis RL** 2000 Crystal structure of human survivin reveals a bow tie-shaped dimer with two unusual alpha-helical extensions. Mol Cell 6:183-189

221. **Kang BH, Altieri DC** 2006 Regulation of survivin stability by the aryl hydrocarbon receptor-interacting protein. J Biol Chem 281:24721-24727

222. **Bordeaux MC, Forcet C, Granger L, Corset V, Bidaud C, Billaud M, Bredesen DE, Edery P, Mehlen P** 2000 The RET proto-oncogene induces apoptosis: a novel mechanism for Hirschsprung disease. EMBO J 19:4056-4063

223. **Zhao Y, Meng XM, Wei YJ, Zhao XW, Liu DQ, Cao HQ, Liew CC, Ding JF** 2003 Cloning and characterization of a novel cardiac-specific kinase that interacts specifically with cardiac troponin I. J Mol Med 81:297-304

224. **Chahal HS, Chapple JP, Frohman LA, Grossman AB, Korbonits M** 2010 Clinical, genetic and molecular characterization of patients with familial isolated pituitary adenomas (FIPA). Trends Endocrinol Metab 21:419-427

225. **Barlier A, Vanbellinghen JF, Daly AF, Silvy M, Jaffrain-Rea ML, Trouillas J, Tamagno G, Cazabat L, Bours V, Brue T, Enjalbert A, Beckers A** 2007 Mutations in the aryl hydrocarbon receptor interacting protein gene are not highly prevalent among subjects with sporadic pituitary adenomas. J Clin Endocrinol Metab 92:1952-1955

226. **Georgitsi M, De ME, Cannavo S, Makinen MJ, Tuppurainen K, Pauletto P, Curto L, Weil RJ, Paschke R, Zielinski G, Wasik A, Lubinski J, Vahteristo P, Karhu A, Aaltonen LA** 2008 Aryl hydrocarbon receptor interacting protein (AIP) gene mutation analysis in children and adolescents with sporadic pituitary adenomas. Clin Endocrinol (Oxf) 69:621-627

227. **Buchbinder S, Bierhaus A, Zorn M, Nawroth PP, Humpert P, Schilling T** 2008 Aryl hydrocarbon receptor interacting protein gene (AIP) mutations are rare in patients with hormone secreting or non-secreting pituitary adenomas. Exp Clin Endocrinol Diabetes 116:625-628

228. **Cazabat L, Libe R, Perlemoine K, Rene-Corail F, Burnichon N, Gimenez-Roqueplo AP, Dupasquier-Fediaevsky L, Bertagna X, Clauser E, Chanson P, Bertherat J, Raffin-Sanson ML** 2007 Germline inactivating mutations of the aryl hydrocarbon receptor-interacting protein gene in a large cohort of sporadic acromegaly: mutations are found in a subset of young patients with macroadenomas. Eur J Endocrinol 157:1-8

229. **Raitila A, Georgitsi M, Karhu A, Tuppurainen K, Makinen MJ, Birkenkamp-Demtroder K, Salmenkivi K, Orntoft TF, Arola J, Launonen V, Vahteristo P, Aaltonen LA** 2007 No evidence of somatic aryl hydrocarbon receptor interacting protein mutations in sporadic endocrine neoplasia. Endocr Relat Cancer 14:901-906

230. **Yu R, Bonert V, Saporta I, Raffel LJ, Melmed S** 2006 Aryl hydrocarbon receptor interacting protein variants in sporadic pituitary adenomas. J Clin Endocrinol Metab 91:5126-5129

231. **Georgitsi M, Karhu A, Winqvist R, Visakorpi T, Waltering K, Vahteristo P, Launonen V, Aaltonen LA** 2007 Mutation analysis of aryl hydrocarbon receptor interacting protein (AIP) gene in colorectal, breast, and prostate cancers. Br J Cancer 96:352-356

232. **Toledo RA, Mendonca BB, Fragoso MC, Soares IC, Almeida MQ, Moraes MB, Lourenco-Jr DM, Alves VA, Bronstein MD, Toledo SP** 2010 Isolated familial somatotropinoma: 11q13-loh and gene/protein expression

analysis suggests a possible involvement of aip also in non-pituitary tumorigenesis. Clinics (Sao Paulo) 65:407-415

233. **Jennings J, Georgitsi M, Holdaway I, Daly A, Tichomirowa M, Beckers A, Aaltonen L, Karhu A, Cameron F** 2009 Aggressive pituitary adenomas occurring in young patients in a large Polynesian kindred with a germline R271W mutation in the AIP gene. Eur J Endocrinol 161:799-804

234. **Wajchenberg BL, Albergaria Pereira MA, Medonca BB, Latronico AC, Campos CP, Alves VA, Zerbini MC, Liberman B, Carlos GG, Kirschner MA** 2000 Adrenocortical carcinoma: clinical and laboratory observations. Cancer 88:711-736

235. **Heppner C, Reincke M, Agarwal SK, Mora P, Allolio B, Burns AL, Spiegel AM, Marx SJ** 1999 MEN1 gene analysis in sporadic adrenocortical neoplasms. J Clin Endocrinol Metab 84:216-219

236. **Kjellman M, Roshani L, Teh BT, Kallioniemi OP, Hoog A, Gray S, Farnebo LO, Holst M, Backdahl M, Larsson C** 1999 Genotyping of adrenocortical tumors: very frequent deletions of the MEN1 locus in 11q13 and of a 1-centimorgan region in 2p16. J Clin Endocrinol Metab 84:730-735

237. **Nord KH, Magnusson L, Isaksson M, Nilsson J, Lilljebjorn H, Domanski HA, Kindblom LG, Mandahl N, Mertens F** 2010 Concomitant deletions of tumor suppressor genes MEN1 and AIP are essential for the pathogenesis of the brown fat tumor hibernoma. Proc Natl Acad Sci USA 107:21122-21127

238. **Li J, Yen C, Liaw D, Podsypanina K, Bose S, Wang SI, Puc J, Miliaresis C, Rodgers L, McCombie R, Bigner SH, Giovanella BC, Ittmann M, Tycko B, Hibshoosh H, Wigler MH, Parsons R** 1997 PTEN, a putative protein tyrosine phosphatase gene mutated in human brain, breast, and prostate cancer. Science 275:1943-1947

239. **Avizienyte E, Loukola A, Roth S, Hemminki A, Tarkkanen M, Salovaara R, Arola J, Butzow R, Husgafvel-Pursiainen K, Kokkola A, Jarvinen H, Aaltonen LA** 1999 LKB1 somatic mutations in sporadic tumors. Am J Pathol 154:677-681

240. **Ali IU, Schriml LM, Dean M** 1999 Mutational spectra of PTEN/MMAC1 gene: a tumor suppressor with lipid phosphatase activity. J Natl Cancer Inst 91:1922-1932

241. **Sanchez-Cespedes M, Parrella P, Esteller M, Nomoto S, Trink B, Engles JM, Westra WH, Herman JG, Sidransky D** 2002 Inactivation of LKB1/STK11 is a common event in adenocarcinomas of the lung. Cancer Res 62:3659-3662

242. **Kasuki Jomori de PL, Vieira NL, Armondi Wildemberg LE, Gasparetto EL, Marcondes J, de Almeida NB, Takiya CM, Gadelha MR** 2010 Low aryl hydrocarbon receptor-interacting protein expression is a better marker

of invasiveness in somatotropinomas than ki-67 and p53. Neuroendocrinology (Epub ahead of print)

243. **Sherr CJ, Roberts JM** 1999 CDK inhibitors: positive and negative regulators of G1-phase progression. Genes Dev 13:1501-1512

244. **Sheaff RJ, Groudine M, Gordon M, Roberts JM, Clurman BE** 1997 Cyclin E-CDK2 is a regulator of p27Kip1. Genes Dev 11:1464-1478

245. **Vlach J, Hennecke S, Amati B** 1997 Phosphorylation-dependent degradation of the cyclin-dependent kinase inhibitor p27. EMBO J 16:5334-5344

246. **Carrano AC, Eytan E, Hershko A, Pagano M** 1999 SKP2 is required for ubiquitin-mediated degradation of the CDK inhibitor p27. Nat Cell Biol 1:193-199

247. **Besson A, Hwang HC, Cicero S, Donovan SL, Gurian-West M, Johnson D, Clurman BE, Dyer MA, Roberts JM** 2007 Discovery of an oncogenic activity in p27Kip1 that causes stem cell expansion and a multiple tumor phenotype. Genes Dev 21:1731-1746

248. **Dijkers PF, Medema RH, Pals C, Banerji L, Thomas NS, Lam EW, Burgering BM, Raaijmakers JA, Lammers JW, Koenderman L, Coffer PJ** 2000 Forkhead transcription factor FKHR-L1 modulates cytokine-dependent transcriptional regulation of p27(KIP1). Mol Cell Biol 20:9138-9148

249. **Servant MJ, Coulombe P, Turgeon B, Meloche S** 2000 Differential regulation of p27(Kip1) expression by mitogenic and hypertrophic factors: Involvement of transcriptional and posttranscriptional mechanisms. J Cell Biol 148:543-556

250. **Millard SS, Yan JS, Nguyen H, Pagano M, Kiyokawa H, Koff A** 1997 Enhanced ribosomal association of p27(Kip1) mRNA is a mechanism contributing to accumulation during growth arrest. J Biol Chem 272:7093-7098

251. **Bellodi C, Krasnykh O, Haynes N, Theodoropoulou M, Peng G, Montanaro L, Ruggero D** 2010 Loss of function of the tumor suppressor DKC1 perturbs p27 translation control and contributes to pituitary tumorigenesis. Cancer Res 70:6026-6035

252. **Pagano M, Tam SW, Theodoras AM, Beer-Romero P, Del SG, Chau V, Yew PR, Draetta GF, Rolfe M** 1995 Role of the ubiquitin-proteasome pathway in regulating abundance of the cyclin-dependent kinase inhibitor p27. Science 269:682-685

253. **Visone R, Russo L, Pallante P, De M, I, Ferraro A, Leone V, Borbone E, Petrocca F, Alder H, Croce CM, Fusco A** 2007 MicroRNAs (miR)-221 and miR-222, both overexpressed in human thyroid papillary carcinomas,

regulate p27Kip1 protein levels and cell cycle. Endocr Relat Cancer 14:791-798

254. **Karnik SK, Hughes CM, Gu X, Rozenblatt-Rosen O, McLean GW, Xiong Y, Meyerson M, Kim SK** 2005 Menin regulates pancreatic islet growth by promoting histone methylation and expression of genes encoding p27Kip1 and p18INK4c. Proc Natl Acad Sci USA 102:14659-14664

255. **Kolluri SK, Weiss C, Koff A, Gottlicher M** 1999 p27(Kip1) induction and inhibition of proliferation by the intracellular Ah receptor in developing thymus and hepatoma cells. Genes Dev 13:1742-1753

256. **Drosten M, Hilken G, Bockmann M, Rodicker F, Mise N, Cranston AN, Dahmen U, Ponder BA, Putzer BM** 2004 Role of MEN2A-derived RET in maintenance and proliferation of medullary thyroid carcinoma. J Natl Cancer Inst 96:1231-1239

257. **Slingerland J, Pagano M** 2000 Regulation of the cdk inhibitor p27 and its deregulation in cancer. J Cell Physiol 183:10-17

258. **Chu IM, Hengst L, Slingerland JM** 2008 The Cdk inhibitor p27 in human cancer: prognostic potential and relevance to anticancer therapy. Nat Rev Cancer 8:253-267

259. **Park MS, Rosai J, Nguyen HT, Capodieci P, Cordon-Cardo C, Koff A** 1999 p27 and Rb are on overlapping pathways suppressing tumorigenesis in mice. Proc Natl Acad Sci USA 96:6382-6387

260. **Di CA, De AM, Koff A, Cordon-Cardo C, Pandolfi PP** 2001 Pten and p27KIP1 cooperate in prostate cancer tumor suppression in the mouse. Nat Gen 27:222-224

261. **Philipp-Staheli J, Payne SR, Kemp CJ** 2001 p27(Kip1): regulation and function of a haploinsufficient tumor suppressor and its misregulation in cancer. Exp Cell Res 264:148-168

262. **Morosetti R, Kawamata N, Gombart AF, Miller CW, Hatta Y, Hirama T, Said JW, Tomonaga M, Koeffler HP** 1995 Alterations of the p27KIP1 gene in non-Hodgkin's lymphomas and adult T-cell leukemia/lymphoma. Blood 86:1924-1930

263. **Kawamata N, Morosetti R, Miller CW, Park D, Spirin KS, Nakamaki T, Takeuchi S, Hatta Y, Simpson J, Wilcyznski S, .** 1995 Molecular analysis of the cyclin-dependent kinase inhibitor gene p27/Kip1 in human malignancies. Cancer Res 55:2266-2269

264. **Spirin KS, Simpson JF, Takeuchi S, Kawamata N, Miller CW, Koeffler HP** 1996 p27/Kip1 mutation found in breast cancer. Cancer Res 56:2400-2404

265. **Wlodarska I, Baens M, Peeters P, Aerssens J, Mecucci C, Brock P, Marynen P, van den Berghe H** 1996 Biallelic alterations of both ETV6 and

CDKN1B genes in a t(12;21) childhood acute lymphoblastic leukemia case. Cancer Res 56:2655-2661

266. **Korbonits M, Chahal HS, Kaltsas G, Jordan S, Urmanova Y, Khalimova Z, Harris PE, Farrell WE, Claret FX, Grossman AB** 2002 Expression of phosphorylated p27(Kip1) protein and Jun activation domain-binding protein 1 in human pituitary tumors. J Clin Endocrinol Metab 87:2635-2643

267. **Bamberger CM, Fehn M, Bamberger AM, Ludecke DK, Beil FU, Saeger W, Schulte HM** 1999 Reduced expression levels of the cell-cycle inhibitor p27Kip1 in human pituitary adenomas. Eur J Endocrinol 140:250-255

268. **Lidhar K, Korbonits M, Jordan S, Khalimova Z, Kaltsas G, Lu X, Clayton RN, Jenkins PJ, Monson JP, Besser GM, Lowe DG, Grossman AB** 1999 Low expression of the cell cycle inhibitor p27Kip1 in normal corticotroph cells, corticotroph tumors, and malignant pituitary tumors. J Clin Endocrinol Metab 84:3823-3830

269. **Komatsubara K, Tahara S, Umeoka K, Sanno N, Teramoto A, Osamura RY** 2001 Immunohistochemical analysis of p27 (Kip1) in human pituitary glands and in various types of pituitary adenomas. Endocr Pathol 12:181-188

270. **Jin L, Qian X, Kulig E, Sanno N, Scheithauer BW, Kovacs K, Young WF, Jr., Lloyd RV** 1997 Transforming growth factor-beta, transforming growth factor-beta receptor II, and p27Kip1 expression in nontumorous and neoplastic human pituitaries. Am J Pathol 151:509-519

271. **Tanaka C, Yoshimoto K, Yang P, Kimura T, Yamada S, Moritani M, Sano T, Itakura M** 1997 Infrequent mutations of p27Kip1 gene and trisomy 12 in a subset of human pituitary adenomas. J Clin Endocrinol Metab 82:3141-3147

272. **Dahia PL, Aguiar RC, Honegger J, Fahlbush R, Jordan S, Lowe DG, Lu X, Clayton RN, Besser GM, Grossman AB** 1998 Mutation and expression analysis of the p27/kip1 gene in corticotrophin-secreting tumours. Oncogene 16:69-76

273. **Ikeda H, Yoshimoto T, Shida N** 1997 Molecular analysis of p21 and p27 genes in human pituitary adenomas. Br J Cancer 76:1119-1123

274. **Takeuchi S, Koeffler HP, Hinton DR, Miyoshi I, Melmed S, Shimon I** 1998 Mutation and expression analysis of the cyclin-dependent kinase inhibitor gene p27/Kip1 in pituitary tumors. J Endocrinol 157:337-341

275. **Casanueva FF, Molitch ME, Schlechte JA, Abs R, Bonert V, Bronstein MD, Brue T, Cappabianca P, Colao A, Fahlbusch R, Fideleff H, Hadani M, Kelly P, Kleinberg D, Laws E, Marek J, Scanlon M, Sobrinho LG, Wass JA, Giustina A** 2006 Guidelines of the Pituitary Society for the diagnosis and management of prolactinomas. Clin Endocrinol (Oxf) 65:265-273

276. **De ME, Prezant TR** 2002 Isolated familial somatotropinomas: clinical features and analysis of the MEN1 gene. Pituitary 5:11-15

277. **Ferretti E, Jaffrain Rea ML, Asteria C, Di SD, Esposito V, Ferrante L, Daniele P, Tiberti C, Gallucci M, Bosman C, Alesse E, Gulino A, Beck-Peccoz P, Tamburrano G** 2001 Two familial giant pituitary adenomas associated with overweight: clinical, morphological and genetic features. Eur J Endocrinol 144:227-235

278. **Ye S, Dhillon S, Ke X, Collins AR, Day IN** 2001 An efficient procedure for genotyping single nucleotide polymorphisms. Nucleic Acids Res 29:E88

279. **Castellsague E, Gonzalez S, Nadal M, Campos O, Guino E, Urioste M, Blanco I, Frebourg T, Capella G** 2008 Detection of APC gene deletions using quantitative multiplex PCR of short fluorescent fragments. Clin Chem 54:1132-1140

280. **Trevisson E, Salviati L, Baldoin MC, Toldo I, Casarin A, Sacconi S, Cesaro L, Basso G, Burlina AB** 2007 Argininosuccinate lyase deficiency: mutational spectrum in Italian patients and identification of a novel ASL pseudogene. Hum Mutat 28:694-702

281. **Nanzer AM, Khalaf S, Mozid AM, Fowkes RC, Patel MV, Burrin JM, Grossman AB, Korbonits M** 2004 Ghrelin exerts a proliferative effect on a rat pituitary somatotroph cell line via the mitogen-activated protein kinase pathway. Eur J Endocrinol 151:233-240

282. **Lewis BP, Shih IH, Jones-Rhoades MW, Bartel DP, Burge CB** 2003 Prediction of mammalian microRNA targets. Cell 115:787-798

283. **Griffiths-Jones S, Saini HK, van DS, Enright AJ** 2008 miRBase: tools for microRNA genomics. Nucleic Acids Res 36:D154-D158

284. **Thadani R, Tammi MT** 2006 MicroTar: predicting microRNA targets from RNA duplexes. BMC Bioinformatics 7 Suppl 5:S20

285. **Kertesz M, Iovino N, Unnerstall U, Gaul U, Segal E** 2007 The role of site accessibility in microRNA target recognition. Nat Gen 39:1278-1284

286. **Krek A, Grun D, Poy MN, Wolf R, Rosenberg L, Epstein EJ, MacMenamin P, da P, I, Gunsalus KC, Stoffel M, Rajewsky N** 2005 Combinatorial microRNA target predictions. Nat Gen 37:495-500

287. **Betel D, Wilson M, Gabow A, Marks DS, Sander C** 2008 The microRNA.org resource: targets and expression. Nucleic Acids Res 36:D149-D153

288. **Ellard S, Hattersley AT, Brewer CM, Vaidya B** 2005 Detection of an MEN1 gene mutation depends on clinical features and supports current referral criteria for diagnostic molecular genetic testing. Clin Endocrinol (Oxf) 62:169-175

289. **Ogino S, Wilson RB, Gold B, Flodman P** 2007 Bayesian risk assessment in genetic testing for autosomal dominant disorders with age-dependent penetrance. J Genet Couns 16:29-39

290. **Finnerty JR, Wang WX, Hebert SS, Wilfred BR, Mao G, Nelson PT** 2010 The miR-15/107 Group of MicroRNA Genes: Evolutionary Biology, Cellular Functions, and Roles in Human Diseases. J Mol Biol 402:491-509

291. **Garzon R, Pichiorri F, Palumbo T, Visentini M, Aqeilan R, Cimmino A, Wang H, Sun H, Volinia S, Alder H, Calin GA, Liu CG, Andreeff M, Croce CM** 2007 MicroRNA gene expression during retinoic acid-induced differentiation of human acute promyelocytic leukemia. Oncogene 26:4148-4157

292. **Yamakuchi M, Lotterman CD, Bao C, Hruban RH, Karim B, Mendell JT, Huso D, Lowenstein CJ** 2010 P53-induced microRNA-107 inhibits HIF-1 and tumor angiogenesis. Proc Natl Acad Sci USA 107:6334-6339

293. **Cazabat L, Guillaud-Bataille M, Bertherat J, Raffin-Sanson ML** 2009 Mutations of the gene for the aryl hydrocarbon receptor-interacting protein in pituitary adenomas. Horm Res 71:132-141

294. **Verges B, Boureille F, Goudet P, Murat A, Beckers A, Sassolas G, Cougard P, Chambe B, Montvernay C, Calender A** 2002 Pituitary disease in MEN type 1 (MEN1): data from the France-Belgium MEN1 multicenter study. J Clin Endocrinol Metab 87:457-465

295. **Ghataorhe P, Kurian AW, Pickart A, Trapane P, Norton JA, Kingham K, Ford JM** 2007 A carrier of both MEN1 and BRCA2 mutations: case report and review of the literature. Cancer Genet Cytogenet 179:89-92

296. **Papi L, Palli D, Masi L, Putignano AL, Congregati C, Zanna I, Marini F, Giusti F, Luzi E, Tonelli F, Genuardi M, Brandi ML, Falchetti A** 2009 Germline mutations in MEN1 and BRCA1 genes in a woman with familial multiple endocrine neoplasia type 1 and inherited breast-ovarian cancer syndromes: a case report. Cancer Genet Cytogenet 195:75-79

297. **Pitteloud N, Quinton R, Pearce S, Raivio T, Acierno J, Dwyer A, Plummer L, Hughes V, Seminara S, Cheng YZ, Li WP, Maccoll G, Eliseenkova AV, Olsen SK, Ibrahimi OA, Hayes FJ, Boepple P, Hall JE, Bouloux P, Mohammadi M, Crowley W** 2007 Digenic mutations account for variable phenotypes in idiopathic hypogonadotropic hypogonadism. J Clin Invest 117:457-463

298. **Delnatte C, Sanlaville D, Mougenot JF, Vermeesch JR, Houdayer C, Blois MC, Genevieve D, Goulet O, Fryns JP, Jaubert F, Vekemans M, Lyonnet S, Romana S, Eng C, Stoppa-Lyonnet D** 2006 Contiguous gene deletion within chromosome arm 10q is associated with juvenile polyposis of infancy, reflecting cooperation between the BMPR1A and PTEN tumor-suppressor genes. Am J Hum Genet 78:1066-1074

299. **Salviati L, Patricelli M, Guariso G, Sturniolo GC, Alaggio R, Bernardi F, Zuffardi O, Tenconi R** 2006 Deletion of PTEN and BMPR1A on chromosome 10q23 is not always associated with juvenile polyposis of infancy. Am J Hum Genet 79:593-596

300. **Loeper S, Ezzat S** 2008 Acromegaly: re-thinking the cancer risk. Rev Endocr Metab Disord 9:41-58

301. **Hemminki K, Forsti A, Ji J** 2007 Incidence and familial risks in pituitary adenoma and associated tumors. Endocr Relat Cancer 14:103-109

302. **Gopfert U, Kullmann M, Hengst L** 2003 Cell cycle-dependent translation of p27 involves a responsive element in its 5'-UTR that overlaps with a uORF. Hum Mol Genet 12:1767-1779

303. **Petrulis JR, Perdew GH** 2002 The role of chaperone proteins in the aryl hydrocarbon receptor core complex. Chem Biol Interact 141:25-40

304. **Peltonen L** 1997 Molecular background of the Finnish disease heritage. Ann Med 29:553-556

305. **Krawczak M, Ball EV, Cooper DN** 1998 Neighboring-nucleotide effects on the rates of germ-line single-base-pair substitution in human genes. Am J Hum Genet 63:474-488

306. **Khoo SK, Pendek R, Nickolov R, Luccio-Camelo DC, Newton TL, Massie A, Petillo D, Menon J, Cameron D, Teh BT, Chan SP** 2009 Genome-wide scan identifies novel modifier loci of acromegalic phenotypes for isolated familial somatotropinoma. Endocr Relat Cancer 16:1057-1063

307. **Brandi ML, Gagel RF, Angeli A, Bilezikian JP, Beck-Peccoz P, Bordi C, Conte-Devolx B, Falchetti A, Gheri RG, Libroia A, Lips CJ, Lombardi G, Mannelli M, Pacini F, Ponder BA, Raue F, Skogseid B, Tamburrano G, Thakker RV, Thompson NW, Tomassetti P, Tonelli F, Wells SA, Jr., Marx SJ** 2001 Guidelines for diagnosis and therapy of MEN type 1 and type 2. J Clin Endocrinol Metab 86:5658-5671

308. **Polster BJ, Westaway SK, Nguyen TM, Yoon MY, Hayflick SJ** 2010 Discordant expression of miR-103/7 and pantothenate kinase host genes in mouse. Mol Genet Metab 101:292-295

309. **Takahashi Y, Forrest AR, Maeno E, Hashimoto T, Daub CO, Yasuda J** 2009 MiR-107 and MiR-185 can induce cell cycle arrest in human non small cell lung cancer cell lines. PLoS One 4:e6677

310. **Martello G, Rosato A, Ferrari F, Manfrin A, Cordenonsi M, Dupont S, Enzo E, Guzzardo V, Rondina M, Spruce T, Parenti AR, Daidone MG, Bicciato S, Piccolo S** 2010 A MicroRNA targeting dicer for metastasis control. Cell 141:1195-1207

311. **Roldo C, Missiaglia E, Hagan JP, Falconi M, Capelli P, Bersani S, Calin GA, Volinia S, Liu CG, Scarpa A, Croce CM** 2006 MicroRNA expression

abnormalities in pancreatic endocrine and acinar tumors are associated with distinctive pathologic features and clinical behavior. J Clin Oncol 24:4677-4684

312. **Wilfred BR, Wang WX, Nelson PT** 2007 Energizing miRNA research: a review of the role of miRNAs in lipid metabolism, with a prediction that miR-103/107 regulates human metabolic pathways. Mol Genet Metab 91:209-217

313. **Ladeiro Y, Couchy G, Balabaud C, Bioulac-Sage P, Pelletier L, Rebouissou S, Zucman-Rossi J** 2008 MicroRNA profiling in hepatocellular tumors is associated with clinical features and oncogene/tumor suppressor gene mutations. Hepatology 47:1955-1963

314. **Corcoran DL, Pandit KV, Gordon B, Bhattacharjee A, Kaminski N, Benos PV** 2009 Features of mammalian microRNA promoters emerge from polymerase II chromatin immunoprecipitation data. PLoS One 4:e5279

315. **Li X, Zhang Y, Shi Y, Dong G, Liang J, Han Y, Wang X, Zhao Q, Ding J, Wu K, Fan D** 2010 MicroRNA-107, an oncogene microRNA that regulates tumor Invasion and metastasis by targeting DICER1 in gastric cancer: miR-107 promotes gastric cancer invasion and metastasis. J Cell Mol Med (Epub ahead of print)

316. **O'Donnell KA, Wentzel EA, Zeller KI, Dang CV, Mendell JT** 2005 c-Myc-regulated microRNAs modulate E2F1 expression. Nature 435:839-843

317. **Pekarsky Y, Croce CM** 2010 Is miR-29 an oncogene or tumor suppressor in CLL? Oncotarget 1:224-227

318. **Santanam U, Zanesi N, Efanov A, Costinean S, Palamarchuk A, Hagan JP, Volinia S, Alder H, Rassenti L, Kipps T, Croce CM, Pekarsky Y** 2010 Chronic lymphocytic leukemia modeled in mouse by targeted miR-29 expression. Proc Natl Acad Sci USA 107:12210-12215

319. **Welch C, Chen Y, Stallings RL** 2007 MicroRNA-34a functions as a potential tumor suppressor by inducing apoptosis in neuroblastoma cells. Oncogene 26:5017-5022

320. **Wang WX, Rajeev BW, Stromberg AJ, Ren N, Tang G, Huang Q, Rigoutsos I, Nelson PT** 2008 The expression of microRNA miR-107 decreases early in Alzheimer's disease and may accelerate disease progression through regulation of beta-site amyloid precursor protein-cleaving enzyme 1. J Neurosci 28:1213-1223

321. **Pallasch CP, Patz M, Park YJ, Hagist S, Eggle D, Claus R, Debey-Pascher S, Schulz A, Frenzel LP, Claasen J, Kutsch N, Krause G, Mayr C, Rosenwald A, Plass C, Schultze JL, Hallek M, Wendtner CM** 2009 miRNA deregulation by epigenetic silencing disrupts suppression of the oncogene PLAG1 in chronic lymphocytic leukemia. Blood 114:3255-3264

322. **Lee KH, Lotterman C, Karikari C, Omura N, Feldmann G, Habbe N, Goggins MG, Mendell JT, Maitra A** 2009 Epigenetic silencing of MicroRNA miR-107 regulates cyclin-dependent kinase 6 expression in pancreatic cancer. Pancreatology 9:293-301

323. **Wang WX, Wilfred BR, Madathil SK, Tang G, Hu Y, Dimayuga J, Stromberg AJ, Huang Q, Saatman KE, Nelson PT** 2010 miR-107 regulates granulin/progranulin with implications for traumatic brain injury and neurodegenerative disease. Am J Pathol 177:334-345

324. **Wang WX, Wilfred BR, Xie K, Jennings MH, Hu Y, Stromberg AJ, Nelson PT** 2010 Individual microRNAs (miRNAs) display distinct mRNA targeting "rules". RNA Biol 7:373-380

325. **Bohlig L, Friedrich M, Engeland K** 2011 p53 activates the PANK1/miRNA-107 gene leading to downregulation of CDK6 and p130 cell cycle proteins. Nucleic Acids Res 39:440-453

326. **Long D, Lee R, Williams P, Chan CY, Ambros V, Ding Y** 2007 Potent effect of target structure on microRNA function. Nat Struct Mol Biol 14:287-294

327. **Sun G, Li H, Rossi JJ** 2010 Sequence context outside the target region influences the effectiveness of miR-223 target sites in the RhoB 3'UTR. Nucleic Acids Res 38:239-252

328. **Kedde M, Strasser MJ, Boldajipour B, Oude Vrielink JA, Slanchev K, le SC, Nagel R, Voorhoeve PM, van DJ, Orom UA, Lund AH, Perrakis A, Raz E, Agami R** 2007 RNA-binding protein Dnd1 inhibits microRNA access to target mRNA. Cell 131:1273-1286

329. **Clark AM, Goldstein LD, Tevlin M, Tavare S, Shaham S, Miska EA** 2010 The microRNA miR-124 controls gene expression in the sensory nervous system of Caenorhabditis elegans. Nucleic Acids Res 38:3780-3793

330. **Doench JG, Sharp PA** 2004 Specificity of microRNA target selection in translational repression. Genes Dev 18:504-511

331. **Daly AF, Tichomirowa MA, Petrossians P, Heliovaara E, Jaffrain-Rea ML, Barlier A, Naves LA, Ebeling T, Karhu A, Raappana A, Cazabat L, De ME, Montanana CF, Raverot G, Weil RJ, Sane T, Maiter D, Neggers S, Yaneva M, Tabarin A, Verrua E, Eloranta E, Murat A, Vierimaa O, Salmela PI, Emy P, Toledo RA, Sabate MI, Villa C, Popelier M, Salvatori R, Jennings J, Longas AF, Labarta Aizpun JI, Georgitsi M, Paschke R, Ronchi C, Valimaki M, Saloranta C, De HW, Cozzi R, Guitelman M, Magri F, Lagonigro MS, Halaby G, Corman V, Hagelstein MT, Vanbellinghen JF, Barra GB, Gimenez-Roqueplo AP, Cameron FJ, Borson-Chazot F, Holdaway I, Toledo SP, Stalla GK, Spada A, Zacharieva S, Bertherat J, Brue T, Bours V, Chanson P, Aaltonen LA, Beckers A** 2010 Clinical characteristics and therapeutic responses in

patients with germ-line AIP mutations and pituitary adenomas: an international collaborative study. J Clin Endocrinol Metab 95:E373-E383

332. **Kanno Y, Takane Y, Izawa T, Nakahama T, Inouye Y** 2006 The inhibitory effect of aryl hydrocarbon receptor repressor (AhRR) on the growth of human breast cancer MCF-7 cells. Biol Pharm Bull 29:1254-1257

333. **Yang X, Liu D, Murray TJ, Mitchell GC, Hesterman EV, Karchner SI, Merson RR, Hahn ME, Sherr DH** 2005 The aryl hydrocarbon receptor constitutively represses c-myc transcription in human mammary tumor cells. Oncogene 24:7869-7881

334. **Schlezinger JJ, Liu D, Farago M, Seldin DC, Belguise K, Sonenshein GE, Sherr DH** 2006 A role for the aryl hydrocarbon receptor in mammary gland tumorigenesis. Biol Chem 387:1175-1187

335. **Zudaire E, Cuesta N, Murty V, Woodson K, Adams L, Gonzalez N, Martinez A, Narayan G, Kirsch I, Franklin W, Hirsch F, Birrer M, Cuttitta F** 2008 The aryl hydrocarbon receptor repressor is a putative tumor suppressor gene in multiple human cancers. J Clin Invest 118:640-650

336. **Hahn ME, Allan LL, Sherr DH** 2009 Regulation of constitutive and inducible AHR signaling: complex interactions involving the AHR repressor. Biochem Pharmacol 77:485-497

337. **Yaneva M, Daly AF, Tichomirowa MA, Vanbellinghen JF, Hagelstein MT, Bours V, Zacharieva S, Beckers A** 2008 Aryl hydrocarbon receptor interacting protein gene mutations in bulgarian FIPA and young sporadic pituitary adenoma patients. Proc of the 90th Annual Meet of the Endocrine SocP3-520

338. **Toledo RA, Mendonca BB, Longuini VC, Lourenco DM, Jr., Moyses CB, Bronstein MD, Toledo SP** 2008 Familial somatotropinoma and adrenocortical carcinoma due to a novel germline mutation and loss of the wild-type allele of the *AIP* gene. Proc of the 90th Annual Meet of the Endocrine Soc P1-488

339. **Beckers A, Vanbellinghen JF, Boikos S, Martari M, Verma S, Daly AF, Raygada M, Keil M, Papademetriou J, Drori-Herishanu L, Horvath A, Nesterova M, Tichomirowa MA, Bours V, Marx S, Agarwal SK, Salvatori R, Stratakis CA** 2008 Germline *AIP*, *MEN1, PRKAR1A*, *CDKN1B (p27^{Kip1})* and *CDKN2C* (*p18^{INK4c}*) gene mutations in a large cohort of pediatric patients with pituitary adenomas occurring in isolation or with associated syndromic features. Proc of the 90th Annual Meet of the Endocrine Soc OR38-1

340. **Ju H, Lim B, Kim M, Kim YS, Kim WH, Ihm C, Noh SM, Han DS, Yu HJ, Choi BY, Kang C** 2009 A regulatory polymorphism at position -309 in PTPRCAP is associated with susceptibility to diffuse-type gastric cancer and gene expression. Neoplasia 11:1340-1347

341. **Chahal HS, Igreja SC, Gueorguiev M, Quinton R, Wass JA, Popovic V, Ribeiro-Oliveira A, Jr., Akker SA, Gallego P, Gallego P, Orme SM, Goldstone AP, Bevan JS, Cheetham TD, Davis JR, Clayton RN, Flanagan D, Frohman LA, Grossman AB, Korbonits M** 2009 The clinical and genetic characteristics of patients with familial isolated pituitary adenoma. Endocrine Abstracts 19:OC40

342. **Montanana CF, Daly AF, Tichomirowa MA, Vanbellinghen JF, Theodoropoulou M, Serrano CT, Suarez PR, Vela JG, Hagelstein MT, Bours V, Beckers A** 2008 Occurrence of AIP mutations in sporadic pituitary adenomas and familial isolated pituitary adenomas kindreds in Valencia, Spain. Proc of the 90th Annual Meet of the Endocrine Soc P3-775